IMMUNE CELL METABOLISM: A PIVOT IN TISSUE ENGINEERING

By

Chima Victor Maduka

A DISSERTATION

Submitted to
Michigan State University
in partial fulfillment of the requirements
for the degree of

Comparative Medicine and Integrative Biology—Doctor of Philosophy

2022

ABSTRACT

IMMUNE CELL METABOLISM: A PIVOT IN TISSUE ENGINEERING

By

Chima Victor Maduka

Chapter 1 introduces emerging concepts in tissue engineering as well as the dynamic metabolism of immune cells, both of which underlie the motivation for my dissertation. Central to tissue engineering is the application of implanted biomaterials. By unraveling the underlying cause of immune cell activation by a widely used biomaterial (polylactide, PLA), Chapter 2 challenges a long-held theory behind host immune responses to PLA in the biomaterial microenvironment. Instead, a role for altered bioenergetics and metabolic reprogramming is postulated. Leveraging this discovery, Chapter 3 demonstrates that metabolic reprogramming can explain the reason why PLA stereochemistry is a determinant of immune cellular activation. Metabolic reprogramming could involve changes in glycolysis as well as oxidative phosphorylation. Consequently, Chapter 4 elucidates the role of glycolysis in chronic inflammation by polyethylene particles, polyethylene being another clinically used implant. Chapter 5 unravels the specific role mitochondrial respiration plays in chronic inflammation by PE particles. Lastly, Chapter 6 summarizes the overall findings in this dissertation, outlining ongoing and future experimental work. Chapters 2, 3, 4 and 5 are preprints of submitted articles.

To my family—Suzan (my wife), Chimamanda (my daughter), Ann (my mom), Francis (my late dad), Eucharia & Kambili (my sisters), Ikenna & Hillary (my brothers).

ACKNOWLEDGEMENTS

I am grateful to God Almighty, in whom I live, I move and I have my being. I express sincere gratitude to my mentor, Dr. Christopher H. Contag. Thank you for believing in and supporting me. To the members of my guidance committee—Drs. Kurt D. Hankenson, Adam J. Moeser, Xanthippi Chatzistavrou— I've always felt at home and among distinguished faculty who have my best interests at heart. To my mentees who contributed in many ways to the success of my experiments, including Oluwatosin M. Habeeb, Maxwell M. Kuhnert, Maxwell Hakun and Hunter Pope: working with you has been a pleasure! To members of the Contag Lab (Cody Madsen, Harada Yuki, Anthony Tundo, Emily Greeson, Victoria Toomajian, Seock-Jin Chung, Ehsanul Hoque Apu) who made the Lab space a memorable workplace, thank you. In particular, I worked closely with Ashley Makela and Evran Ural who enchanted me with their charisma. Brenda Lippincott has been kind, ensuring that I met with Dr. Contag at a moment's notice. Both Drs. Vilma Yuzbasiyan-Gurkan and Susan Conrad continue to inspire me. During my experiments, I variously received help from Jeffrey Leipprandt, Drs Anthony Schilmiller, Danielle Ferguson and Erika Lisabeth. Shout out to our incredible collaborators, including Kylie Smith, Jeremy Hix, Shoue Chen, Vittorio Mottini, Axel Schmitter, Drs. Ramani Narayan, Kurt Hankenson, Stuart B. Goodman, Mohammed Alhaj, Alex Dooneys, Kurt Zinn, Sangbum Park, Nureddin Ashammakhi, Jennifer Elisseeff and Jinxing Li! Outside the Lab, Mike Nestor, Abii-Tah Chungong, Chinwe and Philip Effiong, David Filipovic and Wenjie Qi have been my biggest support system. I'd recommend the CMIB program to any incoming PhD student; with Dimity, Drs. Colleen Hegg and Sreevatsan Srinand, you get first-rate support!

TABLE OF CONTENTS

LIST OF TABLES

LIST OF FIGURES

CHAPTER 1: Introduction

Background

Tissue engineering primarily involves using implanted biomaterials to guide tissue regeneration after injury or damage[1]. Factors, small molecules, cells etc. may be included in this process. Historically, the "best" biomaterials were inert, eliciting almost no inflammatory responses in the human or animal body. Advances in tissue engineering now show that, in fact, biomaterials that regulate inflammatory events in the implant microenvironment are most promising[2,3]. Such materials could guide pro-regenerative outcomes, since inflammation is a normal part of healing and integration of tissues to implants. Stability resulting from successful integration of implants to tissues precludes implant failures, and is of particular relevance in bone regenerative engineering.

Two biomaterials which are clinically and commonly applied in tissue engineering are polylactide (PLA) and polyethylene (PE). Whereas PLA breaks down (biodegradable) and is absorbed (bioresorbable) over time in the body, PE is neither biodegradable nor bioresorbable. It has long been assumed that PLA degradation into oligomers and monomers of lactic acid cause localized chronic inflammation by reducing surrounding tissue pH[4]. Of note, the basis for this theory is correlational not causal[5,6]. Similarly, chronic inflammation could arise from non-degradable particles of PE generated by frictional wear at joint articulations[7]; in either case, macrophages and fibroblasts are key cells in the biomaterial microenvironment that drive resulting pathologies.

In infectious conditions, macrophage and fibroblast activation during inflammation is a tightly regulated metabolic and bioenergetic process[8,9]. However, the underlying metabolism and bioenergetics of immune cells in the biomaterial microenvironment remain undefined. Therefore, the objective of my dissertation is to uncover the role of macrophage

and fibroblast metabolism as it relates to inflammation by PE particles and PLA degradation, advancing the field of tissue engineering.

REFERENCES

REFERENCES

1 (NIBIB), N. I. o. B. I. a. B. *Tissue Engineering and Regenerative Medicine*, <https://www.nibib.nih.gov/science-education/science-topics/tissue-engineering-and-regenerative-medicine> (2022).

2 Li, C. *et al.* Design of biodegradable, implantable devices towards clinical translation. *Nature Reviews Materials* **5**, 61-81 (2020).

3 Sadtler, K. *et al.* Design, clinical translation and immunological response of biomaterials in regenerative medicine. *Nature Reviews Materials* **1**, 1-17 (2016).

4 Agrawal, C. M. & Athanasiou, K. A. Technique to control pH in vicinity of biodegrading PLA-PGA implants. *J Biomed Mater Res* **38**, 105-114, doi:10.1002/(sici)1097-4636(199722)38:2<105::aid-jbm4>3.0.co;2-u (1997).

5 Taylor, M. S., Daniels, A. U., Andriano, K. P. & Heller, J. Six bioabsorbable polymers: in vitro acute toxicity of accumulated degradation products. *J Appl Biomater* **5**, 151-157, doi:10.1002/jab.770050208 (1994).

6 Ignatius, A. A. & Claes, L. E. In vitro biocompatibility of bioresorbable polymers: poly(L, DL-lactide) and poly(L-lactide-co-glycolide). *Biomaterials* **17**, 831-839, doi:10.1016/0142-9612(96)81421-9 (1996).

7 Sivananthan, S., Goodman, S. & Burke, M. in *Joint Replacement Technology* 373-402 (Elsevier, 2021).

8 O'Neill, L. A. & Pearce, E. J. in *J Exp Med* Vol. 213 15-23 (2016).

9 Pålsson-McDermott, E. M. & O'Neill, L. A. Targeting immunometabolism as an anti-inflammatory strategy. *Cell research* **30**, 300-314 (2020).

CHAPTER 2: Polylactide Degradation Activates Immune Cells by Metabolic Reprogramming

This chapter is a preprint of the following manuscript, currently under revision in Nature Biomedical Engineering:

Polylactide Degradation Activates Immune Cells by Metabolic Reprogramming

Chima V. Maduka, Mohammed Alhaj, Evran Ural, Michael O. Habeeb, Max M. Kuhnert, Seock-Jin Chung, Maxwell Hakun, Ashley V. Makela, Kurt D. Hankenson, Stuart B. Goodman, Ramani Narayan, Christopher H. Contag

Abstract

Polylactide (PLA) is the most widely utilized biopolymer in medicine. However, chronic inflammation and excessive fibrosis resulting from its degradation remain significant obstacles to extended clinical use. Immune cell activation has been correlated to the acidity of breakdown products, yet methods to neutralize the pH have not significantly reduced adverse responses. Using a bioenergetic model, we observed delayed cellular changes that were not apparent in the short-term. Amorphous and semi-crystalline PLA degradation products, including monomeric L-lactic acid, mechanistically remodel metabolism in cells leading to a reactive immune microenvironment characterized by elevated proinflammatory cytokines. Selective inhibition of metabolic reprogramming and altered bioenergetics both reduces these undesirably high cytokine levels and stimulates anti-inflammatory signals. Our results present a new biocompatibility paradigm by identifying metabolism as a target for immunomodulation to increase tolerance to biomaterials, ensuring safe clinical

application of PLA-based implants for soft- and hard-tissue regeneration, and advancing nanomedicine and drug delivery.

Keywords: Polylactide, Metabolic Reprogramming, Immune Cells, Tissue Regeneration, Biocompatibility

Introduction

Polylactide (PLA) is the most widely utilized biopolymer[1], with applications in nanotechnology, drug delivery and adult reconstructive surgery for tissue regeneration. However, after surgical implantation, PLA elicits adverse immune responses in up to 44% of human patients, often requiring further interventions[2,3]. In animals, a 66% incidence of excessive fibrosis from long-term inflammation with capsules which significantly limit implant-tissue integration has been reported[4]. PLA degrades by hydrolysis into D- or L-lactic acid, with semi-crystalline PLA degrading slower and tending to contain less D-content than amorphous PLA[1,5]. Adverse responses to PLA are exacerbated by mechanical loading and increasing implant size[6], and occur after prolonged exposure to large amounts of PLA degradation products[2,7-9]. It is speculated that adverse responses are mediated by PLA degradation reducing pH in surrounding tissue[10], the historical basis of which involved *Photobacterium phosphoreum*[11]. This bacterium expresses a luciferase whose reduced metabolic activity, measured by bioluminescence, can infer toxicity. In this study, breakdown products (extract) of PLA were obtained either in sterile water or Tris buffer; addition of acidic extract correlated with reduced luminescence. However, the study was not performed on mammalian cells, did not reflect the buffered in-vivo microenvironment or simulate

prolonged exposure times to accumulated PLA degradation products. Establishing that a decrease in pH correlates with PLA degradation has informed the current strategy in regenerative medicine to neutralize acidic PLA degradation products both in-vitro and in-vivo using polyphosphazene[12], calcium carbonate, sodium bicarbonate and calcium hydroxyapatite salts[10], bioglass[13] and composites containing alloys or hydroxides of magnesium[14,15] despite reports of failures[16]. The lack of a clearly described mechanism of immune cell activation by PLA degradation remains a major obstacle in the safe application of large-PLA based implants in load-bearing applications as reflected by their paucity in FDA approvals[17], and in soft tissue surgery where neutralizing ceramics cannot be applied[18].

Metabolic reprogramming refers to significant changes in oxidative phosphorylation and glycolytic flux patterns, and is a driver of fibrosis and bacterial lipopolysaccharide (LPS)-induced inflammation[19,20]. Here we set out to establish a molecular mechanism that directly links metabolic reprogramming to inflammation and fibrosis, consequent to cellular interactions with PLA degradation products. Foremost, we develop and validate a bioenergetic model of prolonged immune cell interaction with accumulated PLA degradation products. Only after prolonged exposure to amorphous or semi-crystalline PLA degradation products did macrophages and fibroblasts mechanistically undergo metabolic reprogramming and marked bioenergetic changes, with higher PLA crystallinity delaying onset. Using our model, we observed that PLA breakdown products markedly increase proinflammatory cytokine (protein) expression in primary macrophages through lactate signaling. Targeting different glycolytic steps using small molecule inhibitors modulated proinflammatory and stimulated anti-inflammatory cytokine expression by inhibiting metabolic reprogramming and altered bioenergetics in a dose-dependent manner. This

process is highly specific and not cytotoxic to surrounding unaffected immune cells. Our findings establish a new biocompatibility paradigm by identifying altered metabolism as a target for immunomodulation of PLA-based implants, fundamentally differing from previous strategies aimed at neutralizing PLA. Therefore, major advances in the use of PLA for human and veterinary applications are anticipated.

Results

Bioenergetic model for evaluating cellular responses to PLA degradation

To simulate in-vivo buffer conditions, breakdown products of PLA, generally referred to as extracts[21], were generated in serum-containing medium and used after 12 days (d) of incubation in a shaker at 37 °C (Fig. 1a). This in-vitro degradation method was designed to mimic PLA degradation in-vivo, with agitation to accelerate PLA degradation relative to static methods[22]. Together, studies in rodents, dogs and humans indicate that adverse immune responses occur after accumulation of PLA degradation products over several weeks or months[8,23-25]. To account for these extended exposure times in our model, we maintained immune cells in PLA-extract for 12 d, and this required initiating our cultures with small numbers of cells per well in both control and treatment groups. Mouse embryonic fibroblasts (NIH 3T3 cells) were stably transfected with a Sleeping Beauty transposon plasmid (pLuBIG) having a bidirectional promoter driving an improved firefly luciferase gene (fLuc) and a fusion gene encoding a Blasticidin-resistance marker (BsdR) linked to eGFP (BGL)[26]. Seeding the same cell number across control and treatment groups resulted in constant levels of luciferase and we exposed cells to equal levels of D-luciferin and oxygen in all assays. In this manner, ATP was rate-limiting and changes in ATP were measured by

bioluminescence using in-vivo imaging system (IVIS; Fig. 1b). Use of bioluminescence as an indicator of ATP levels was inexpensive, rapid (on the order of seconds) and allowed for high throughput spatiotemporal bioenergetic analysis in live cells. Additionally, in our model, each well of a 96-well plate had a total of 200 µl of medium, of which 100 µl was freshly prepared. The additional 100 µl for control wells was medium that had been in the shaker at 37 °C for 12 d to account for potential nutrient degradation that could confound results. Similarly, the additional 100 µl for treatment wells was medium in which PLA had been degraded under the same conditions. Dose-bioenergetic response of amorphous and crystalline PLA extracts revealed altered ATP levels for all tested doses (Fig. S1a). Therefore, we selected 100 or 150 µl of extract, as indicated in figure legends, to mimic accumulation of voluminous PLA breakdown products[2,7].

Highly crystalline and amorphous PLA samples were selected for their high molecular weights and represent a range of physicochemical properties (crystallinity, stereochemistry, degradation period) which constitute important considerations in selecting PLA for hard and soft tissue engineering[8,10,25]. Before using these PLA materials, we authenticated their physicochemical and thermal properties (Table S1). Lastly, we used the non-transformed, immortalized NIH 3T3 fibroblast cell line that typifies primary fibroblasts, as well as primary bone-marrow derived macrophages, both of which are key cellular mediators of prolonged inflammation and excessive fibrosis that occur in response to PLA degradation[12,23].

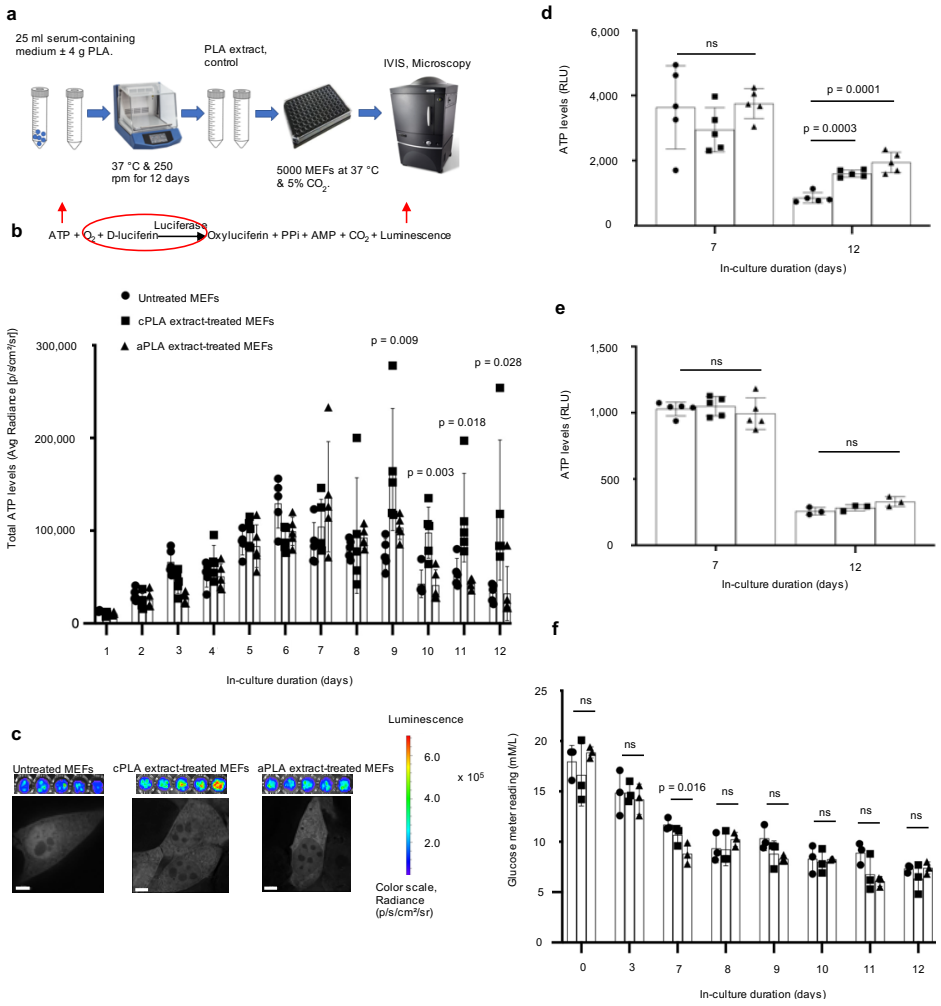

Figure 1. Bioenergetic (ATP) levels are elevated in mouse embryonic fibroblasts (MEFs) only after prolonged exposure to polylactide (PLA) degradation products (extract). **a**, Workflow showing our in-vitro bioenergetic model. **b**, Keeping luciferase, oxygen and D-luciferin levels constant (red circle) allows for changes in ATP (red arrow) to be measured by luminescence (red arrow). Using in-vivo imaging system (IVIS) and in comparison to controls, ATP levels in live cells are increased in blasticidin-eGFP-luciferase (BGL)-transfected MEFs after prolonged exposure to crystalline PLA (cPLA) degradation products. **c**, Representative microscopic (scale bars, 5 µM) and IVIS images show differential nucleoli number and luminescence, respectively. **d**, Measuring ATP in cell lysates of wild-type MEFs revealed that prolonged exposure to both amorphous PLA (aPLA) and cPLA results in elevated ATP levels. **e**, Addition of PLA does not affect the biochemical reaction by which ATP is measured. **f**, Between groups on the same day, glucose levels are similar in our in-vitro bioenergetic model. Not significant (ns), mean (SD), n = 5 (Fig. 1b, 1d and day 7 for 1e) or n = 3 (Fig. 1f and day 12 for 1e), one-way ANOVA followed by Tukey's post-hoc test; 100 µl of control or PLA extract was used.

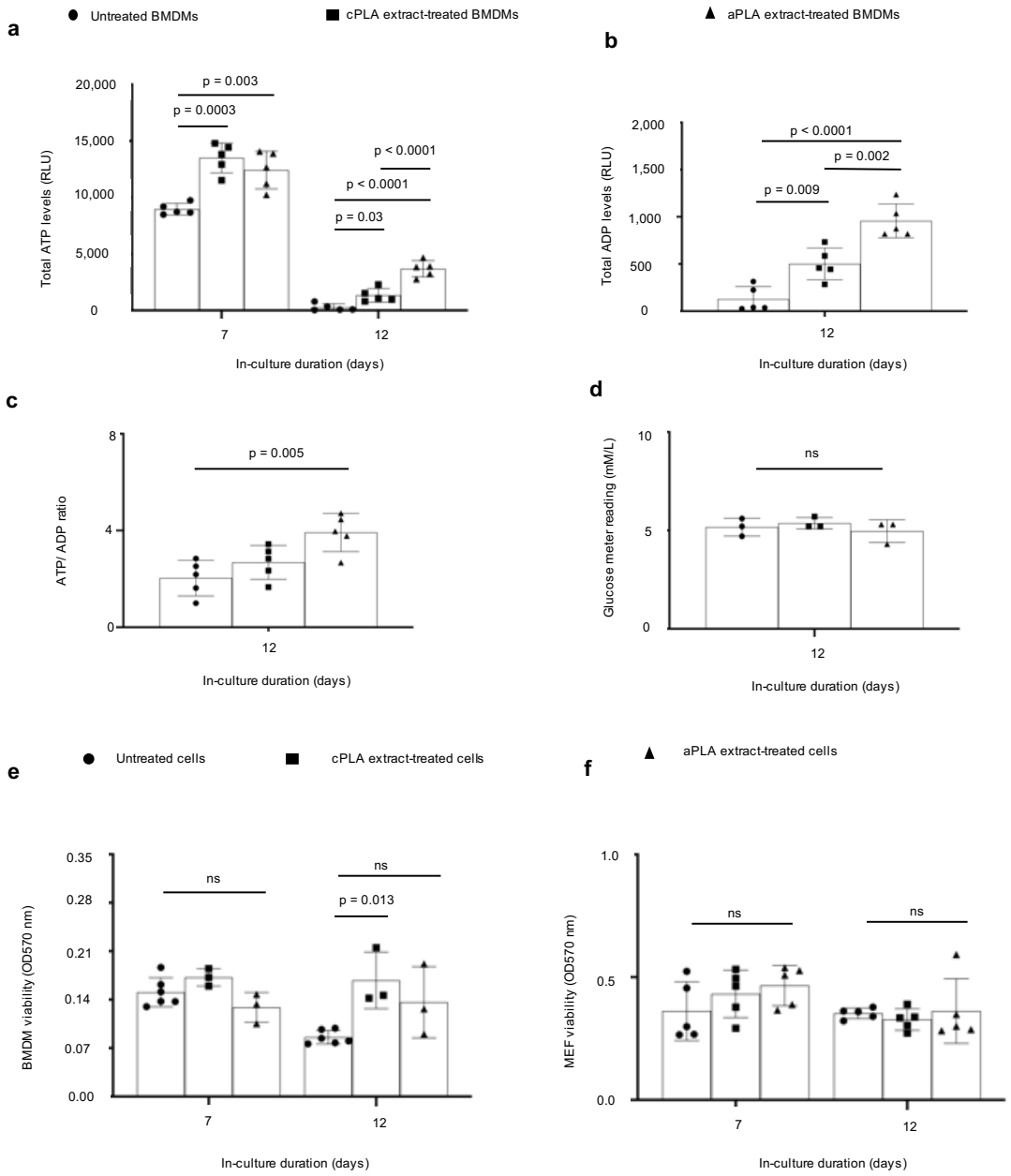

Figure 2. Bioenergetics is increased in primary bone marrow-derived macrophages (BMDMs) after prolonged exposure to polylactide (PLA) degradation products (extract). **a**, ATP levels **b**, ADP levels **c**, and ATP/ADP ratios are increased in BMDMs after prolonged exposure to amorphous PLA (aPLA) or crystalline PLA (cPLA) degradation products (extracts) in comparison to controls. **d**, Glucose levels between groups on day 12 are similar. **e-f**, Cell number between groups are similar for BMDMs (**e**) and MEFs (**f**). Not significant (ns), mean (SD), n = 5 (Fig. 2a, b, c, f), n = 3 (Fig. 2d), n = 3-6 (Fig. 2e), one-way ANOVA followed by Tukey's post-hoc test; 100 µl of control or PLA extract was used.

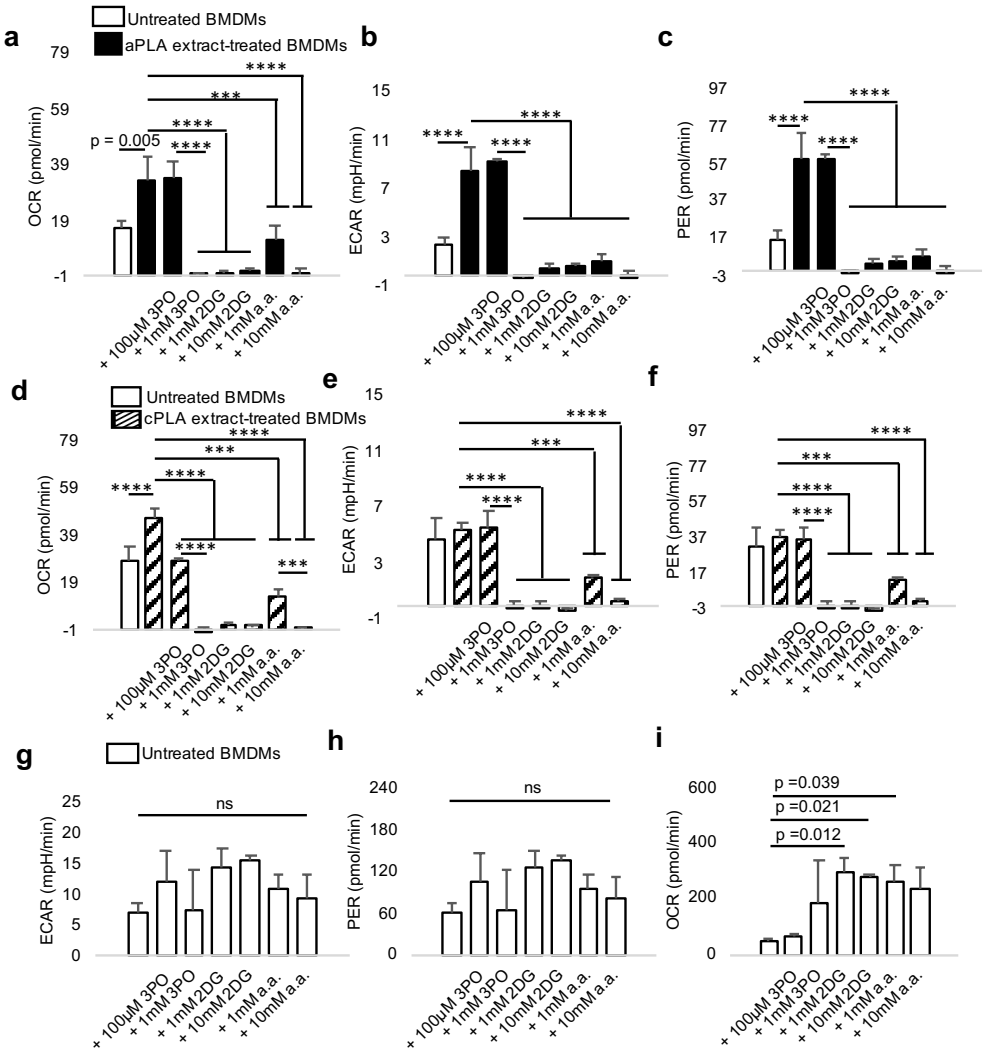

Figure 3. Functional metabolic indices are altered in primary bone marrow-derived macrophages (BMDMs) after prolonged exposure to polylactide (PLA) degradation products (extract), and can be modulated by glycolytic inhibitors. **a-c**, Following exposure to amorphous PLA (aPLA) extract, oxygen consumption rate (OCR) (**a**), extracellular acidification rate (ECAR) (**b**) and proton efflux rate (PER) (**c**) are increased relative to controls, and this abnormal increase can be dose-dependently controlled by various small molecule inhibitors. **d-f**, OCR (**d**) and not ECAR (**e**) and PER (**f**) are increased relative to controls in groups exposed to crystalline PLA (cPLA) extract, and functional metabolic indices can be controlled by pharmacologic inhibitors of glycolysis. **g-h**, ECAR (**g**) and PER (**h**) are not affected by glycolytic inhibitors in untreated BMDMs. **i**, Compensatory increase in OCR occurs in untreated BMDMs after treatment with some inhibitors. Not significant (ns), ***p<0.001, ****p<0.0001, mean (SD), n = 3, one-way ANOVA followed by Tukey's post-hoc test; 3-(3-pyridinyl)-1-(4-pyridinyl)-2-propen-1-one (3PO), 2-deoxyglucose (2DG) and aminooxyacetic acid (a.a.); 100 μl of control or PLA extract was used for 7 days.

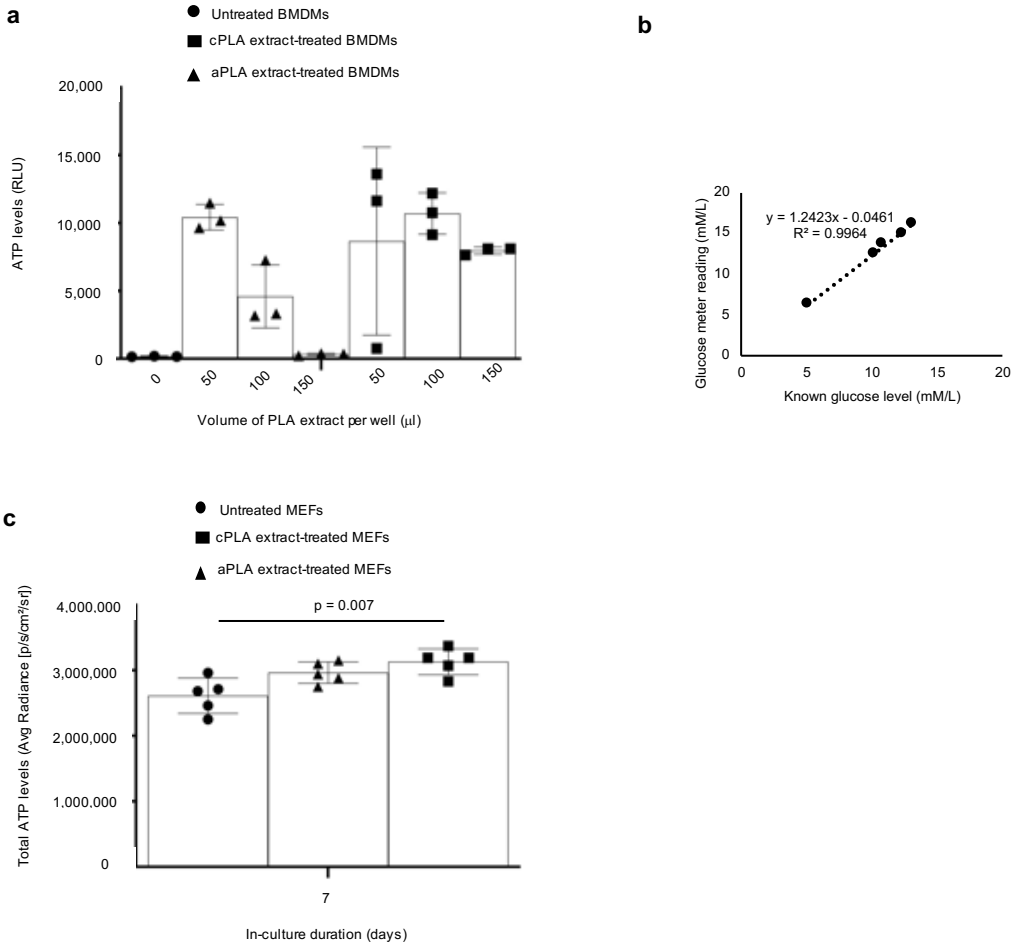

Figure S1. Different doses of polylactide (PLA) extract alter bioenergetic (ATP) levels in primary bone marrow-derived macrophages (BMDMs) and using the glucose meter can measure glucose levels in cell culture medium. a, Dose-bioenergetic response of the different PLA extracts on BMDMs revealed tendencies to alter ATP levels for all tested doses. **b**, Known glucose levels in cell culture medium linearly correlated (R square = 0.9964) with measurements from the glucose meter. **c**, Bioenergetic (ATP) levels are higher in mouse embryonic fibroblasts (MEFs) exposed to PLA extracts in comparison to controls. Mean (SD), n = 3 (Supplementary Fig. 1a), n = 5 (Supplementary Fig. 1c), simple linear regression, one-way ANOVA followed by Tukey's post-hoc test; crystalline PLA (cPLA), amorphous PLA (aPLA); 100 µl of control or PLA extract was used in Supplementary Fig. 1c.

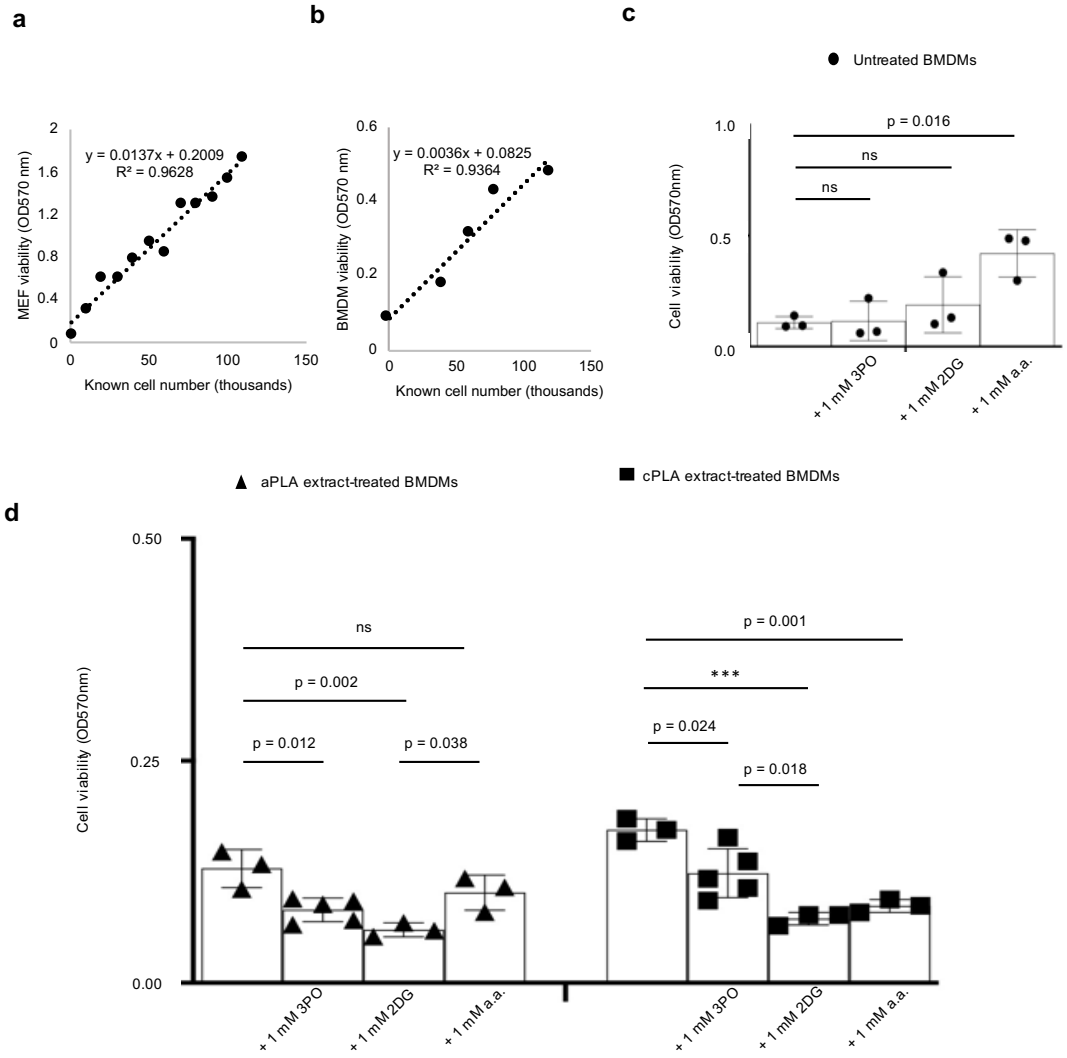

Figure S2. Crystal violet assay can measure cell viability and cytotoxicity was selective for cells exposed to polylactide (PLA) following treatment with glycolytic inhibitors. a-b, Known cell numbers linearly correlated with absorbance for **a**, mouse embryonic fibroblasts (MEF; R square = 0.9628) and **b**, primary bone marrow-derived macrophages (BMDMs; R square = 0.9364). **c-d**, Although cell viability was not decreased in untreated BMDMs following exposure to glycolytic inhibitors (**c**), BMDMs exposed to amorphous PLA (aPLA) or crystalline PLA (cPLA) degradation products (extract) decreased in cell viability after treatment with glycolytic inhibitors (**d**). Not significant (ns), *** $p < 0.001$, mean (SD), n = 3 (Supplementary Fig. 2c), n = 3-5 (Supplementary Fig. 2d), one-way ANOVA followed by Tukey's post-hoc test; 3-(3-pyridinyl)-1-(4-pyridinyl)-2-propen-1-one (3PO), 2-deoxyglucose (2DG) and aminooxyacetic acid (a.a.); 100 µl of control or PLA extract was used on day 7.

Bioenergetics is altered in immune cells after exposure to PLA degradation products

Whereas in the short-term (days 0-5) there were no changes in ATP levels, prolonged (days 6-12) exposure of fibroblasts to either amorphous or crystalline PLA increased ATP levels in live cells (Fig. 1b-c). Upon high resolution z-stack imaging, there were apparent changes in nucleoli number (Fig. 1c) after prolonged exposure to either amorphous or crystalline PLA extract, which could represent a stress response[27]. To exclude the possibility that changing luciferase expression (by transcription or translation) was responsible for observed bioenergetic changes, we lysed wild-type cells after exposure to PLA extract and added controlled amounts of luciferase and D-luciferin in the standard ATP assay. By day 12, there was a 1.9- and 2.3-fold increase in ATP levels among cells exposed to crystalline and amorphous PLA extract, respectively (Fig. 1d). To exclude the possibility that PLA extracts affect the biochemical reaction (Fig. 1b) underlying bioenergetic measurements, lysed fibroblasts were exposed to D-luciferin, luciferase and control or PLA extract. No difference in ATP levels was observed, confirming that treatment with PLA extract did not affect this biochemical reaction (Fig. 1e).

To determine whether glucose levels changed between groups on the same day because of the extended exposure times in our model, glucose meter readings were optimized in mammalian cell culture medium (Fig. S1b). Glucose levels were similar between groups on each day (Fig. 1f). On day 7, when untreated groups had higher glucose levels (Fig. 1f), corresponding bioenergetic measurement revealed that PLA extract-treated fibroblasts had higher ATP levels (Fig. S1c), excluding changing glucose levels as a confounding factor in our bioenergetic model. Because NIH 3T3 cells are normal immortalized fibroblasts, changing cell number from proliferation could account for bioenergetic changes. To exclude

this, we optimized the crystal violet assay for cell number measurement[28] in fibroblasts (Fig. S2a). Next, we isolated mouse primary bone marrow-derived macrophages (BMDMs) which, unlike NIH 3T3 cells, do not proliferate[29]. In BMDMs and consistent with our observations in fibroblasts, we observed marked increases in ATP and ADP levels (Fig. 2a, b) or ATP/ADP ratios (Fig. 2c) which were not due to changing glucose levels (Fig. 2d). After optimizing the crystal violet assay for macrophages (Fig. S2b), overall, cell numbers could not account for observed bioenergetic changes (Fig. 2e). Furthermore, fibroblast numbers were similar for cultures that were untreated or exposed to PLA extracts (Fig. 2f), excluding changing cell number as a confounder in our model.

Table S1. Authentication of physicochemical and thermal properties of commercial polylactide (PLA).

Criteria	PLA 3100HP (Crystalline PLA)	PLA 4060D (Amorphous PLA)
Optical purity (%)	99.04	81.47
L-content (%)	99.40	90.54
Glass transition temperature T_g (^oC)‡	62.20	59.05
Melting temperature T_m (^oC)‡	175.85	N/A
Crystallinity (pellet, %)†	51.46	0
Crystallinity (resin, %)‡	42.49	0
Number average molecular weights M_n (Da)	87,390	113,270
Weight average molecular weights M_w (Da)	157,060	200,200
Polydispersity index	1.797	1.767

†Percentage crystallinity of pellets was determined based on the first heating cycle.
‡Percentage crystallinity of the resin, T_g, and T_m were determined based on the second heating cycle. Molecular weights were based on a calibration curve of polystyrene standards.

Table S2. Molecular weights of polylactide (PLA) samples decrease after extraction in medium or water.

Extracted in:		Initial molecular weight (Da)		Final molecular weight (Da)		Decrease (%)	
	PLA sample	M_n	M_w	M_n	M_w	M_n	M_w
Serum-containing medium	cPLA	87,390 ± 2,840	157,060 ± 3,640	75,155 ± 1,340	140,540 ± 2,390	14.0	10.5
	aPLA	113,270 ± 1,880	200,200 ± 2,150	100,923 ± 3,380	185,365 ± 3,900	10.9	7.4
Milli-Q water	cPLA	--	--	75,155 ± 1,340	140,540 ± 2,390	14.0	10.5
	aPLA	--	--	103,302 ± 2,180	185,250 ± 3,560	8.8	7.5

Number average molecular weight (M_n) and weight average molecular weight (M_w) are expressed as mean (SD) and based on a calibration curve of polystyrene standards, n=3; crystalline PLA (cPLA), amorphous PLA (aPLA); Dashed line indicates that initial weights are the same for PLA, irrespective of whether PLA will be extracted in water or complete medium.

Exposure of macrophages to PLA breakdown products selectively results in metabolic reprogramming

To determine the metabolic pathways responsible for the bioenergetic changes we had observed, Seahorse assays were used to measure oxygen consumption rate (OCR), extracellular acidification rate (ECAR) and lactate-linked proton efflux rate (PER) in a customized medium (pH 7.4); this technique has not been previously used to examine PLA-induced adverse responses. PLA extract was removed and washed off of the cells prior to running the Seahorse assay at a pH of 7.4. Seahorse assays measure ECAR as an index of glycolytic flux, OCR as an index of oxidative phosphorylation and PER as an index of monocarboxylate transporter function[30] in live cells; and are used to assess for metabolic reprogramming[31-33]. Primary BMDMs exposed to amorphous PLA extract were metabolically altered, showing a 2-fold increase in oxidative phosphorylation (OCR; Fig. 3a), 3.5-fold increase in glycolytic flux (ECAR; Fig. 3b) and 3.5-fold increase in monocarboxylate transporter activity (PER; Fig. 3c) in comparison to untreated BMDMs. Similar amounts (100 µl) of crystalline PLA extract resulted in a 1.6-fold increase in OCR (Fig. 3d) but no change in ECAR (Fig. 3e) or PER (Fig. 3f). However, higher amounts (150 µl) of crystalline PLA extract resulted in 3.2-, 3.8-, and 3.8-fold increases in OCR, ECAR and PER, respectively (Fig. S3a-c) compared to controls, suggesting that greater volume of PLA extract is required for reprogramming using crystalline than amorphous PLA.

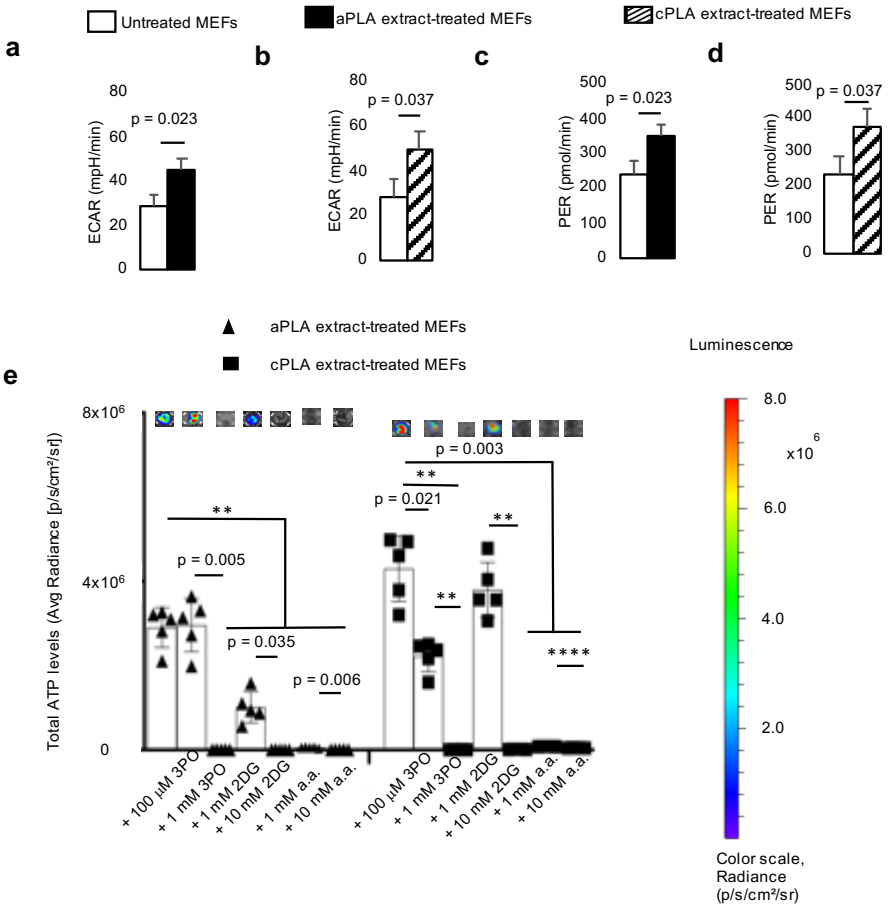

Figure 4. Functional metabolism is altered in mouse embryonic fibroblasts (MEFs) after exposure to polylactide (PLA) degradation products (extract). **a-b**, Following exposure to amorphous PLA (aPLA; **a**) or crystalline PLA (cPLA; **b**) extracts, extracellular acidification rate (ECAR) is increased. **c-d**, Proton efflux rate (PER) is elevated in MEFs after exposure to aPLA (**c**) or cPLA (**d**) extract. **e**, Bioenergetic levels in MEFs exposed to aPLA or cPLA extracts are decreased in a dose-dependent manner by 3-(3-pyridinyl)-1-(4-pyridinyl)-2-propen-1-one (3PO), 2-deoxyglucose (2DG) and aminooxyacetic acid (a.a.; representative wells are shown). ** p = 0.002, **** p < 0.0001, mean (SD), n = 3 (Fig. 4a, b, c, d), n = 5 (Fig. 4e), two-tailed unpaired t-test or Brown-Forsythe and Welch ANOVA followed by Dunnett's T3 multiple comparisons test; 100 µl of control or PLA extract was used for 7 days.

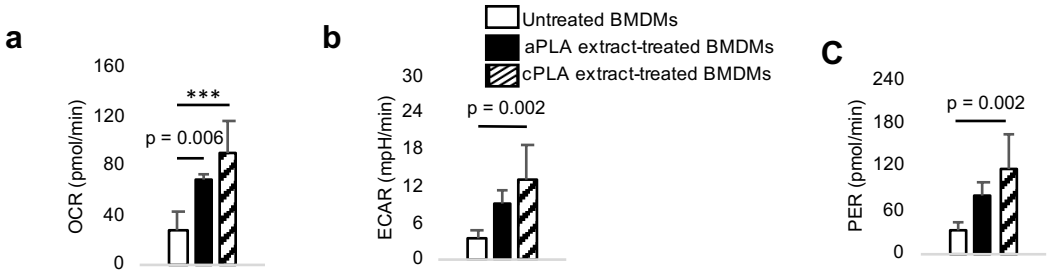

Figure S3. Functional metabolic indices are increased in primary bone marrow-derived macrophages (BMDMs) after exposure to crystalline PLA (cPLA) degradation products (extracts). a-c, Oxygen consumption rate (OCR, **a**), extracellular acidification rate (ECAR, **b**) and proton efflux rate (PER, **c**) are increased following exposure to cPLA extracts. *** $p < 0.001$, mean (SD), n=5, one-way ANOVA followed by Tukey's post-hoc test; 150 µl of control or PLA extract was used on day 7.

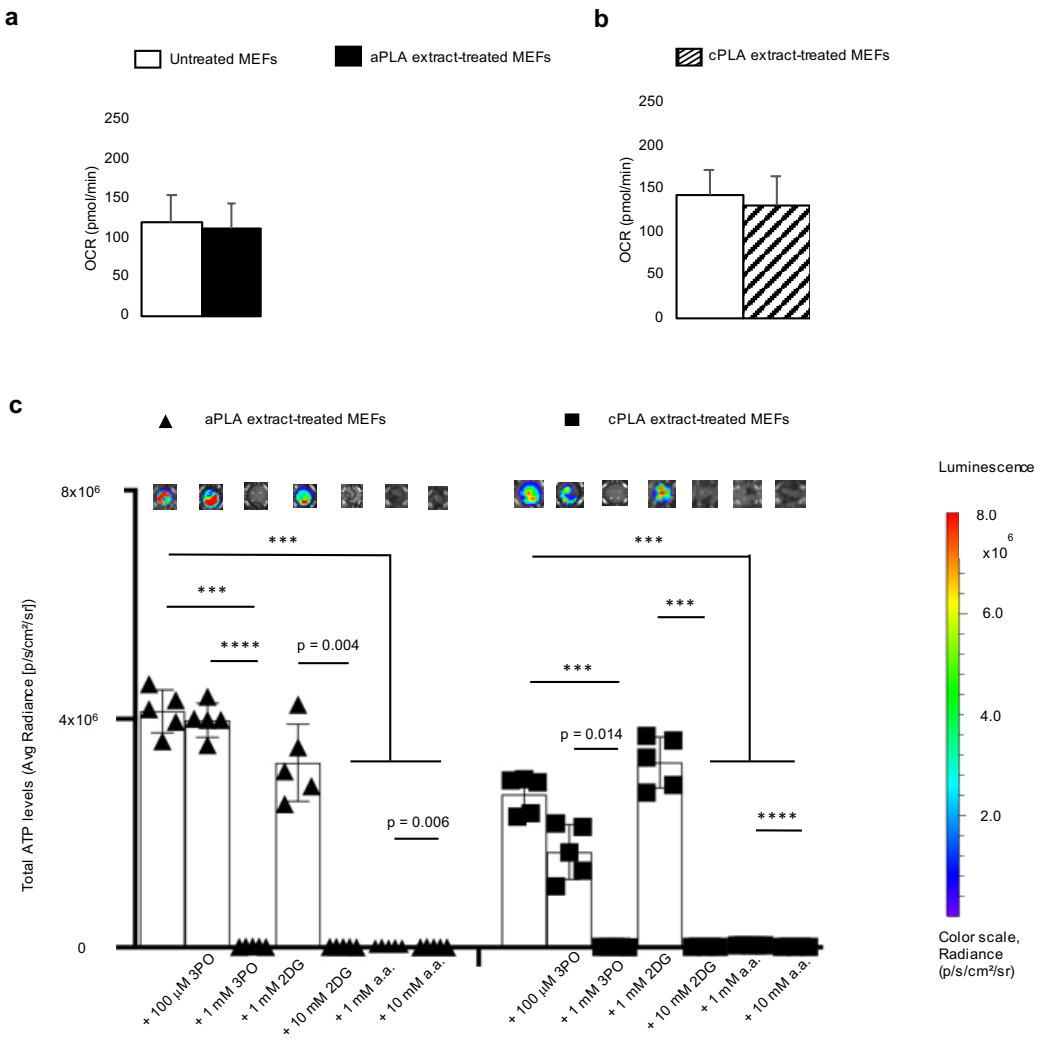

Figure S4. Oxygen consumption rate (OCR) is not altered in mouse embryonic fibroblasts (MEFs) following prolonged exposure to polylactide (PLA) degradation products (extract). **a-b**, Following exposure to amorphous PLA (aPLA; **a**) or crystalline PLA (cPLA; **b**) extracts, OCR is unaffected. **c**, Bioenergetic levels on day 12 in MEFs exposed to aPLA or cPLA extracts are decreased in a dose-dependent manner by 3-(3-pyridinyl)-1-(4-pyridinyl)-2-propen-1-one (3PO), 2-deoxyglucose (2DG) and aminooxyacetic acid (a.a.). *** $p < 0.001$, **** $p < 0.0001$, mean (SD), n = 3 (Supplementary Fig. 4a, b), n = 5 (Supplementary Fig. 4c), two-tailed unpaired t-test or Brown-Forsythe and Welch ANOVA followed by Dunnett's T3 multiple comparisons test; 100 µl of control or PLA extract was used on day 7 (Supplementary Fig. 4a, b) or 12 (Supplementary Fig. 4c).

Next, we targeted different steps in the glycolytic pathway using three small molecule inhibitors: 3-(3-pyridinyl)-1-(4-pyridinyl)-2-propen-1-one (3PO), 2-deoxyglucose (2DG) and aminooxyacetic acid (a.a.). Whereas 3PO specifically inhibits 6- phosphofructo-2-kinase which is the rate limiting glycolytic enzyme[34], 2DG inhibits hexokinase, the first enzyme in glycolysis[33], and aminooxyacetic acid prevents uptake of glycolytic substrates[35]. Dose-dependently, 3PO, 2DG and a.a. inhibited metabolic reprogramming following exposure to amorphous PLA (Fig. 3a-c) or crystalline PLA extract (Fig. 3-f) but not in untreated BMDMs (Fig. 3g-i). This demonstrates cellular uptake of 3PO, 2DG and a.a., yet with selective pharmacologic effects. Notably and under the same experimental conditions, cell viability was not reduced in untreated BMDMs after exposure to glycolytic inhibitors (Fig. S2c), demonstrating the absence of cytotoxicity[28]. However, when BMDMs were treated with amorphous or crystalline PLA extract, where metabolism was abnormally remodeled, 3PO, 2DG and a.a. mildly but selectively reduced cell viability (Fig. S2d). Therefore, pharmacologically targeting altered metabolism in primary BMDMs following exposure to PLA extract is highly specific with limited toxicity to immune cells that have normal metabolic profiles.

Fibroblasts are glycolytically reprogrammed after exposure to PLA breakdown products

After prolonged exposure of fibroblasts to amorphous and crystalline PLA extracts, glycolytic flux (ECAR; Fig. 4a-b) is increased by 1.6- and 1.7-fold, respectively. Furthermore, monocarboxylate transporter function is increased in amorphous or crystalline PLA extract-treated fibroblasts by 1.6- and 1.5-fold, respectively (Fig. 4c-d). However, oxidative

phosphorylation remains similar between untreated fibroblasts and cells exposed to amorphous or crystalline PLA extracts (OCR; Fig. S4a-b). Remarkably, increased bioenergetic (ATP) levels in amorphous or crystalline PLA extract-treated fibroblasts are inhibited by 3PO, 2DG and a.a. in a spatiotemporal and dose-dependent manner (Fig. 4e; Fig. S4c).

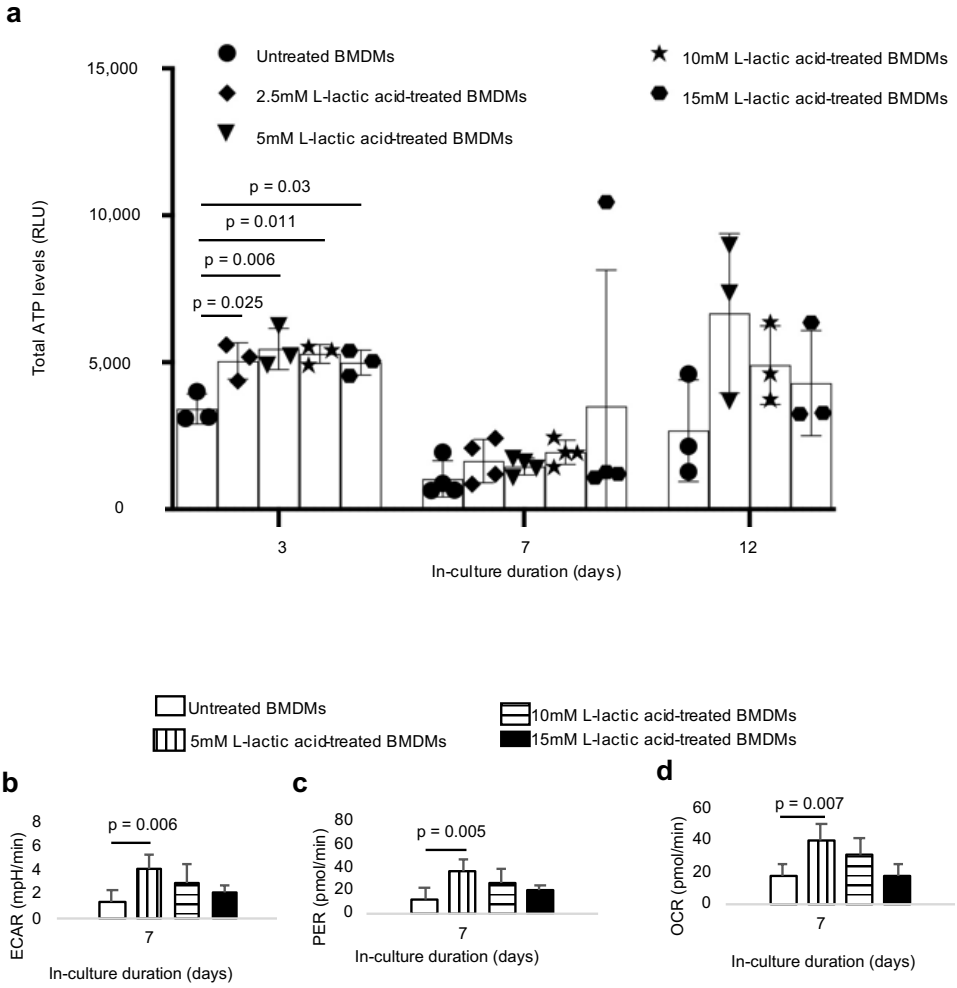

Figure 5. Treatment of primary bone marrow-derived macrophages (BMDMs) with L-lactic acid altered bioenergetic (ATP) levels and functional metabolism. a, Treatment with different doses of monomeric L-lactic acid resulted in changes in ATP levels. **b-d**, Following exposure to L-lactic acid extracellular acidification rate (ECAR, **b**), proton efflux rate (PER, **c**) and oxygen consumption rate (OCR, **d**) are increased. One-way ANOVA followed by Tukey's post-hoc test, mean (SD), n = 3-4 (Fig. 5a), n = 5 (Fig. 5b, c, d).

Short- and long-term exposure to L-lactic acid alters bioenergetics and results in metabolic reprogramming

As previously reported for short-term hydrolytic degradation of PLA[8], there was no reduction in mass of PLA after our 12 d extraction, but there were detectable changes in molecular weight (Table S2). Using the standard D/L-lactic acid enzyme-based determination assays could not effectively measure levels in serum-containing medium. However, in milliQ water and relative to controls, we observed a 7.8- and 5.2-fold increase in L-lactic acid in amorphous and crystalline PLA extracts, respectively, although these increments were not significant (Table S3). Similarly, we observed a 2.7- and 2.8-fold increase in D-lactic acid in amorphous and crystalline PLA extracts, respectively (Table S3). Therefore, we exposed BMDMs to various doses of L-lactic acid, ranging from 2.5- to 15-fold higher levels in comparison to untreated cells. We observed that bioenergetic levels are altered in the short-term (day 3; Fig. 5a) for all doses of L-lactic acid treatment, resulting in a 1.5 to 1.6-fold increase in ATP levels. After prolonged (day 7) exposure to L-lactic acid and even when bioenergetic alterations were not apparent, glycolytic flux (ECAR; Fig. 5b), monocarboxylate transporter function (PER; Fig. 5c) and oxidative phosphorylation (OCR; Fig. 5d) were increased by 2.8-, 2.8- and 2.3-fold, mechanistically reproducing observations made with amorphous and crystalline PLA extracts in our bioenergetic model. Moreover, these changes were not dependent on alterations in cell number (Fig. S5c). Of note, highly acidic groups (5-15 mM L-lactic acid) did not result in reduction in viability of primary macrophages either at day 7 or 12, relative to controls (Fig. S5c).

Table S3. Monomers of L- and D-lactic acid are detectable in extracts of polylactide.

	L-lactic acid (OD565nm)	D-lactic acid (OD565nm)
Crystalline PLA (cPLA) extract	0.0034 ± 0.0025	0.0021 ± 0.0010
Amorphous PLA (aPLA) extract	0.0051 ± 0.0036	0.0023 ± 0.0002
Control (milli-Q water)	0.0007 ± 0.0004	0.0008 ± 0.0001

Lactic acid absorbance is expressed as mean (SD), n=2-3.

Glycolytic inhibition modulates proinflammatory and stimulates anti-inflammatory cytokine expression

Using a magnetic bead-based chemokine and cytokine assay[36], we observed that, prolonged exposure of primary macrophages to amorphous and crystalline PLA extracts resulted in 228- and 319-fold increases, respectively, in IL-6 protein expression (Fig. 6a) compared to untreated macrophages. We confirmed this observation by ELISA (Fig. S6a). Similarly, exposure of macrophages to lactic acid resulted in elevated IL-6 protein expression by 2.3-fold (Fig. S6a). Amorphous PLA extracts increased MCP-1 (Fig. 6b), TNF-α (Fig. 6c) and IL-1β (Fig 6d) levels by 1.2-fold, 21-fold, and 567-fold, respectively. Likewise, crystalline PLA extracts increased MCP-1 (Fig. 6b), TNF-α (Fig. 6c) and IL-1β (Fig 6d) levels by 4.7-fold, 27-fold, and 1,378-fold, respectively.

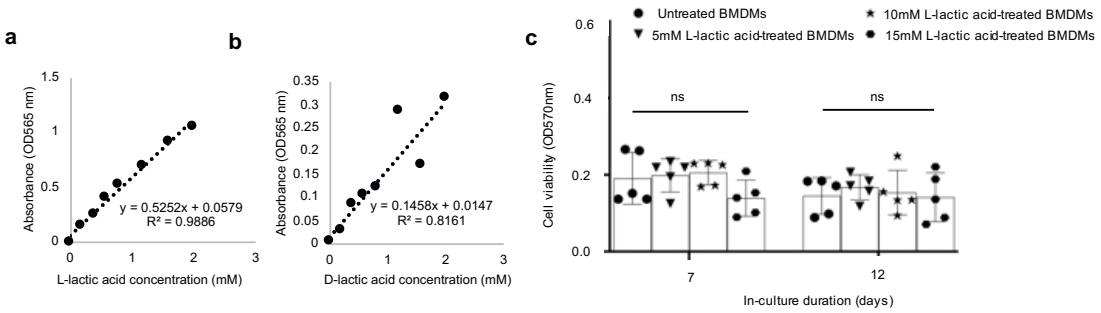

Figure S5. D- and L-lactic acid levels can be detected by absorbance and cell viability is similar among macrophages treated with L-lactic acid. a-b, Known concentrations of L-lactic (R square = 0.9886; **a**) and D-lactic (R square = 0.8161; **b**) acid linearly correlate with absorbance. **c**, Viability of primary bone marrow-derived macrophages (BMDMs) is similar after treatment with L-lactic acid over time. Not significant (ns), one-way ANOVA, mean (SD), n=5

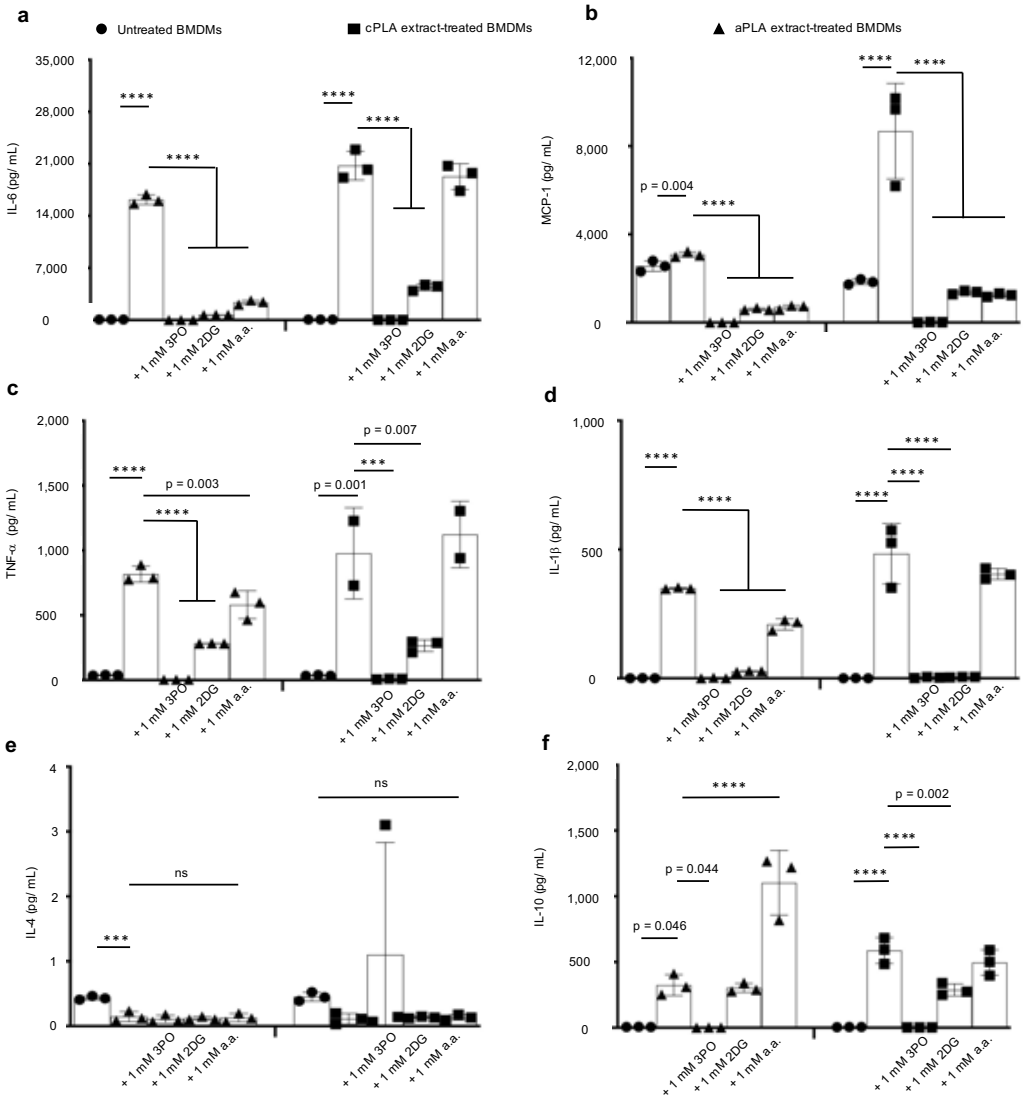

Figure 6. In macrophages exposed to PLA breakdown products, glycolytic inhibitors modulate elevated proinflammatory cytokine expression and stimulate or do not reduce anti-inflammatory cytokine levels. **a-d**, Following exposure to amorphous PLA (aPLA) or crystalline PLA (cPLA) extract, primary bone marrow-derived macrophages (BMDMs) express elevated levels of IL-6 (**a**), MCP-1 (**b**), TNF- (**c**) and IL-1β (**d**) in comparison to untreated BMDMs, and these elevated proinflammatory cytokine levels can be modulated by various small molecule inhibitors of glycolysis. **e,** Addition of glycolytic inhibitors to PLA does not reduce IL-4 expression. **f**, Expression of IL-10 is increased by inhibiting glycolysis using aminooxyacetic acid (a.a.) in amorphous PLA. Not significant (ns), ***p<0.001, ****p<0.0001, mean (SD), n = 3 in all except the cPLA group in TNF- where n=2-3, one-way ANOVA followed by Tukey's post-hoc test; 3-(3-pyridinyl)-1-(4-pyridinyl)-2-propen-1-one (3PO), 2-deoxyglucose (2DG); 100 µl of aPLA or 150 µl of cPLA extract with corresponding controls were used on day 7.

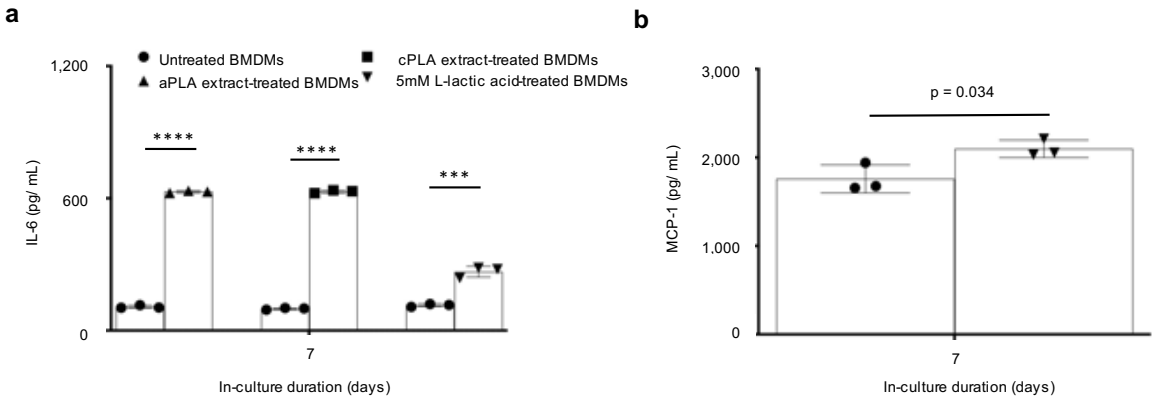

Figure S6. IL-6 and MCP-1 protein levels are increased following prolonged exposure of primary bone marrow-derived macrophages (BMDMs) to L-lactic acid in comparison to untreated BMDMs. a, Using ELISA reproduced changes in IL-6 levels following exposure of BMDMs to amorphous PLA (aPLA), crystalline PLA (cPLA) or L-lactic acid. **b**, Similarly, MCP-1 levels are increased after exposing BMDMs to L-lactic acid as measured by the MILLIPLEX assay. ***p<0.001, ****p<0.0001, mean (SD), n=3, two-tailed unpaired t-test; 100 µl of aPLA or 150 µl of cPLA with corresponding controls were used; whereas corresponding controls for PLA were incubated for 12 days, the controls for L-lactic acid were not.

Abnormally increased levels of IL-6, MCP-1, TNF-α and IL-1β were modulated by addition of 3PO, 2DG or a.a. (Fig. 6a-d). Increased MCP-1 levels in macrophages also occurred after exposure to L-lactic acid (Fig. S6b). Levels of IFN-γ and IL-13 were unchanged by PLA extract (data not shown) but exposure to amorphous PLA extract decreased IL-4 protein levels by 3-fold (Fig. 6e) relative to untreated macrophages. Remarkably, with the exception of 3PO, IL-10 expression was either unchanged (crystalline PLA) or increased by 3.4-fold (amorphous PLA) upon addition of a.a. (Fig. 6f) relative to macrophages exposed to PLA extract.

Discussion

We describe a bioenergetic model of immune cell activation to PLA degradation, revealing that altered bioenergetics and metabolic reprogramming underlie adverse responses, including persistent inflammation and excessive fibrosis, to PLA breakdown products. For decades, the hypothesis in regenerative medicine has been that acidity drives immune cell activation to PLA degradation[10]. However, this observation was founded on correlation not causation[11,21]. Consequently, methods based on neutralizing acidity have been inadequate in controlling adverse responses to PLA degradation[7,16].

Importantly, our in-vitro model extends the short time periods that have been previously studied[37]. By adapting our bioenergetic model for high throughput analysis, we observed delayed immune cell changes not apparent in the short-term. In patients, PLA slowly degrades into oligomers and monomers of lactic acid. Ultimately, due to bulk degradation, PLA breakdown exceeds immune cellular clearance, resulting in accumulation of oligomers and monomers of lactic acid[25]. We illustrate that only after prolonged exposure to PLA degradation products do fibroblasts and macrophages become activated.

Mechanistically, PLA degradation not only alters bioenergetic homeostasis in immune cells, it results in metabolic reprogramming. We identified PLA degradation products to include monomeric L-lactic acid and reproduced bioenergetic alterations and metabolic reprogramming using L-lactic acid. Following exposure of macrophages to PLA degradation products, metabolic reprogramming is characterized by concomitantly elevated oxidative phosphorylation and glycolysis, resulting in increased IL-6, MCP-1, TNF-α and IL-1β protein expression, potent proinflammatory cytokines. Increased glycolysis, a fundamental proinflammatory metabolic phenotype, is likely mediated by HIF-1α[33]. Human fibroblasts in lactate-enriched medium stabilize HIF-1α resulting in increased glycolysis[38] which underlies activation of fibroblasts in several profibrotic pathologies[19]. Similarly, increased oxidative phosphorylation is required for macrophages to function as antigen presenting cells as part of inflammation[39] or its resolution[20].

Inhibiting different steps in the glycolytic pathway produced similar effects, decreasing proinflammatory cytokine expression by modulating metabolic reprogramming and altered bioenergetics. Unlike bacterial LPS-mediated glycolytic reprogramming that is uniquely dependent on IL-1β[33], PLA degradation products additionally affect IL-6, MCP-1 and TNF-α. Of note, modulating proinflammatory cytokine expression using aminooxyacetic acid stimulated IL-10 protein expression, an anti-inflammatory cytokine[31]. Collectively, these findings are important for at least four reasons. First, it explains the "Oppenheimer phenomenon", where long-term PLA implantation results in neoplasia in some humans and up to 80% of rodents[6] since IL-6 directly links persistent inflammation from PLA to cellular transformation[40]. Second, stimulating IL-10 is critical to tissue repair by driving wound resolution and angiogenesis[41]. In fact, IL-10 is a key immunomodulatory cytokine secreted

by mesenchymal stem cells[42], and is crucial in macrophage-stem cell crosstalk[43,44] for tissue engineering. Third, macrophages that have normal metabolism are unaffected by the small molecule inhibitors studied. In fact, cytotoxicity is selective for macrophages having altered metabolism, making this technique particularly desirable. Fourth, it provides a basis to study lactate signaling in tumor initiation, with the potential to stop neoplastic initiation.

Lactate is a signaling molecule in immunity[45] and cancer progression[46-48]. Its role when combined with LPS is conflicting, with reports of proinflammatory and anti-inflammatory effects[49,50]. However, a stand-alone ability of lactate to activate immune cells is novel, as prior inflammatory and cancer models did not simulate prolonged exposure times, a critical feature of the cancer and immune microenvironments.

Amorphous PLA which undergoes faster hydrolytic degradation than crystalline PLA results in quicker onset of metabolic reprogramming. Nonetheless, crystalline PLA does eventually result in metabolic remodeling and altered bioenergetics. Furthermore, our data implicate monocarboxylate transporters which mediate the bi-directional flux of lactate across cell membranes[30,49].

Taken together, our findings suggest a model where PLA degradation products, including monomers of L-lactic acid, mechanistically remodel metabolism in cells of the immune microenvironment. This mechanism is specific and leads to increased proinflammatory cytokine expression which can be modulated while stimulating anti-inflammatory cytokines. Our approach will enhance the biocompatibility and safety of biomaterials, including PLA-based implants for soft- and hard-tissue regeneration, significantly advancing tissue engineering.

Methods

Polylactide (PLA) materials and extraction

Highly crystalline PLA 3100HP and amorphous PLA 4060D (both from NatureWorks LLC) were used after their physicochemical and thermal properties were authenticated (Table S1). PLA was sterilized by exposure to ultraviolet radiation for 30 minutes[25]. Afterwards, breakdown products (extracts)[21] of PLA, were obtained by suspending 4 g of PLA pellets in 25 ml of complete medium. Complete medium comprised of DMEM medium, 10% heat-inactivated Fetal Bovine Serum and 100 U/mL penicillin-streptomycin (all from ThermoFisher Scientific). PLA was extracted for 12 days in a shaker at 250 rpm and 37 °C, after which extracts were decanted. Volume of extracts used for each experiment is specified in figure legends.

Bioenergetic assessment

Bioluminescence was measured using the IVIS Spectrum in vivo imaging system (PerkinElmer) after adding 150 μg/mL of D-luciferin (PerkinElmer). Living Image (Version 4.5.2, PerkinElmer) was used for acquiring bioluminescence on the IVIS Spectrum. Standard ATP/ADP kits (Sigma-Aldrich) containing D-luciferin, luciferase and cell lysis buffer were used to according to manufacturer's instructions. Luminescence at integration time of 1000 ms was obtained using the SpectraMax M3 Spectrophotometer (Molecular Devices) using SoftMax Pro (Version 7.0.2, Molecular Devices).

Microscopy

Z-stack microscopy was accomplished by using the DeltaVision deconvolution imaging system (GE Healthcare) and softWoRx software (Version 7.2.1, GE Healthcare) at excitation and emission wavelengths of 525 and 558 nm, respectively for FITC. Section thickness of 0.2 μm for 64 to 128 sections were obtained at 40x and 100x magnification.

Glucose measurement

Glucose levels in complete medium was evaluated by a hand-held GM-100 glucose meter (BioReactor Sciences) according to manufacturer's instruction.

Cells

Mouse embryonic fibroblast cell line (NIH 3T3 cell line; ATCC) and murine primary bone-marrow derived macrophages (BMDMs) were used. In each experiment, either 5,000 fibroblasts or 50,000 BMDMs were initially seeded. BMDMs were sourced from male and female C57BL/6J mice (Jackson Laboratories) of 3-4 months[29,32]. NIH 3T3 cells were stably transfected with a Sleeping Beauty transposon plasmid (pLuBIG) having a bidirectional promoter driving an improved firefly luciferase gene (fLuc) and a fusion gene encoding a Blasticidin-resistance marker (BsdR) linked to eGFP (BGL)[26]; enabling us to simultaneously monitor morphological and bioenergetic changes in live cells[51,52]. All cells were cultured in complete medium.

Materials

3-(3-pyridinyl)-1-(4-pyridinyl)-2-propen-1-one (MilliporeSigma), 2-deoxyglucose (MilliporeSigma) and aminooxyacetic acid (Sigma-Aldrich) were used for glycolytic inhibition and L-lactic acid (Sigma-Aldrich) was used at various concentrations to reproduce the effects of PLA degradation products.

Cell viability

Cell viability was assessed using the crystal violet assay[28]. Absorbance (optical density) was acquired at 570 nm using the the SpectraMax M3 Spectrophotometer (Molecular Devices) and SoftMax Pro software (Version 7.0.2, Molecular Devices).

Functional metabolism

Basal measurements of oxygen consumption rate (OCR), extracellular acidification rate (ECAR) and lactate-linked proton efflux rate (PER) were obtained in real-time using the Seahorse XFe-96 Extracellular Flux Analyzer (Agilent Technologies)[31-33]. Prior to running the assay, cell culture medium was replaced by the Seahorse XF DMEM medium (pH 7.4) supplemented with 25 mM D-glucose and 4 mM Glutamine. The Seahorse ATP rate and cell energy phenotype assays were run according to manufacturer's instruction and all reagents for the Seahorse assays were sourced from Agilent Technologies. Wave software (Version 2.6.1) was used to export Seahorse data directly as means ± standard deviation (SD).

Chemokine and cytokine measurements

Cytokine and chemokine levels were measured using a MILLIPLEX MAP mouse magnetic bead multiplex kit (MilliporeSigma)[36] to assess for IL-6, MCP-1, TNF-α, IL-1β, IL-4, IL-10, IFN-λ and 1L-13 protein expression in supernatants. Data was acquired using Luminex 200 (Luminex Corporation) by the xPONENT software (Version 3.1, Luminex Corporation). Using the glycolytic inhibitor, 3PO, expectedly decreased cytokine values to < 3.2 pg/ mL in some experiments. For statistical analyses, those values were expressed as 3.1 pg/ mL. Values exceeding the dynamic range of the assay, in accordance with manufacturer's instruction, were excluded. Additionally, IL-6 ELISA kits (RayBiotech) for supernatants were used according to manufacturer's instructions.

D/L-lactic acid determination assays

Measurements of L- and D-lactic acid were using standard D- and L-lactate assay kits (Sigma-Aldrich) according to manufacturer's instruction. Negative absorbance values which were outside the dynamic range for the assay were excluded during analysis.

Optical rotation

Polarimetry was used to characterize the L-content and optical purity of the PLA samples with a P-2000 polarimeter (Jasco) by the Spectra Manager software (Version 2.13.00, Jasco). The optical rotation, $[\alpha]_{25}$, was measured and averaged for three samples of each polymer in chloroform (Omnisolv), at a concentration of 1 g/100 mL. Conditions were set at 25 ºC and 589 nm wavelength. Sucrose was used as a standard reference material, and its specific optical rotation was reported as approximately 67 º.

Gel permeation chromatography

Gel permeation chromatography (GPC) was conducted to characterize the polymer molecular weights using a 600 controller (Waters) equipped with Optilab T-rEX refractive index (RI) and TREOS II multi-angle light scattering (MALS) detectors (Wyatt Technology Corporation), and a PLgel 5µm MIXED-C column (Agilent Technologies) with chloroform eluent (1 mL/min). ASTRA software (Version 7.3.2.21, Wyatt Technology Corporation) was used. Polystyrene standards (Alfa Aesar) with M_n ranging from 35,000 to 900,000 Da were used for calibration.

Differential scanning calorimetry

Differential scanning calorimetry (DSC) was conducted with a DSC Q20 (TA Instruments) to analyse the melting temperature (T_m), glass transition temperature (T_g), and percent crystallinity of the PLA grades. Thermal Advantage software (Version 5.5.23, TA Instruments) was used. Temperature was first equilibrated to 0 ºC, then ramped up to 200 ºC at a heating rate of 10 ºC/ min; temperature was then held isothermally for 5 minutes. Afterwards, the sample was cooled back to 0 ºC at a rate of 10 ºC/min, then held isothermally for 2 minutes. Finally, the material was heated back to 200 ºC at 10 ºC/ min.

Statistics and reproducibility

Statistical software (GraphPad Prism) was used to analyse data presented as mean with standard deviation (SD). Significance level was set at $p < 0.05$, and details of statistical tests and sample sizes, which are biological replicates, are provided in figure legends. Exported data (mean, SD) from Wave in Seahorse experiments had the underlying assumption of

normality and similar variance, and thus were tested using corresponding parametric tests as indicated in figure legends.

Reporting summary

Further information on experimental design is available in the Nature Research Reporting Summary linked to this article.

Data availability

The data supporting the findings of this study are available within the paper and its Supplementary Information.

Acknowledgements

Euthanized C57BL/6J mice were a gift from RR Neubig (facilitated by J Leipprandt) and the Campus Animal Resources at Michigan State University (MSU). Funding for this work was provided in part by the James and Kathleen Cornelius Endowment at MSU.

Author contributions

Conceptualization, C.V.M. and C.H.C.; Methodology, C.V.M., K.D.H., S.B.G., R.N. and C.H.C.; Investigation, C.V.M., M.A., E.U., M.O.B., M.M.K., S.J.C., M.H. and A.V.M.; Writing – Original Draft, C.V.M.; Writing – Review & Editing, C.V.M., M.A., E.U., M.O.B., M.M.K., S.J.C., M.H., A.V.M., K.D.H., S.B.G., R.N. and C.H.C.; Funding Acquisition, C.H.C.; Resources, R.N. and C.H.C.; Supervision, K.D.H., S.B.G., R.N. and C.H.C.

Competing interests

The authors declare no competing interests.

REFERENCES

REFERENCES

1 Farah, S., Anderson, D. G. & Langer, R. Physical and mechanical properties of PLA, and their functions in widespread applications - A comprehensive review. *Adv Drug Deliv Rev* **107**, 367-392, doi:10.1016/j.addr.2016.06.012 (2016).

2 Givissis, P. K., Stavridis, S. I., Papagelopoulos, P. J., Antonarakos, P. D. & Christodoulou, A. G. Delayed foreign-body reaction to absorbable implants in metacarpal fracture treatment. *Clinical Orthopaedics and Related Research*® **468**, 3377-3383 (2010).

3 Laine, P., Kontio, R., Lindqvist, C. & Suuronen, R. Are there any complications with bioabsorbable fixation devices?: a 10 year review in orthognathic surgery. *International journal of oral and maxillofacial surgery* **33**, 240-244 (2004).

4 Chalidis, B., Kitridis, D., Savvidis, P., Papalois, A. & Givissis, P. Does the Inion OTPStm absorbable plating system induce higher foreign-body reaction than titanium implants? An experimental randomized comparative study in rabbits. *Biomedical Materials* **15**, 065011 (2020).

5 Poh, P. S. *et al.* Polylactides in additive biomanufacturing. *Advanced Drug Delivery Reviews* **107**, 228-246 (2016).

6 Ramot, Y., Haim-Zada, M., Domb, A. J. & Nyska, A. Biocompatibility and safety of PLA and its copolymers. *Adv Drug Deliv Rev* **107**, 153-162, doi:10.1016/j.addr.2016.03.012 (2016).

7 Mosier-LaClair, S., Pike, H. & Pomeroy, G. Intraosseous bioabsorbable poly-L-lactic acid screw presenting as a late foreign-body reaction: a case report. *Foot & ankle international* **22**, 247-251 (2001).

8 Athanasiou, K. A., Agrawal, C. M., Barber, F. A. & Burkhart, S. S. Orthopaedic applications for PLA-PGA biodegradable polymers. *Arthroscopy* **14**, 726-737, doi:10.1016/s0749-8063(98)70099-4 (1998).

9 Waris, E. *et al.* Long-term bone tissue reaction to polyethylene oxide/polybutylene terephthalate copolymer (Polyactive®) in metacarpophalangeal joint reconstruction. *Biomaterials* **29**, 2509-2515 (2008).

10 Agrawal, C. M. & Athanasiou, K. A. Technique to control pH in vicinity of biodegrading PLA-PGA implants. *J Biomed Mater Res* **38**, 105-114, doi:10.1002/(sici)1097-4636(199722)38:2<105::aid-jbm4>3.0.co;2-u (1997).

11 Taylor, M. S., Daniels, A. U., Andriano, K. P. & Heller, J. Six bioabsorbable polymers: in vitro acute toxicity of accumulated degradation products. *J Appl Biomater* **5**, 151-157, doi:10.1002/jab.770050208 (1994).

12 Deng, M. *et al.* Dipeptide-based Polyphosphazene and Polyester Blends for Bone Tissue Engineering. *Biomaterials* **31**, 4898-4908, doi:10.1016/j.biomaterials.2010.02.058 (2010).

13 Pajares-Chamorro, N. *et al.* Silver-doped bioactive glass particles for in vivo bone tissue regeneration and enhanced methicillin-resistant Staphylococcus aureus (MRSA) inhibition. *Materials Science and Engineering: C* **120**, 111693 (2021).

14 Lih, E. *et al.* A Bioinspired Scaffold with Anti-Inflammatory Magnesium Hydroxide and Decellularized Extracellular Matrix for Renal Tissue Regeneration. *ACS Cent Sci* **5**, 458-467, doi:10.1021/acscentsci.8b00812 (2019).

15 Xu, T. O., Kim, H. S., Stahl, T. & Nukavarapu, S. P. Self-neutralizing PLGA/magnesium composites as novel biomaterials for tissue engineering. *Biomed Mater* **13**, 035013, doi:10.1088/1748-605X/aaaa29 (2018).

16 Kamata, M., Sakamoto, Y. & Kishi, K. Foreign-body reaction to bioabsorbable plate and screw in craniofacial surgery. *Journal of Craniofacial Surgery* **30**, e34-e36 (2019).

17 Narayanan, G., Vernekar, V. N., Kuyinu, E. L. & Laurencin, C. T. Poly (lactic acid)-based biomaterials for orthopaedic regenerative engineering. *Advanced drug delivery reviews* **107**, 247-276 (2016).

18 Gonzalez-Lomas, G., Cassilly, R. T., Remotti, F. & Levine, W. N. Is the etiology of pretibial cyst formation after absorbable interference screw use related to a foreign body reaction? *Clinical Orthopaedics and Related Research*® **469**, 1082-1088 (2011).

19 Xie, N. *et al.* Glycolytic reprogramming in myofibroblast differentiation and lung fibrosis. *American journal of respiratory and critical care medicine* **192**, 1462-1474 (2015).

20 O'Neill, L. A. & Pearce, E. J. in *J Exp Med* Vol. 213 15-23 (2016).

21 Ignatius, A. A. & Claes, L. E. In vitro biocompatibility of bioresorbable polymers: poly(L, DL-lactide) and poly(L-lactide-co-glycolide). *Biomaterials* **17**, 831-839, doi:10.1016/0142-9612(96)81421-9 (1996).

22 Yang, Y. *et al.* In vitro degradation of porous poly (l-lactide-co-glycolide)/β-tricalcium phosphate (PLGA/β-TCP) scaffolds under dynamic and static conditions. *Polymer Degradation and Stability* **93**, 1838-1845 (2008).

23 Bostman, O. M. & Pihlajamaki, H. K. Adverse tissue reactions to bioabsorbable fixation devices. *Clin Orthop Relat Res*, 216-227 (2000).

24 Choueka, J. *et al.* Canine bone response to tyrosine-derived polycarbonates and poly(L-lactic acid). *J Biomed Mater Res* **31**, 35-41, doi:10.1002/(sici)1097-4636(199605)31:1<35::aid-jbm5>3.0.co;2-r (1996).

25 Athanasiou, K. A., Niederauer, G. G. & Agrawal, C. M. Sterilization, toxicity, biocompatibility and clinical applications of polylactic acid/polyglycolic acid copolymers. *Biomaterials* **17**, 93-102, doi:10.1016/0142-9612(96)85754-1 (1996).

26 Kanada, M. *et al.* Differential fates of biomolecules delivered to target cells via extracellular vesicles. *Proceedings of the National Academy of Sciences* **112**, E1433-E1442 (2015).

27 Frottin, F. *et al.* The nucleolus functions as a phase-separated protein quality control compartment. *Science* **365**, 342-347 (2019).

28 Feoktistova, M., Geserick, P. & Leverkus, M. Crystal violet assay for determining viability of cultured cells. *Cold Spring Harbor Protocols* **2016**, pdb. prot087379 (2016).

29 Gonçalves, R. & Mosser, D. M. The isolation and characterization of murine macrophages. *Current protocols in immunology* **111**, 14.11. 11-14.11. 16 (2015).

30 Tan, Z. *et al.* in *The Journal of biological chemistry* Vol. 290 46-55 (2015).

31 Ip, W. E., Hoshi, N., Shouval, D. S., Snapper, S. & Medzhitov, R. Anti-inflammatory effect of IL-10 mediated by metabolic reprogramming of macrophages. *Science* **356**, 513-519 (2017).

32 Mills, E. L. *et al.* Succinate Dehydrogenase Supports Metabolic Repurposing of Mitochondria to Drive Inflammatory Macrophages. *Cell* **167**, 457-470.e413, doi:10.1016/j.cell.2016.08.064 (2016).

33 Tannahill, G. *et al.* Succinate is a danger signal that induces IL-1β via HIF-1α. *Nature* **496**, 238-242, doi:10.1038/nature11986 (2013).

34 Clem, B. *et al.* Small-molecule inhibition of 6-phosphofructo-2-kinase activity suppresses glycolytic flux and tumor growth. *Molecular cancer therapeutics* **7**, 110-120 (2008).

35 Kauppinen, R. A., Sihra, T. S. & Nicholls, D. G. Aminooxyacetic acid inhibits the malate-aspartate shuttle in isolated nerve terminals and prevents the mitochondria from utilizing glycolytic substrates. *Biochim Biophys Acta* **930**, 173-178, doi:10.1016/0167-4889(87)90029-2 (1987).

36 Sprague, L. *et al.* Dendritic cells: in vitro culture in two-and three-dimensional collagen systems and expression of collagen receptors in tumors and atherosclerotic microenvironments. *Experimental cell research* **323**, 7-27 (2014).

37 Pariente, J.-L., Kim, B.-S. & Atala, A. In vitro biocompatibility evaluation of naturally derived and synthetic biomaterials using normal human bladder smooth muscle cells. *The Journal of urology* **167**, 1867-1871 (2002).

38 Kozlov, A. M., Lone, A., Betts, D. H. & Cumming, R. C. Lactate preconditioning promotes a HIF-1α-mediated metabolic shift from OXPHOS to glycolysis in normal human diploid fibroblasts. *Scientific reports* **10**, 1-16 (2020).

39 Olive, A. J., Kiritsy, M. & Sassetti, C. (Am Assoc Immnol, 2021).

40 Iliopoulos, D., Hirsch, H. A. & Struhl, K. An epigenetic switch involving NF-κB, Lin28, Let-7 MicroRNA, and IL6 links inflammation to cell transformation. *Cell* **139**, 693-706 (2009).

41 Eming, S. A., Wynn, T. A. & Martin, P. Inflammation and metabolism in tissue repair and regeneration. *Science* **356**, 1026-1030 (2017).

42 Jiang, W. & Xu, J. Immune modulation by mesenchymal stem cells. *Cell proliferation* **53**, e12712 (2020).

43 Pajarinen, J. *et al.* Mesenchymal stem cell-macrophage crosstalk and bone healing. *Biomaterials* **196**, 80-89 (2019).

44 Swartzlander, M. D. *et al.* Immunomodulation by mesenchymal stem cells combats the foreign body response to cell-laden synthetic hydrogels. *Biomaterials* **41**, 79-88 (2015).

45 Manoharan, I., Prasad, P. D., Thangaraju, M. & Manicassamy, S. Lactate-Dependent Regulation of Immune Responses by Dendritic Cells and Macrophages. *Frontiers in Immunology*, 3062 (2021).

46 Zhang, A. *et al.* Lactate-induced M2 polarization of tumor-associated macrophages promotes the invasion of pituitary adenoma by secreting CCL17. *Theranostics* **11**, 3839 (2021).

47 Lin, S. *et al.* Lactate-activated macrophages induced aerobic glycolysis and epithelial-mesenchymal transition in breast cancer by regulation of CCL5-CCR5 axis: a positive metabolic feedback loop. *Oncotarget* **8**, 110426 (2017).

48 Romero-Garcia, S., Moreno-Altamirano, M. M. B., Prado-Garcia, H. & Sánchez-García, F. J. Lactate contribution to the tumor microenvironment: mechanisms, effects on immune cells and therapeutic relevance. *Frontiers in immunology* **7**, 52 (2016).

49 Samuvel, D. J., Sundararaj, K. P., Nareika, A., Lopes-Virella, M. F. & Huang, Y. Lactate boosts TLR4 signaling and NF-κB pathway-mediated gene transcription in macrophages via monocarboxylate transporters and MD-2 up-regulation. *The Journal of Immunology* **182**, 2476-2484 (2009).

50 Yang, K. *et al.* Lactate Suppresses Macrophage Pro-Inflammatory Response to LPS Stimulation by Inhibition of YAP and NF-κB Activation via GPR81-Mediated Signaling. *Frontiers in Immunology* **11**, 2610 (2020).

51 Kanada, M. *et al.* Microvesicle-mediated delivery of minicircle DNA results in effective gene-directed enzyme prodrug cancer therapy. *Molecular cancer therapeutics* **18**, 2331-2342 (2019).

52 Negrin, R. S. & Contag, C. H. In vivo imaging using bioluminescence: a tool for probing graft-versus-host disease. *Nature Reviews Immunology* **6**, 484-490 (2006).

CHAPTER 3: Stereochemistry Determines Immune Cellular Responses to Polylactide Implants

This chapter is a preprint of the following manuscript, currently under review in Acta Biomaterialia:

Stereochemistry Determines Immune Cellular Responses to Polylactide Implants

Chima V. Maduka, Mohammed Alhaj, Evran Ural, Maxwell M. Kuhnert, Oluwatosin M. Habeeb, Kurt D. Hankenson, Stuart B. Goodman, Ramani Narayan, Christopher H. Contag

Abstract

Repeating L- and D-chiral configurations determine polylactide (PLA) stereochemistry which affects its thermal and physicochemical properties, including degradation profiles. Clinically, degradation of PLA implants promotes prolonged inflammation and excessive fibrosis, but the role of PLA stereochemistry is unclear. Additionally, although PLA of varied stereochemistries cause differential immune responses in-vivo, this observation has yet to be effectively modeled in-vitro. A bioenergetic model was applied to study immune cellular responses to PLA containing > 99% L-lactide (PLLA), > 99% D-lactide (PDLA) and a 50/50 melt-blend of PLLA and PDLA (stereocomplex PLA). Stereocomplex PLA breakdown products increased IL-1β, TNF-α and IL-6 protein levels but not MCP-1. Expression of these proinflammatory cytokines is mechanistically driven by increases in glycolysis in primary macrophages. In contrast, PLLA and PDLA degradation products selectively increase MCP-1 protein expression. Whereas both oxidative phosphorylation and glycolysis are increased with PDLA, only oxidative phosphorylation is increased with PLLA. For each biomaterial, glycolytic inhibition reduces proinflammatory cytokines and markedly increases anti-

inflammatory (IL-10) protein levels; differential metabolic changes in fibroblasts were observed. These findings provide mechanistic explanations for the diverse immune responses to PLA of different stereochemistries. Immune cellular metabolism plays a pivotal role in biomaterial biocompatibility for controlling host immune responses.

Keywords: Polylactide, stereochemistry, Immune Cells, Immunometabolism, Biomaterials, Biocompatibility

Introduction

The host immune response to biomaterials and material properties comprise the most important considerations for biodegradable implants to safely perform their intended function[1]. An important material property of polylactide (PLA), a biodegradable biomaterial widely used to make implants, is its stereochemistry as PLA hydrolyzes into D- or L-lactic acid; with meso-lactide being optically inactive. The stereochemistry of PLA determines its mechanical and thermal properties, crystallinity and degradation rate; higher L-lactide content increases mechanical strength, melting point and crystallinity but slows degradation[2]. Consequently, whereas PLA containing > 99% L-lactide (PLLA) takes more than 5 years to completely breakdown after implantation in animals and humans, PLA containing > 99% D-lactide (PDLA) takes only 1.5 years[1]. Furthermore, melt-blending a 50/50 ratio of PLLA and PDLA results in stereocomplex PLA that has higher mechanical strength, melting point and crystallinity, and slower degradation rate than either homopolymer because of its more compact crystal orientation[3]. Hydrolytic degradation of PLLA, PDLA and stereocomplex has been characterized[4]. Degradation products of PLA,

including oligomers and monomers of lactic acid, drive adverse host immune responses such as long-term inflammation and excessive fibrosis which impair PLA medical devices from performing their diagnostic, therapeutic or regenerative functions.

Historically, adverse responses to PLA have been attributed to the accompanying acidity from breakdown products[5]. Recently, an alternative mechanism for immune cell activation to PLA degradation products was proposed using a bioenergetic in-vitro model simulating events in patients[6]. In the study, altered bioenergetic homeostasis and functional metabolic profiles were discovered to underlie adverse immune responses to amorphous and crystalline PLA degradation. However, spanning over decades, adverse responses to PLA have been controversial. While there have been some studies showing only mild proinflammatory responses to PLA degradation products[7-9], other studies have demonstrated that PLA degradation is accompanied by severe adverse immune responses[10-14] which could necessitate intervention in patients[15-17]. Differing PLA stereochemistry which determines its diverse physicochemical and thermal properties could account for these markedly different outcomes following surgical implantation. As a result, breakdown products from PLLA and PDLA which are widely applied materials in patients, and stereocomplex PLA were examined herein to determine the role of PLA stereochemistry in activating macrophages and fibroblasts, key immune cells involved in host immune responses.

Materials and methods

Polylactide (PLA) materials and extraction

Polylactide (PLA) containing > 99% L-lactide (PLLA) and > 99% D-lactide (PDLA) were obtained from NatureWorks LLC as PLA L175 and PLA D120, respectively. To produce stereocomplex PLA, pre-mixtures of 50% PLLA and 50% PDLA were melt-blended in a co-rotating twin-screw extruder type ZSE 27 HP–PH (Leistritz). The screws used possessed a diameter of 27 mm and an L/ D ratio of 40/ 1; screw elements are interchangeable to allow for optimization of varied material specifications. The temperature profile range was 150 to 220 °C. After quenching the filament in a cold-water bath, the product was pelletized and then placed in a tray for drying for 24 h at 45 °C. Prior to using them, polylactide pellets were confirmed to be of similar curved surface area and sterilized by autoclaving at 121 °C for 20 minutes[18]. Extracts were made as previously described[6] using 4g of biomaterial in 25 mL of complete medium (see section 2.5), and the amount of extract used in each experiment is indicated in figure legends; extracts in water were also made for comparison.

pH measurements

pH of extracts was assessed using an Orion Star A111 Benchtop pH Meter (ThermoFisher Scientific) under room temperature conditions (20 °C).

Bioenergetic assessment

ATP levels in live cells were assessed by bioluminescence on the IVIS Spectrum in vivo imaging system (PerkinElmer) after adding 150 μg/mL of D-luciferin (PerkinElmer). For

lysed cells, the standard ATP/ADP kits (Sigma-Aldrich) were used according to manufacturer's instructions.

Microscopy

The DeltaVision imaging system and softWoRx software (GE Healthcare) were used for imaging in z-stack at 40x magnification.

Cells

Both mouse embryonic fibroblast cell line (NIH 3T3; ATCC) and murine primary bone-marrow derived macrophages (BMDMs) were used as previously described in bioenergetic models used in studying polylactide biocompatibility[6]. BMDMs were sourced from C57BL/6J mice (Jackson Laboratories) of 3-4 months[19,20]. In addition, NIH 3T3 cells with a Sleeping Beauty transposon plasmid (pLuBIG) having a bidirectional promoter driving an improved firefly luciferase gene (fLuc) and a fusion gene encoding a Blasticidin-resistance marker (BsdR) linked to eGFP (BGL)[21] were used to assess ATP levels in live cells by making ATP the rate limiting factor as previously described[6]. Thus, monitor morphological and bioenergetic changes in live cells could be concurrently monitored[22,23]. In each well of a 96-well plate, 5,000 fibroblasts or 50,000 macrophages were cultured in complete medium containing DMEM, 10% heat-inactivated Fetal Bovine Serum and 100 U/mL penicillin-streptomycin (all from ThermoFisher Scientific); the amount of extract used in each experiment is indicated in figure legends.

Materials

For pharmacologic inhibition of glycolytic flux, 3-(3-pyridinyl)-1-(4-pyridinyl)-2-propen-1-one (MilliporeSigma), 2-deoxyglucose (MilliporeSigma) and aminooxyacetic acid (Sigma-Aldrich) were used.

Cell viability

As previously described, cell viability was assessed using the crystal violet assay[24].

Functional metabolism

Oxygen consumption rate (OCR), extracellular acidification rate (ECAR) and lactate-linked proton efflux rate (PER) were measured using the Seahorse XFe-96 Extracellular Flux Analyzer (Agilent Technologies) as previously described[6].

Chemokine and cytokine measurements

Levels of proinflammatory and anti-inflammatory cytokines and chemokines were evaluated from BMDM supernatants using using a MILLIPLEX MAP mouse magnetic bead multiplex kit (MilliporeSigma)[25] to assess for IL-6, MCP-1, TNF-α, IL-1β, IL-4, IL-10, IFN-λ and 1L-13 protein expression in supernatants. Using the glycolytic inhibitor, 3PO, expectedly decreased cytokine values to < 3.2 pg/ mL in some experiments. For statistical analyses, those values were expressed as 3.1 pg/ mL. Additionally, IL-6 ELISA kits (RayBiotech) for supernatants were used according to manufacturer's instructions.

Optical rotation

Polarimetry was used to characterize the L-content and optical purity of the PLA samples with a P-2000 polarimeter (Jasco). The optical rotation, $[\alpha]_{25}$, was measured and averaged for three samples of each polymer in chloroform (Omnisolv), at a concentration of 1 g/100 mL. Conditions were set at 25 °C and 589 nm wavelength. Sucrose was used as a standard reference material, and its specific optical rotation was approximately 67°.

Gel permeation chromatography

Gel permeation chromatography (GPC) was conducted to characterize the polymer molecular weights using a 600 controller (Waters) equipped with Optilab T-rEX refractive index (RI) and TREOS II multi-angle light scattering (MALS) detectors (Wyatt Technology Corporation), and a PLgel 5µm MIXED-C column (Agilent Technologies) with chloroform eluent (1 mL/min). Polystyrene standards (Alfa Aesar) with M_n ranging from 35,000 to 900,000 Da were used for calibration. Dissolving stereocomplex PLA in chloroform/1,1,1,3,3,3-hexafluoro-2-propanol [90/10(v/v)] has been described for obtaining its molecular weight[26]. However, this did not dissolve our stereocomplex PLA even after heating below boiling temperatures of chloroform, likely from the high crystallinity thickness of stereocomplex PLA[26]. As such, we refer to the molecular weights of the PLLA and PDLA used in producing stereocomplex PLA.

Differential scanning calorimetry

Differential scanning calorimetry (DSC) was conducted with a DSC Q20 (TA Instruments) to analyse the melting temperature (T_m), glass transition temperature (T_g), and percent

crystallinity of the PLA grades. For PLLA and PDLA, the temperature was first equilibrated to 0 °C, then ramped up to 200 °C at a heating rate of 10 °C/ min; temperature was then held isothermally for 5 minutes. Afterwards, the sample was cooled back to 0 °C at a rate of 10 °C/min, then held isothermally for 2 minutes. Finally, the material was heated back to 200 °C at 10 °C/ min. However, for stereocomplex PLA, after equilibrating to 0 °C, the temperature was ramped up to 260 °C at a heating rate of 10 °C/ min. A second heating scan was not run because, above its melting temperature (~240 °C), stereocomplex PLA thermally dissociates into its constituent homopolymers.

Attenuated total reflectance – Fourier transform infrared (ATR–FTIR) spectroscopy

PLA stereocomplexation was confirmed using an IRAffinity-1 spectrophotometer (Shimadzu) where the changes in the conformation of PLA chains could be observed using ATR-FTIR spectroscopy as previously described[27].

Statistics and reproducibility

Data were presented as mean with standard deviation (SD). For data analysis, statistical software (GraphPad Prism) was used with significance level set at $p < 0.05$. Specific details of statistical tests and sample sizes are provided in figure legends.

Results

We validated the physicochemical and thermal properties of polylactide (PLA) containing > 99% L-lactide (PLLA), > 99% D-lactide (PDLA) and stereocomplex PLA (melt-blend of 50/50 PLLA and PDLA) prior to using them (Table S4). Stereocomplexation was

confirmed by both differential scanning calorimetry (DSC) thermograms and attenuated total reflectance–Fourier transform infrared (ATR–FTIR) spectroscopy. DSC thermograms revealed a melting peak of 240 °C (Fig. S7A). With ATR-FTIR spectroscopy, the α helix (wavenumber 921 cm^{-1}) which is characteristic of PLLA and PDLA is transformed into a more compact β helix (wavenumber 908 cm-1) in stereocomplex PLA (Fig. S7B, C)[27]. Using a bioenergetic model we had developed and optimized[6], we degraded polylactide (PLA) to obtain breakdown products over 12-days, also referred to as extracts in complete (serum containing) medium. There were no changes in pH over the 12-day extraction period for serum-containing control (no polylactide) medium (pH = 8.0), PLLA (pH = 8.0), PDLA (pH = 8.1) and stereocomplex PLA (pH = 8.1) extracts used on cells; In contrast, extraction in water resulted in changes between control (no polylactide; pH = 8.2), PLLA (pH = 7.5), PDLA (pH = 7.7) and stereocomplex PLA (pH = 7.3) extracts.

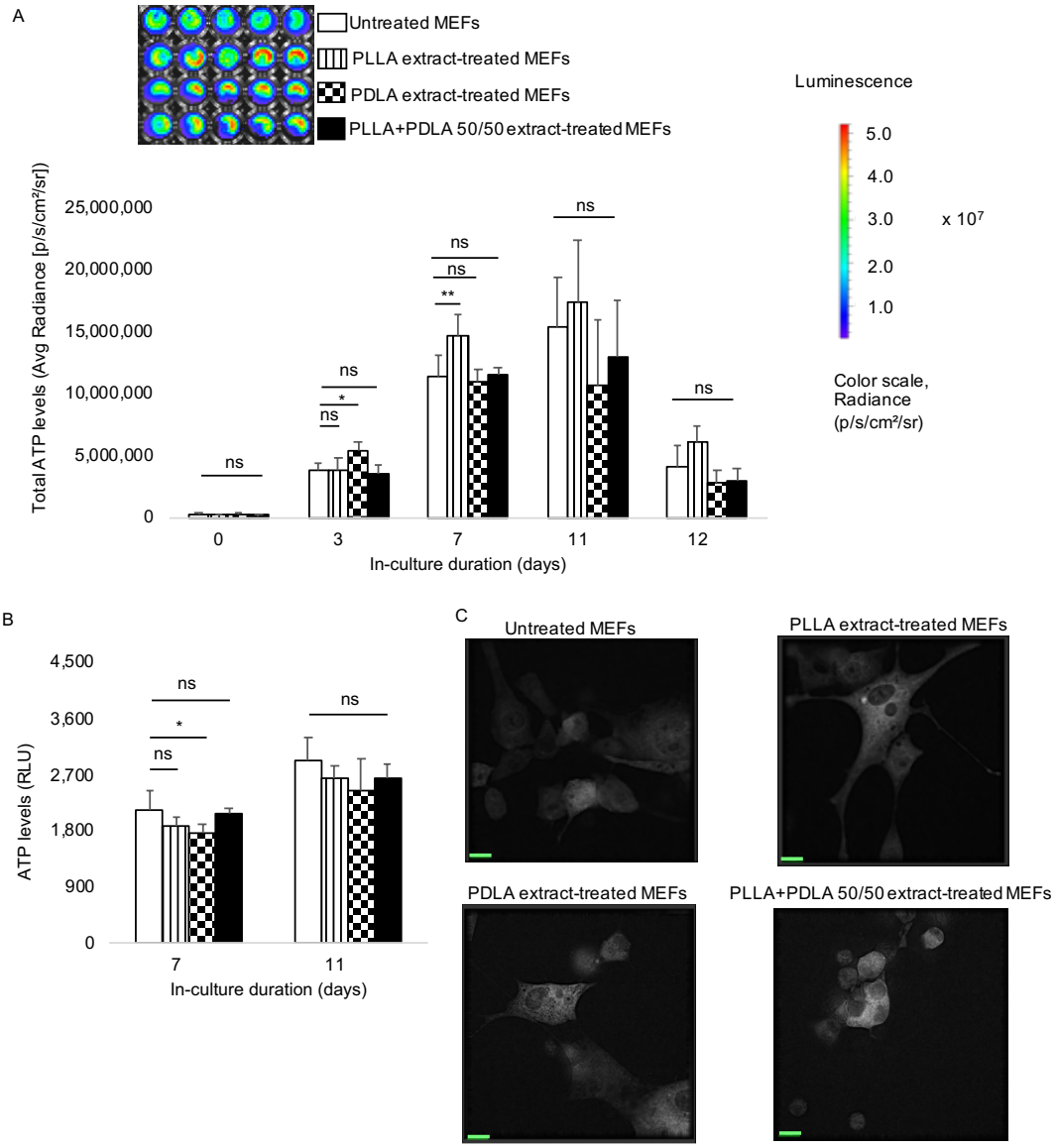

Figure 7. Bioenergetics in fibroblasts. A) Bioenergetic (ATP) levels in mouse embryonic fibroblasts (MEFs) are mostly unaltered after exposure to breakdown products (extracts) of polylactide containing >99% L-isomer (PLLA), >99% D-isomer (PDLA) or a 50/50 melt-blend of PLLA and PDLA (stereocomplex PLA) over time in live cells. Representative images for day 7 are shown. B) In lysed cells, ATP levels are mostly unchanged following exposure to PLLA, PDLA and stereocomplex PLA extracts. C) There were no apparent microscopic changes in MEFs exposed to PLLA or PDLA; cells exposed to stereocomplex PLA extract appeared more rounded in comparison to untreated cells on day 7 (scale bar, 15 µm). Not significant (ns), *p<0.05, **p<0.01, mean (SD), n=3-5, one-way ANOVA followed by Tukey's post-hoc test; 150 µl of control or extract was used.

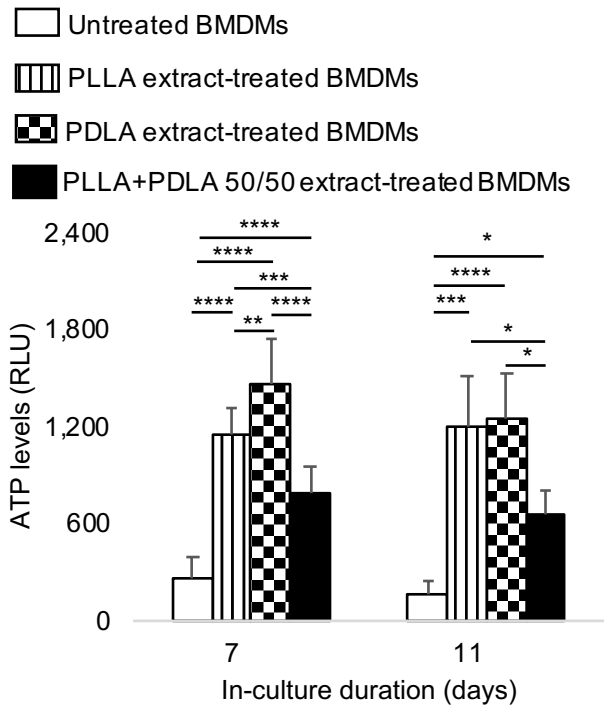

Figure 8. Bioenergetics in macrophages. In primary bone marrow-derived macrophages (BMDMs), bioenergetics is altered after prolonged exposure to breakdown products (extracts) of polylactide containing >99% L-isomer (PLLA), >99% D-isomer (PDLA) or a 50/50 melt-blend of PLLA and PDLA (stereocomplex PLA) over time. *p<0.05, **p<0.01, ***p<0.001, ****p<0.0001, mean (SD), n=4-10, one-way ANOVA followed by Tukey's post-hoc test; 150 µl of control or extract was used.

Table S4. Physical, chemical and thermal properties of polylactides studied.

Criteria	PLA L175 (PLLA)	PLA D120 (PDLA)	Stereocomplex PLA (50% PLLA + 50% PDLA)
Optical purity (%)	99.87	99.55	Not applicable
L-content (%)	99.74	Not applicable	50
D-content (%)	Not applicable	99.87	50
Glass transition temperature T_g (^oC)	63.12	62.19	64.24
Melting temperature T_m (^oC)	175.12	177.53	240.13
Crystallinity (First heating scan, %)	47.49	51.38	55.03
Crystallinity (Second heating scan, %)	6.14	36.02	Not applicable
Number average molecular weights M_n (Da)	102,697	91,760	Not applicable
Weight average molecular weights M_w (Da)	171,675	150,515	Not applicable
Polydispersity index	1.672	1.640	Not applicable

First heating scan was used to determine T_m and T_g for stereocomplex PLA.
Second heating scan was used to determine T_m and T_g for PLLA and PDLA.
Molecular weights were based on a calibration curve of polystyrene standards.

After exposure to extracts of PLA containing > 99% L-lactide (PLLA), > 99% D-lactide (PDLA) or stereocomplex PLA (melt-blend of 50/50 PLLA and PDLA), there were no alterations in ATP levels over time in live (Fig. 7A) or lysed (Fig. 7B) fibroblasts in comparison to untreated cells, despite tendencies for changes on days 3 and 7. In addition, there were no changes in microscopic appearance of fibroblasts exposed to PLLA or PDLA extracts compared to untreated cells (Fig. 7C). However, fibroblasts exposed to stereocomplex PLA extract tended to be more rounded than stellar in appearance (Fig. 7C). In contrast to fibroblasts, primary bone marrow-derived macrophages exposed to PLLA, PDLA or stereocomplex PLA extracts expressed higher ATP levels than untreated cells on days 7 and 11 (Fig. 8). Evaluation of dose-bioenergetic response by adding different volumes of polylactide extracts revealed changes in ATP levels for all doses (Fig. S8), and this guided our subsequent studies.

Next, we sought to find out whether bioenergetic changes were affected by cell numbers. Using the crystal violet assay[24], we observed that numbers of fibroblasts were similar after exposure to PLLA, PDLA or stereocomplex PLA extract in comparison to untreated cells over time (Fig. S9). Observed changes in numbers of macrophages (Fig. S10) were not a confounder after normalizing ATP levels in macrophages (Fig. S11). Bioenergetic alterations from amorphous and crystalline polylactide degradation could be the result of changes in oxidative phosphorylation and glycolytic flux in immune cells[6]. To determine whether PLLA, PDLA or stereocomplex PLA degradation alters functional metabolism, we used the Seahorse assay to measure oxygen consumption rate (OCR; a measure of oxidative phosphorylation), extracellular acidification rate (ECAR; a measure of glycolytic flux) and proton efflux rate (PER; a measure of monocarboxylate transporter function, where

monocarboxylate transporters are responsible for the bidirectional movement of proton linked lactate across cell membranes)[28-30]. Compared to untreated macrophages, extracts of PLLA and PDLA increased OCR (Fig. 9A, B). However, similar amounts of stereocomplex PLA extract did not affect OCR (Fig. 9C). Whereas exposure of macrophages to PLLA extract did not affect ECAR (Fig. 9D), extracts of PDLA and stereocomplex PLA increased ECAR (Fig. 9E, F). Similarly, PER was unchanged after exposure to PLLA extract (Fig. 9G) but exposure to PDLA and stereocomplex PLA extracts increased PER (Fig. 9H, I), suggesting a trend for both PDLA and stereocomplex PLA which each contain ≥ 50% D-lactide. For the volume of extract used in Seahorse assays, cell numbers were similar between untreated macrophages and macrophages exposed to PLLA, PDLA or stereocomplex PLA extract (Fig. S12A-C).

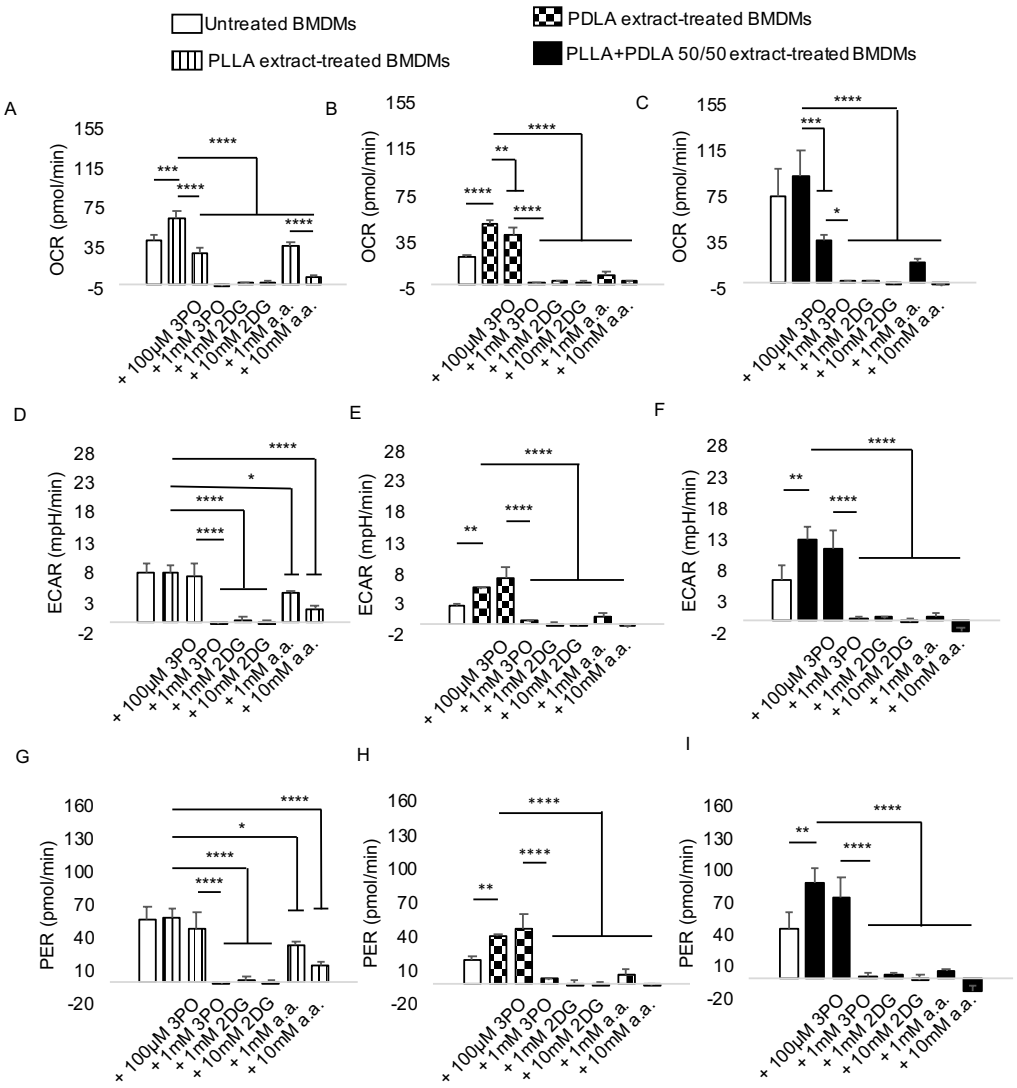

Figure 9. Functional metabolism in macrophages. A-C) In comparison to untreated cells, oxygen consumption rate (OCR) is increased in primary bone marrow-derived macrophages (BMDMs) exposed to breakdown products (extracts) of polylactide containing >99% L-isomer (PLLA) or >99% D-isomer (PDLA) but not a 50/50 melt-blend of PLLA and PDLA (stereocomplex PLA). In cells exposed to polylactide extracts, OCR is dose-dependently controlled by addition of glycolytic inhibitors. D-I) Extracellular acidification rate (ECAR; D-F) and proton efflux rate (PER; G-I) are increased in BMDMs treated with PDLA or stereocomplex PLA but not PLLA extracts. Both ECAR and PER are controlled by addition of glycolytic inhibitors in a dose-dependent manner. *p<0.05, **p<0.01, ***p<0.001, ****p<0.0001, mean (SD), n=3, one-way ANOVA followed by Tukey's post-hoc test; 3-(3-pyridinyl)-1-(4-pyridinyl)-2-propen-1-one (3PO), 2-deoxyglucose (2DG) and aminooxyacetic acid (a.a.); 100 µl of control or extract was used for 7 days.

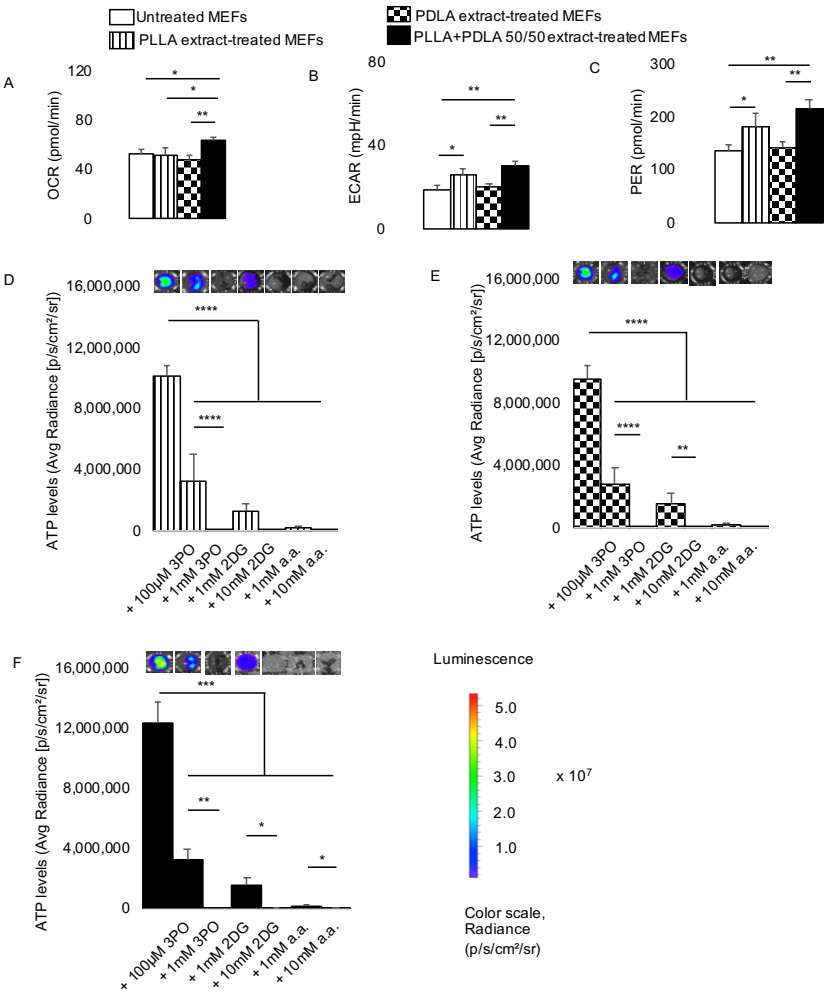

Figure 10. Relating functional metabolism to bioenergetics in fibroblasts. A) Oxygen consumption rate (OCR) is elevated in mouse embryonic fibroblasts (MEFs) exposed to breakdown products (extracts) of stereocomplex PLA compared to untreated, PLLA or PDLA groups. B-C) Extracellular acidification rate (ECAR; B) and proton efflux rate (PER; C) are increased in MEFs exposed to stereocomplex PLA or PLLA extracts in comparison to untreated cells. D-F) Bioenergetics is modulated in MEFs exposed to stereocomplex PLA, PLLA or PDLA extracts in a dose-dependent manner by pharmacologic inhibitors of glycolysis (representative wells are shown). *p<0.05, **p<0.01, ***p<0.001, ****p<0.0001, mean (SD), n=3-5, one-way ANOVA followed by Tukey's post-hoc test or Brown-Forsythe and Welch ANOVA followed by Dunnett multiple comparison test; 3-(3-pyridinyl)-1-(4-pyridinyl)-2-propen-1-one (3PO), 2-deoxyglucose (2DG) and aminooxyacetic acid (a.a.); polylactide containing >99% L-isomer (PLLA), >99% D-isomer (PDLA) and a 50/50 melt-blend of PLLA and PDLA (stereocomplex PLA); 150 µl of control or extract was used for 7 days in Figure 4A-C; 100 µl of control or extract was used for 7 days in in Figure 4D-F.

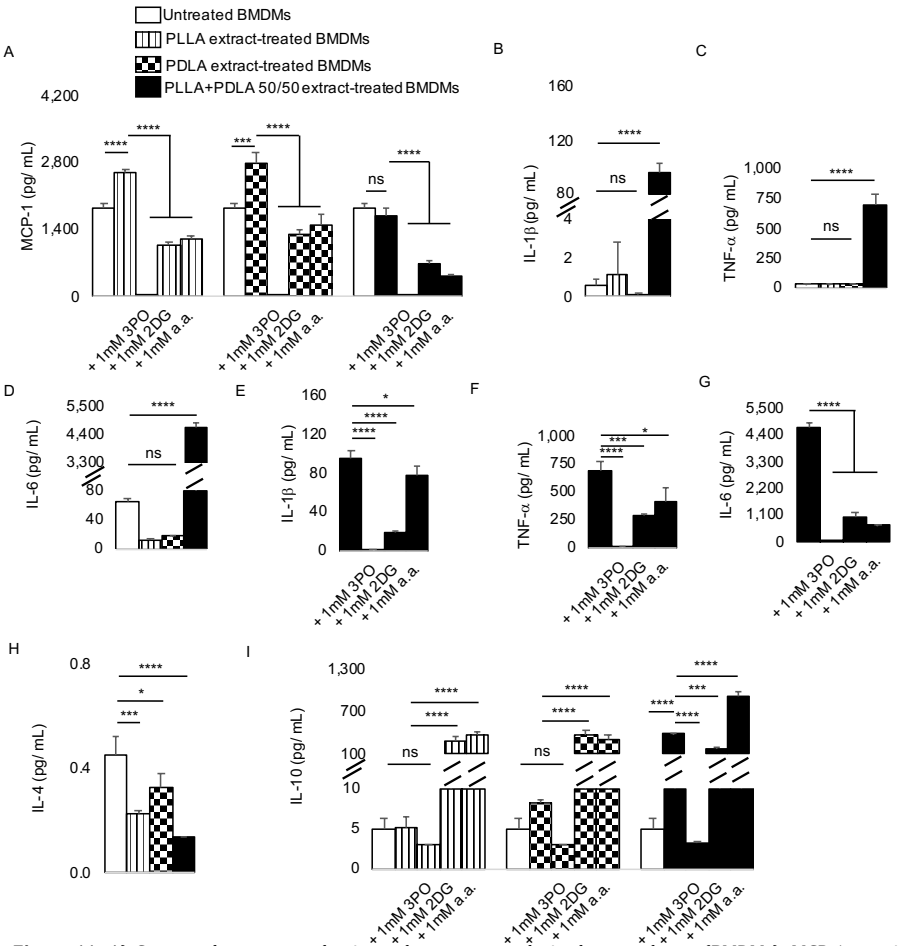

Figure 11. Cytokine and chemokine expression in macrophages. A) Compared to untreated primary bone marrow-derived macrophages (BMDMs), MCP-1 protein expression is increased in cells exposed to breakdown products (extracts) of polylactide containing >99% L-isomer (PLLA) or >99% D-isomer (PDLA) but not a 50/50 melt-blend of PLLA and PDLA (stereocomplex PLA); increased MCP-1 levels are inhibited by different glycolytic inhibitors. B-D) Whereas IL-1β, TNF-α and IL-6 protein levels are similar in BMDMs exposed to PLLA and PDLA, they are elevated in cells exposed to stereocomplex PLA extracts in comparison to untreated cells. E-G) Increased IL-1 β, TNF-α and IL-6 protein expression in BMDMs exposed to stereocomplex PLA extracts is inhibited by different glycolytic inhibitors. H) IL-4 protein expression is decreased in BMDMs exposed to PLLA, PDLA or Stereocomplex PLA compared to untreated cells. I) IL-10 protein expression is unchanged in BMDMs exposed to PLLA or PDLA but not stereocomplex PLA compared to untreated cells; addition of 2-deoxyglucose (2DG) and aminooxyacetic acid (a.a.) but not 3-(3-pyridinyl)-1-(4-pyridinyl)-2-propen-1-one (3PO) increases IL-10 protein expression in comparison to cells exposed to respective polylactide extracts. Not significant (ns), *p<0.05, ***p<0.001, ****p<0.0001, mean (SD), n=3, one-way ANOVA followed by Tukey's post-hoc test; 150 µl of control or extract was used for 7 days.

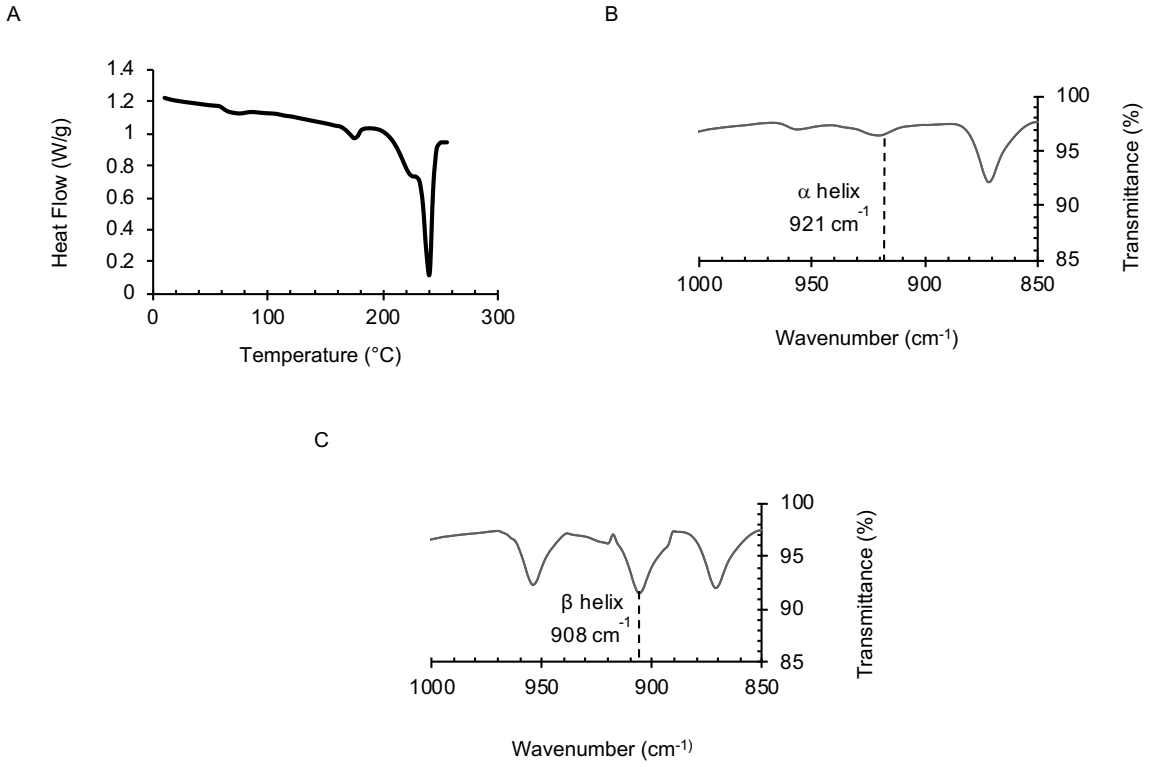

Figure S7. Verifying stereocomplexation of PLA. A) Differential scanning calorimetry (DSC) thermogram for the first heating scan of stereocomplex polylactide (PLA) suggests stereocomplexation occurs. B-C) Attenuated total reflectance–Fourier transform infrared (ATR–FTIR) spectroscopy of PLLA (B) and stereocomplex PLA (C) shows their characteristic helices.

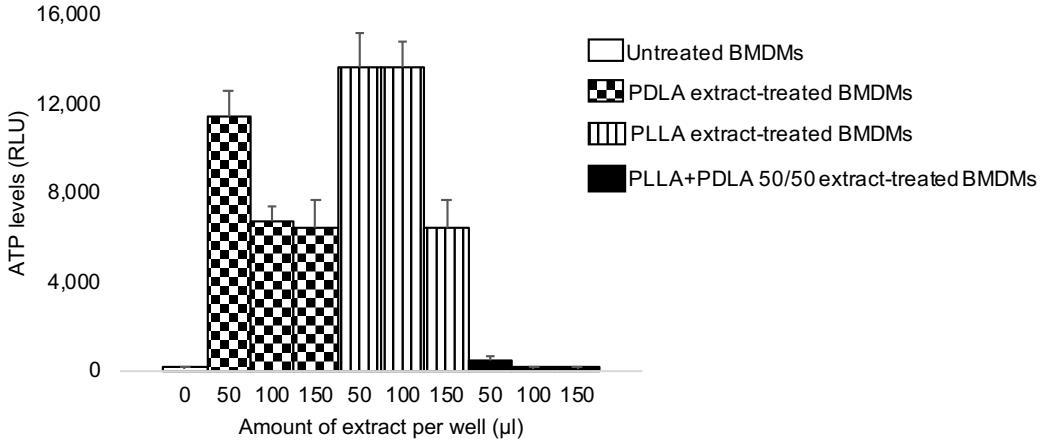

Figure S8. Dose-response to PLA extract. Dose-bioenergetic response of >99% L-isomer (PLLA), >99% D-isomer (PDLA) or a 50/50 melt-blend of PLLA and PDLA (stereocomplex PLA) extracts on primary bone marrow-derived macrophages (BMDMs) reveals an inverse relationship, and tendencies to alter ATP levels for all tested doses. Mean (SD), n = 3, measurements were obtained on day 7.

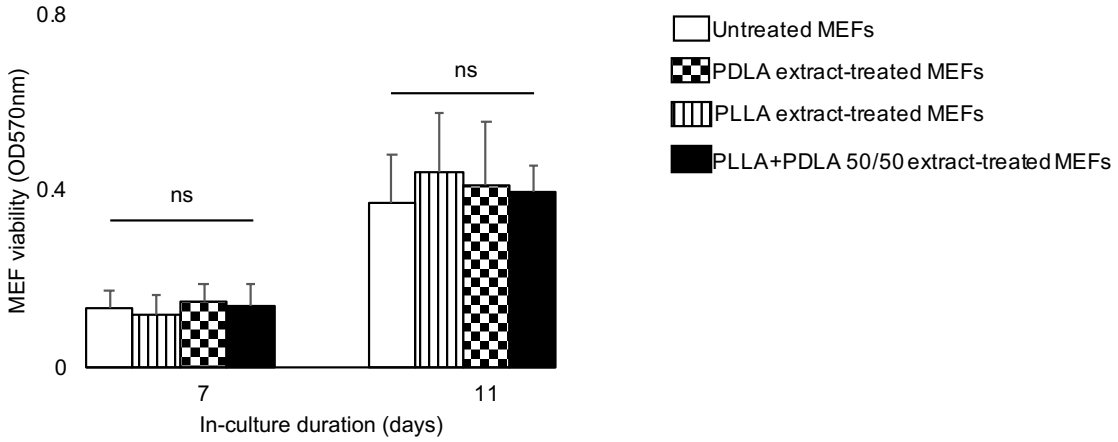

Figure S9. Changes in fibroblast cell number. Cell numbers are similar after exposure of mouse embryonic fibroblasts (MEFs) to >99% L-isomer (PLLA), >99% D-isomer (PDLA) or a 50/50 melt-blend of PLLA and PDLA (stereocomplex PLA) extracts over time. Not significant (ns), mean (SD), n = 5, one-way ANOVA; 150 µl of control or extract was used.

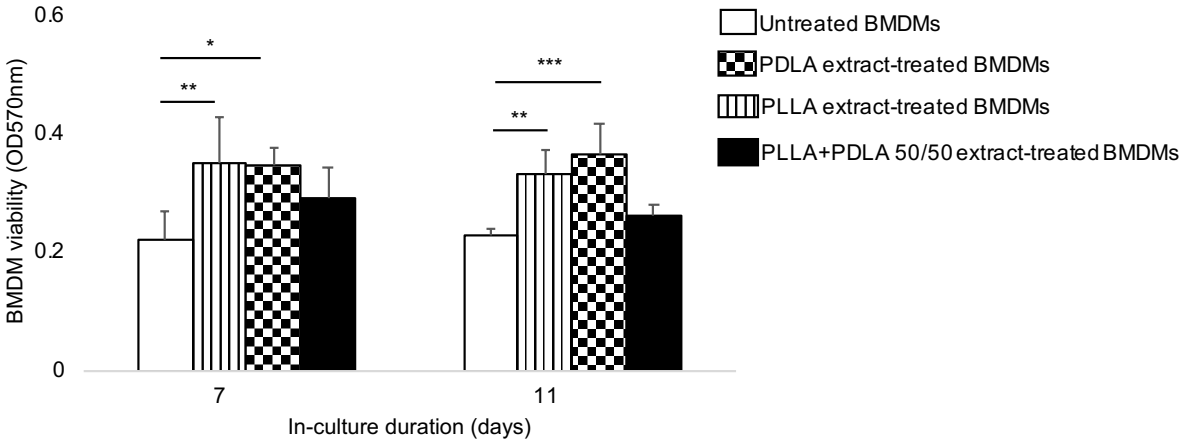

Figure S10. Changes in macrophage cell number. Numbers of primary bone marrow-derived macrophages (BMDMs) are higher after exposure to >99% L-isomer (PLLA) and >99% D-isomer (PDLA) and not a 50/50 melt-blend of PLLA and PDLA (stereocomplex PLA) extracts over time. *p<0.05, **p<0.01, ***p<0.001, mean (SD), n = 5, one-way ANOVA followed by Tukey's post-hoc test; 150 µl of control or extract was used.

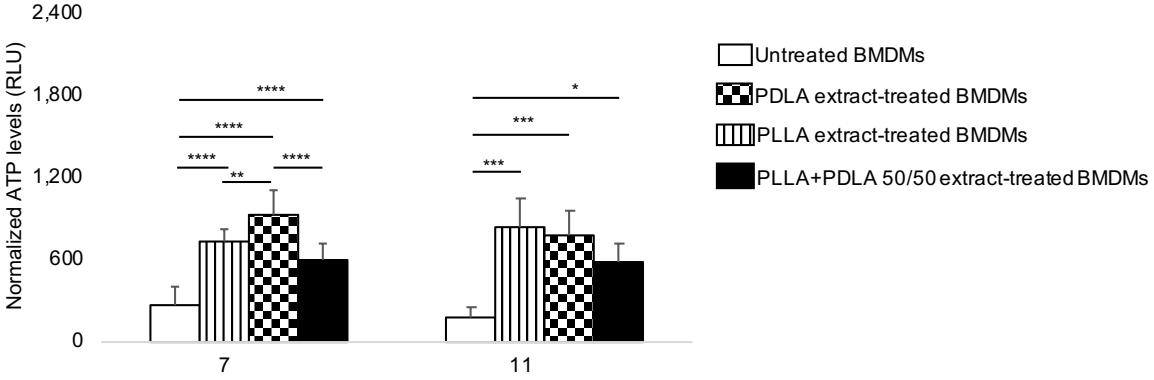

Figure S11. Normalizing macrophage numbers. After normalization to cell numbers, bioenergetics in primary bone marrow-derived macrophages (BMDMs) remains altered after prolonged exposure to extracts of polylactide containing >99% L-isomer (PLLA), >99% D-isomer (PDLA) or a 50/50 melt-blend of PLLA and PDLA (stereocomplex PLA) over time. *p<0.05, **p<0.01, ***p<0.001, ****p<0.0001, mean (SD), n= 4-10, one-way ANOVA followed by Tukey's post-hoc test; 150 µl of control or extract was used; normalization factors were obtained from Figure S3 as 1.6, 1.6 and 1.3 for PLLA, PDLA and stereocomplex PLA, respectively, on day 7; 1.4, 1.6 and 1.4 for PLLA, PDLA and stereocomplex PLA, respectively, on day 11.

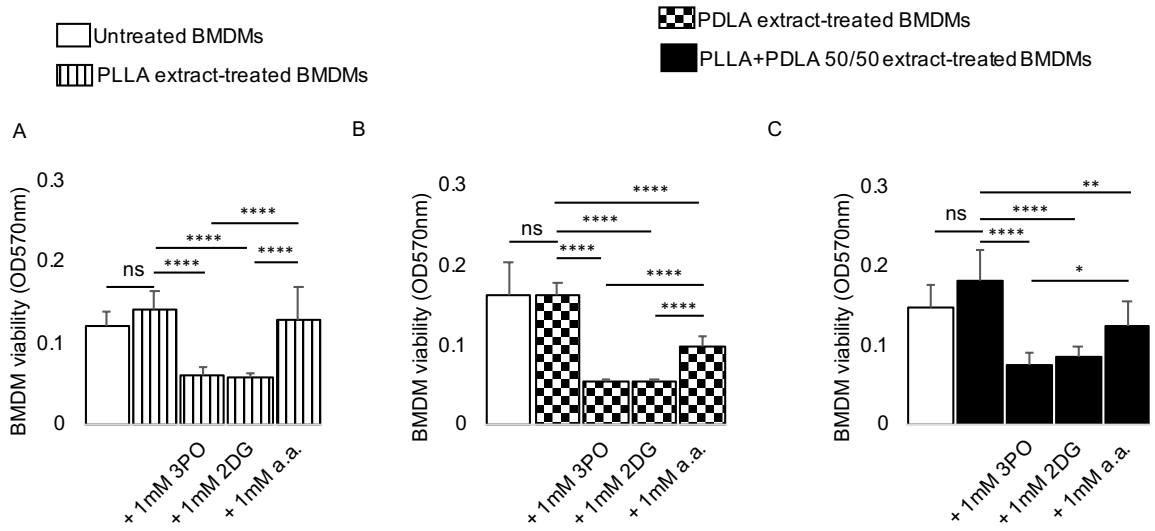

Figure S12. Cytotoxicity of inhibitors. A-C) In comparison to untreated cells, viability of primary bone marrow-derived macrophages (BMDMs) is similar after exposure to polylactide containing >99% L-isomer (PLLA) or >99% D-isomer (PDLA) or a 50/50 melt-blend of PLLA and PDLA (stereocomplex PLA); addition of glycolytic inhibitors reduces cell viability, with aminooxyacetic acid (a.a.) having the least effect. Not significant (ns), *p<0.05, **p<0.01, ****p<0.0001, mean (SD), n = 8, one-way ANOVA followed by Tukey's post-hoc test or Brown-Forsythe and Welch ANOVA followed by Dunnett multiple comparison test; 3-(3-pyridinyl)-1-(4-pyridinyl)-2-propen-1-one (3PO), 2-deoxyglucose (2DG); 100 µl of control or extract was used for 7 days.

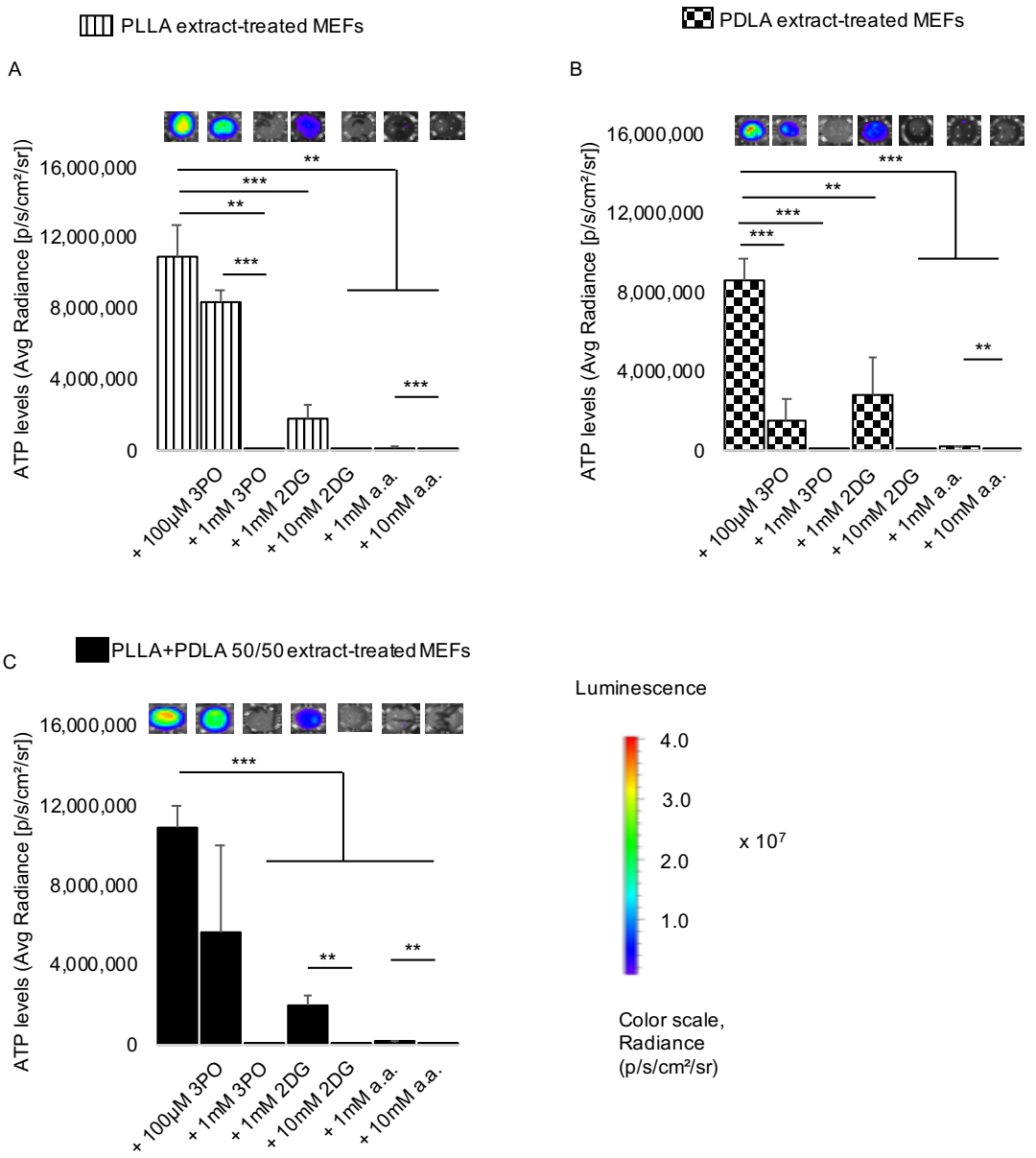

Figure S13. Bioenergetic inhibition in fibroblasts. A-C) Bioenergetics is modulated in mouse embryonic fibroblasts (MEFs) exposed to extracts of polylactide containing >99% L-isomer (PLLA) or >99% D-isomer (PDLA) and a 50/50 melt-blend of PLLA and PDLA (stereocomplex PLA) in a dose-dependent manner by pharmacologic inhibitors of glycolysis (representative wells are shown). **p<0.01, ***p<0.001, ****p<0.0001, mean (SD), n = 5, Brown-Forsythe and Welch ANOVA followed by Dunnett multiple comparison test; 3-(3-pyridinyl)-1-(4-pyridinyl)-2-propen-1-one (3PO), 2-deoxyglucose (2DG) and aminooxyacetic acid (a.a.); 100 µl of control or extract was used for 7 days.

Lactate, the final substrate in glycolysis, is converted to pyruvate which feeds oxidative phosphorylation in the tricarboxylic acid cycle. Reasoning that modulation of glycolysis will also modulate oxidative phosphorylation, different steps in the glycolytic pathway were targeted. Three small molecule inhibitors used were 3-(3-pyridinyl)-1-(4-pyridinyl)-2-propen-1-one (3PO), 2-deoxyglucose (2DG) and aminooxyacetic acid (a.a.) which inhibit 6-phosphofructo-2-kinase/ fructose-2,6-bisphosphatase isozyme 3 (PFKFB3), hexokinase and uptake of glycolytic substrates, respectively[31-33]. Following exposure of macrophages to PLLA, PDLA or stereocomplex PLA extracts, addition of 3PO, 2DG or a.a. resulted in a dose-dependent decrease in OCR, ECAR and PER (Fig. 9A-I). Macrophages with altered metabolic profiles from exposure to PLLA, PDLA or stereocomplex PLA extracts had mildly decreased cell numbers after treatment with pharmacologic inhibitors (Fig. S12A-C).

In fibroblasts, exposure to stereocomplex PLA but not PLLA or PDLA extract increased OCR (Fig. 10A). ECAR and PER increased in fibroblasts exposed to PLLA or stereocomplex PLA extract compared to untreated cells (Fig. 10B, C). In contrast, ECAR and PER were similar in untreated fibroblasts and cells exposed to PDLA extract (Fig. 10B, C). Fibroblasts exposed to PLLA, PDLA, or stereocomplex PLA extracts expressed lower bioenergetic levels after addition of 3PO, 2DG or a.a. in a dose-dependent manner (Fig. 10D-F; Fig. S13A-C).

To determine whether immune activation is the result of altered bioenergetics and metabolic reprogramming, we assayed levels of cytokine and chemokine expression using a magnetic bead-based technique. Both proinflammatory (MCP-1, IL-1β, TNF-α, IL-6 and IFN-γ) and anti-inflammatory (IL-4, IL-13 and IL-10) protein levels were assessed. In comparison to untreated macrophages, PLLA and PDLA but not stereocomplex PLA extract increased

MCP-1 protein levels (Fig. 11A). Targeting glycolytic flux using 3PO, 2DG or a.a. consistently decreased MCP-1 expression (Fig. 11A).

Exposure of macrophages to PLLA or PDLA extracts did not increase IL-1β (Fig. 11B), TNF-α (Fig. 11C), or IL-6 protein levels (Fig. 11D). However, similar amounts of stereocomplex PLA extract increased IL-1β, TNF-α and IL-6 levels by 175.2-, 19.1-, and 70.9-fold respectively (Fig. 11B-D). Independent studies using a different technique (ELISA) revealed similar trends for IL-6 (Fig. S14). The increased levels of IL-1β, TNF-α and IL-6 by stereocomplex PLA were decreased by targeting glycolytic flux using 3PO, 2DG or a.a. (Fig. 11E-G). There were no changes in levels of IL-13 or IFN-γ (data not shown). Macrophages exposed to PLLA, PDLA or stereocomplex PLA extracts decreased IL-4 protein expression (Fig. 11H). Interestingly, neither PLLA nor PDLA extract increased IL-10 levels (Fig. 11I). However, addition of 2DG and a.a. increased IL-10 levels by 55.8- and 71.9-fold, respectively, in macrophages exposed to PLLA extract; by 46.3- and 37-fold, respectively, in macrophages exposed to PDLA extract (Fig. 11I). Stereocomplex PLA extract increased IL-10 levels compared to untreated macrophages (Fig. 11I). Yet, inclusion of a.a. to stereocomplex PLA extract increased IL-10 levels by 2.4-fold in macrophages compared to stereocomplex PLA alone (Fig. 11I).

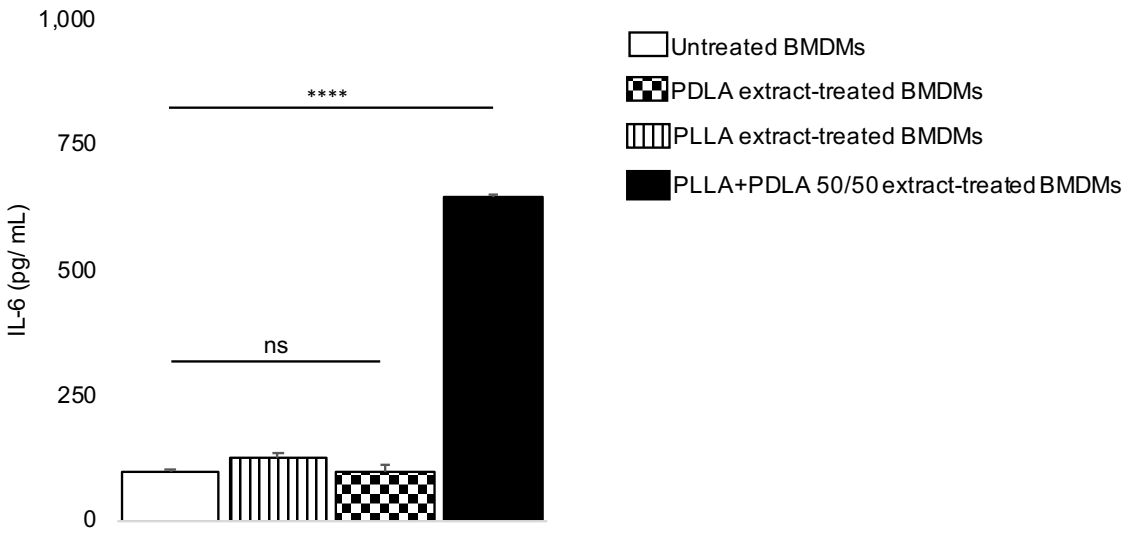

Figure S14. IL-6 expression by ELISA. Using ELISA, IL-6 protein expression is similar in primary bone marrow-derived macrophages (BMDMs) exposed to extracts of polylactide containing >99% L-isomer (PLLA) or >99% D-isomer (PDLA) in comparison to untreated macrophages; but is increased when macrophages are exposed to a 50/50 melt-blend of PLLA and PDLA (stereocomplex PLA) extracts. Not significant (ns), ****$p<0.0001$, mean (SD), n = 3, one-way ANOVA followed by Tukey's post-hoc test; 150 µl of control or extract was used for 7 days.

Discussion

There have been numerous in-vivo studies characterizing the host immune cellular responses to polylactide (PLA)[7-17]. While being highly informative, the complexity of the in-vivo microenvironment where PLA is implanted could preclude a thorough understanding of mechanistic events therein. To deconvolute in-vivo events, several in-vitro studies have been undertaken[34-38] . However, many prior in-vitro models on PLA biocompatibility focused on acidity, based on prior correlation between reduced pH and the adverse immune responses elicited by PLA[5,18]. Instead, this study builds on observed alterations in bioenergetics as well as metabolic reprogramming as drivers of adverse immune responses to amorphous and crystalline PLA[6]. Comparatively, our bioenergetic model more robustly simulates sterile inflammatory protein expression, without the need to include IFN-γ[39] or bacterial endotoxins[40] in polylactide in-vitro studies. Moreover, the use of murine primary macrophages directly isolated from the bone marrow better simulates in-vivo scenarios than monocyte-macrophage cell lines.

Bioenergetics and metabolic reprogramming are emerging mechanisms in the cell biology of immune cellular activation[19,28,31,41,42]. Perhaps the greatest advantage of PLA-based implants is their biodegradability; it is thought that PLA degradation products are "normally" metabolized by the tricarboxylic acid cycle (TCA) to make ATP[43]. However, this had not been previously investigated. We reveal that bioenergetic imbalances occur in primary macrophages following exposure to PLA containing > 99% L-lactide (PLLA), > 99% D-lactide (PDLA) or stereocomplex PLA (melt-blend of 50/50 PLLA and PDLA), all of which are highly crystalline and different than we had previously studied[6]. Furthermore, our observation that PLLA, PDLA and stereocomplex PLA degradation products differentially

reprogram metabolism (glycolytic flux and oxidative phosphorylation) in macrophages offers mechanistic insight into the different host immune responses to PLA of varied stereochemistries and, consequently, mechanical and thermal properties, crystallinity and degradation rates. Increased glycolytic flux, oxidative phosphorylation (OXPHOS) and monocarboxylate transporter (MCT) function are mechanistic drivers of the inflammatory response mediated by macrophages [29,41,44,45].

Elevated glycolytic flux, OXPHOS or MCT function from exposure to PLLA, PDLA or stereocomplex PLA extracts were decreased upon addition of small molecule inhibitors, including 3-(3-pyridinyl)-1-(4-pyridinyl)-2-propen-1-one (3PO), 2-deoxyglucose (2DG) and aminooxyacetic acid (a.a.), which target different steps in glycolysis; these decreases were accompanied by slight reductions in cell numbers. However, cell numbers alone could not fully account for observed reductions in glycolytic flux, OXPHOS or MCT function. In contrast, untreated macrophages exposed to these pharmacologic inhibitors for the same duration neither exhibited decreased functional metabolism nor reduced cell numbers, suggesting selectivity for macrophages having altered metabolism only following exposure to different types of PLA[6]. Of note, one of the small molecule inhibitors, a.a. (pKa: 3.16) is a stronger acid than lactic acid (pKa: 3.78), yet a.a. modulated inflammatory responses to the various PLA types studied, suggesting acidity may not necessarily be the driver of adverse immune responses to polylactide. Similar to macrophages, fibroblasts respond differently to degradation products of PLLA, PDLA or stereocomplex PLA in terms of bioenergetics and functional metabolism. In both macrophages and fibroblasts, there is efficient cellular uptake of 3PO, 2DG or a.a. as candidate pharmacologic agents to modulate metabolic reprogramming and altered bioenergetics.

PLA degradation products are known to drive immune cellular activation [7-17]. Since PLLA and PDLA degrade faster than stereocomplex PLA[4], we expected PLLA and PDLA degradation products to elicit more adverse immune cellular responses. Paradoxically, among proinflammatory cytokines, IL-1β, TNF-α and IL-6 protein levels were unchanged after exposure to PLLA or PDLA degradation products; however, stereocomplex PLA products remarkably increased IL-1β, TNF-α and IL-6 protein levels. Interestingly, studies that have thoroughly characterized extracts of PLLA, PDLA and stereocomplex PLA over durations relevant to this study indicate that uniquely shorter oligomers of lactic acid are produced by stereocomplex PLA hydrolysis compared to its constituent homopolymers (PLLA, PDLA)[4]. Making and characterizing PLA extracts is a standardized process as outlined by the International Standard Organization (ISO 10993-5:2009 - Biological evaluation of medical devices). Over the 12-day extraction for this study, there were no pH changes in serum-containing DMEM medium used. This is likely because DMEM medium is highly buffered with sodium bicarbonate salts for cell culture in CO_2 incubators, and included serum; within CO_2 incubators, the pH of DMEM medium normalizes to 7.4[46,47]. Therefore, because pH was similar across groups in our study, acidity was not a confounder in our model, and could not have accounted for the dramatic immune cellular outcomes that we observed. If our extractions are performed in water, we reproduce decreased pH which is consistent with prior in-vitro models because water lacks buffers, such as serum and bicarbonates which are present in blood. Remarkably, stereocomplex PLA extracts in water were more acidic than either PLLA or PDLA extracts as previously reported[4].

Monomeric lactic acid acts as a potent signaling molecule, transcending its role as simply a metabolite both in inflammation and cancer biology. In cancer biology, lactate plays

as immunomodulatory role[48]. However, combined with bacterial lipopolysaccharide (LPS), lactate could stimulate[45] or dampen[49] the activation of immune cells.

For many types of polylactide, reprocessing (by melt-blending) results in faster degradation[50] which could accentuate immune cellular responses. However, that is not the case with stereocomplex PLA which has been reported to degrade slower than either homopolymer despite (owing to) melt-blending[4,50,51]. Consequently, whereas we expected lower immune cellular activation from stereocomplex PLA since it breaks down in a particularly slow manner, we observed quite the opposite.

Intriguingly, PLLA or PDLA degradation products increased MCP-1 (CCL-2) protein levels whereas stereocomplex PLA did not. MCP-1 recruits macrophages to promote inflammation. MCP-1 is also implicated in cartilage destruction and osteolysis, and is required for foreign body giant cell formation [52-54], events that characterize the host immune responses to PLLA and PDLA in-vivo. These different immune cellular responses to PLA of varied stereochemistries could explain conflicting in-vivo study results showing mild and severe host immune responses to different types of PLA[7-17].

Irrespective of the proinflammatory protein (s) generated by the biomaterials studied, targeting metabolism using 3PO, 2DG or a.a. decreased undesirably high cytokine protein levels. Concomitantly, this strategy markedly increased anti-inflammatory cytokines which are crucial for tissue repair and regeneration through remodeling and recruitment of stem or progenitor cell populations [42]. Next generation biomaterials used in diagnostic, therapeutic and regenerative applications will be designed to allow for modulation of their immune microenvironment [1]. Targeting bioenergetics and altered metabolism in immune cells offers opportunities for modulating immune responses for improved outcome.

Manipulating immune cell activation using biologically-derived, decellularized extracellular matrix is very promising [55,56] but complete removal of cellular components, which elicit rejection and risk disease transmission, remain limiting factors[57]; methods aimed at bioenergetics and altered metabolism overcome these limitations.

This study is not focused on the type of PLA that minimizes adverse immune responses but investigates how adverse immune responses from different types of PLA can be modulated. Different types of PLA may be appropriate for different clinical situations, based on their physicochemical properties. For example, highly crystalline PLA with high mechanical strength could be desirable for implants expected to degrade slowly following surgical implantation; whereas, amorphous PLA with reduced mechanical strength could be applied in scenarios where fast degradation is expected. PLA stereochemistry is a key determinant of several of these physicochemical parameters affecting clinical use. By targeting metabolism, we can modulate immune responses to PLA of varied stereochemistries. This could significantly extend the clinical applications of PLA past PLLA and PDLA to formulations of different stereochemistries with minimal concerns about biocompatibility.

The biocompatibility of PLA degradation products presents with conflicting events, partly because "polylactide (PLA)" refers to a broad class of polymer having vast physicochemical, mechanical and thermal properties which are all affected by its stereochemistry. Our findings provide insight into these discrepancies by demonstrating fundamentally different bioenergetic and metabolic signatures in immune cells exposed to degradation products of PLLA, PDLA and their 50/50 combination as stereocomplex PLA. Consequently, varied macrophage polarization occurs. This drives distinctive cytokine and

chemokine secretion, ultimately determining host immune responses. In addition, we present a unifying mechanism by which different forms of PLA drive adverse host responses and new methods to specifically modulate them. Except for 3PO, using glycolytic inhibitors allow for some proinflammatory cytokines to be produced by macrophages. This is important because an appropriate level of inflammation is crucial for tissue healing and regeneration to occur. Moreover, the multiple strategies we have used to modulate immune cellular responses offer options from which to choose and apply in a patient-specific manner.

Conclusion

While different immune outcomes occur following surgical implantation of various types of PLA[7-17], this observation has not been previously modeled in-vitro. Not only do we provide a convincing in-vitro model, we reveal the biological mechanisms that explain the complex relationships among material stereochemistry, immune responses, bioenergetics and metabolic reprogramming. Our findings underscore PLA stereochemistry as a determinant of immune cellular responses. With stereocomplex PLA, expression of proinflammatory cytokines is mechanistically driven by increased glycolytic flux in macrophages. Whereas both oxidative phosphorylation and glycolysis are increased with PDLA, only oxidative phosphorylation is increased with PLLA. Taken together, we: 1) highlight the intricacies underlying metabolic alterations among different cell populations in the immune microenvironment after exposure to PLA of varied stereochemistries; 2) offer mechanistic insights into why various types of PLA elicit markedly different immune responses in patients; 3) underscore metabolic reprogramming and altered bioenergetics in immune cells as a unifying mechanism for PLA-induced host responses; and 4) demonstrate

immunometabolism as a pivot in biomaterial biocompatibility for controlling host immune responses.

Author contributions

Conceptualization, C.V.M. and C.H.C.; Methodology, C.V.M., K.D.H., S.B.G., R.N. and C.H.C.; Investigation, C.V.M., M.A., E.U., M.O.B. and M.M.K.; Writing – Original Draft, C.V.M.; Writing – Review & Editing, C.V.M., M.A., E.U., M.O.B., M.M.K., K.D.H., S.B.G., R.N. and C.H.C.; Funding Acquisition, C.H.C.; Resources, R.N. and C.H.C.; Supervision, K.D.H., S.B.G., R.N. and C.H.C.

Data availability

All data generated during this study are included in this published article and supplementary information files.

Declaration of competing interest

The authors declare no conflict of interest.

Acknowledgements

AV Makela provided expertise for running cytokine and chemokine assays. Euthanized C57BL/6J mice were a gift from RR Neubig (facilitated by J Leipprandt and E Lisabeth) and the Campus Animal Resources at Michigan State University (MSU). Funding for this work was provided in part by the James and Kathleen Cornelius Endowment at MSU.

REFERENCES

REFERENCES

1 Li, C. *et al.* Design of biodegradable, implantable devices towards clinical translation. *Nature Reviews Materials* **5**, 61-81 (2020).

2 Da Silva, D. *et al.* Biocompatibility, biodegradation and excretion of polylactic acid (PLA) in medical implants and theranostic systems. *Chemical Engineering Journal* **340**, 9-14 (2018).

3 Im, S. H. *et al.* Stereocomplex Polylactide for Drug Delivery and Biomedical Applications: A Review. *Molecules* **26**, 2846 (2021).

4 Andersson, S. R., Hakkarainen, M., Inkinen, S., Södergård, A. & Albertsson, A.-C. Polylactide stereocomplexation leads to higher hydrolytic stability but more acidic hydrolysis product pattern. *Biomacromolecules* **11**, 1067-1073 (2010).

5 Agrawal, C. M. & Athanasiou, K. A. Technique to control pH in vicinity of biodegrading PLA-PGA implants. *J Biomed Mater Res* **38**, 105-114, doi:10.1002/(sici)1097-4636(199722)38:2<105::aid-jbm4>3.0.co;2-u (1997).

6 Maduka, C. V. *et al.* Polylactide degradation activates immune cells by metabolic reprogramming. *Nature Biomedical Engineering* **(under revision)**.

7 Mainil-Varlet, P., Rahn, B. & Gogolewski, S. Long-term in vivo degradation and bone reaction to various polylactides: 1. One-year results. *Biomaterials* **18**, 257-266 (1997).

8 Von Schroeder, H. P., Kwan, M., Amiel, D. & Coutts, R. D. The use of polylactic acid matrix and periosteal grafts for the reconstruction of rabbit knee articular defects. *Journal of biomedical materials research* **25**, 329-339 (1991).

9 Athanasiou, K. A., Agrawal, C. M., Barber, F. A. & Burkhart, S. S. Orthopaedic applications for PLA-PGA biodegradable polymers. *Arthroscopy* **14**, 726-737, doi:10.1016/s0749-8063(98)70099-4 (1998).

10 Apikian, M., Roberts, S. & Goodman, G. Adverse reactions to polylactic acid injections in the periorbital area. *Journal of cosmetic dermatology* **6**, 95-101 (2007).

11 Chalidis, B., Kitridis, D., Savvidis, P., Papalois, A. & Givissis, P. Does the Inion OTPStm absorbable plating system induce higher foreign-body reaction than titanium implants? An experimental randomized comparative study in rabbits. *Biomedical Materials* **15**, 065011 (2020).

12 Xue, A. S. *et al.* Local foreign-body reaction to commercial biodegradable implants: an in vivo animal study. *Craniomaxillofacial trauma & reconstruction* **7**, 27-33 (2014).

13 Wittwer, G. *et al.* Complications after zygoma fracture fixation: is there a difference between biodegradable materials and how do they compare with titanium osteosynthesis? *Oral Surgery, Oral Medicine, Oral Pathology, Oral Radiology, and Endodontology* **101**, 419-425 (2006).

14 Givissis, P. K., Stavridis, S. I., Papagelopoulos, P. J., Antonarakos, P. D. & Christodoulou, A. G. Delayed foreign-body reaction to absorbable implants in metacarpal fracture treatment. *Clinical Orthopaedics and Related Research*® **468**, 3377-3383 (2010).

15 Mosier-LaClair, S., Pike, H. & Pomeroy, G. Intraosseous bioabsorbable poly-L-lactic acid screw presenting as a late foreign-body reaction: a case report. *Foot & ankle international* **22**, 247-251 (2001).

16 Gonzalez-Lomas, G., Cassilly, R. T., Remotti, F. & Levine, W. N. Is the etiology of pretibial cyst formation after absorbable interference screw use related to a foreign body reaction? *Clinical Orthopaedics and Related Research*® **469**, 1082-1088 (2011).

17 Kamata, M., Sakamoto, Y. & Kishi, K. Foreign-body reaction to bioabsorbable plate and screw in craniofacial surgery. *Journal of Craniofacial Surgery* **30**, e34-e36 (2019).

18 Athanasiou, K. A., Niederauer, G. G. & Agrawal, C. M. Sterilization, toxicity, biocompatibility and clinical applications of polylactic acid/polyglycolic acid copolymers. *Biomaterials* **17**, 93-102, doi:10.1016/0142-9612(96)85754-1 (1996).

19 Mills, E. L. *et al.* Succinate Dehydrogenase Supports Metabolic Repurposing of Mitochondria to Drive Inflammatory Macrophages. *Cell* **167**, 457-470.e413, doi:10.1016/j.cell.2016.08.064 (2016).

20 Gonçalves, R. & Mosser, D. M. The isolation and characterization of murine macrophages. *Current protocols in immunology* **111**, 14.11. 11-14.11. 16 (2015).

21 Kanada, M. *et al.* Differential fates of biomolecules delivered to target cells via extracellular vesicles. *Proceedings of the National Academy of Sciences* **112**, E1433-E1442 (2015).

22 Kanada, M. *et al.* Microvesicle-mediated delivery of minicircle DNA results in effective gene-directed enzyme prodrug cancer therapy. *Molecular cancer therapeutics* **18**, 2331-2342 (2019).

23 Negrin, R. S. & Contag, C. H. In vivo imaging using bioluminescence: a tool for probing graft-versus-host disease. *Nature Reviews Immunology* **6**, 484-490 (2006).

24 Feoktistova, M., Geserick, P. & Leverkus, M. Crystal violet assay for determining viability of cultured cells. *Cold Spring Harbor Protocols* **2016**, pdb. prot087379 (2016).

25 Sprague, L. *et al.* Dendritic cells: in vitro culture in two-and three-dimensional collagen systems and expression of collagen receptors in tumors and atherosclerotic microenvironments. *Experimental cell research* **323**, 7-27 (2014).

26 Tsuji, H. Poly (lactide) stereocomplexes: formation, structure, properties, degradation, and applications. *Macromolecular bioscience* **5**, 569-597 (2005).

27 Jeong, J., Ayyoob, M., Kim, J.-H., Nam, S. W. & Kim, Y. J. In situ formation of PLA-grafted alkoxysilanes for toughening a biodegradable PLA stereocomplex thin film. *RSC advances* **9**, 21748-21759 (2019).

28 Ip, W. E., Hoshi, N., Shouval, D. S., Snapper, S. & Medzhitov, R. Anti-inflammatory effect of IL-10 mediated by metabolic reprogramming of macrophages. *Science* **356**, 513-519 (2017).

29 Tan, Z. *et al.* in *The Journal of biological chemistry* Vol. 290 46-55 (2015).

30 Payen, V. L., Mina, E., Van Hee, V. F., Porporato, P. E. & Sonveaux, P. Monocarboxylate transporters in cancer. *Mol Metab* **33**, 48-66, doi:10.1016/j.molmet.2019.07.006 (2020).

31 Tannahill, G. *et al.* Succinate is a danger signal that induces IL-1β via HIF-1α. *Nature* **496**, 238-242, doi:10.1038/nature11986 (2013).

32 Clem, B. *et al.* Small-molecule inhibition of 6-phosphofructo-2-kinase activity suppresses glycolytic flux and tumor growth. *Molecular cancer therapeutics* **7**, 110-120 (2008).

33 Kauppinen, R. A., Sihra, T. S. & Nicholls, D. G. Aminooxyacetic acid inhibits the malate-aspartate shuttle in isolated nerve terminals and prevents the mitochondria from utilizing glycolytic substrates. *Biochim Biophys Acta* **930**, 173-178, doi:10.1016/0167-4889(87)90029-2 (1987).

34 Pariente, J.-L., Kim, B.-S. & Atala, A. In vitro biocompatibility evaluation of naturally derived and synthetic biomaterials using normal human bladder smooth muscle cells. *The Journal of urology* **167**, 1867-1871 (2002).

35 Granados-Hernández, M. V. *et al.* In vitro and in vivo biological characterization of poly (lactic acid) fiber scaffolds synthesized by air jet spinning. *Journal of Biomedical Materials Research Part B: Applied Biomaterials* **106**, 2435-2446 (2018).

36 Taylor, M. S., Daniels, A. U., Andriano, K. P. & Heller, J. Six bioabsorbable polymers: in vitro acute toxicity of accumulated degradation products. *J Appl Biomater* **5**, 151-157, doi:10.1002/jab.770050208 (1994).

37 Ignatius, A. A. & Claes, L. E. In vitro biocompatibility of bioresorbable polymers: poly(L, DL-lactide) and poly(L-lactide-co-glycolide). *Biomaterials* **17**, 831-839, doi:10.1016/0142-9612(96)81421-9 (1996).

38 Woo, K. M., Seo, J., Zhang, R. & Ma, P. X. Suppression of apoptosis by enhanced protein adsorption on polymer/hydroxyapatite composite scaffolds. *Biomaterials* **28**, 2622-2630 (2007).

39 Wang, Q. S. *et al.* Reduction of the pro-inflammatory response by tetrandrine-loading poly (l-lactic acid) films in vitro and in vivo. *Journal of Biomedical Materials Research Part A* **102**, 4098-4107 (2014).

40 Correia, C. R., Gaifem, J., Oliveira, M. B., Silvestre, R. & Mano, J. F. The influence of surface modified poly (l-lactic acid) films on the differentiation of human monocytes into macrophages. *Biomaterials science* **5**, 551-560 (2017).

41 Olive, A. J., Kiritsy, M. & Sassetti, C. (Am Assoc Immnol, 2021).

42 Eming, S. A., Wynn, T. A. & Martin, P. Inflammation and metabolism in tissue repair and regeneration. *Science* **356**, 1026-1030 (2017).

43 Hollinger, J. O. & Battistone, G. C. Biodegradable bone repair materials: synthetic polymers and ceramics. (1985).

44 Kornberg, M. D. *et al.* Dimethyl fumarate targets GAPDH and aerobic glycolysis to modulate immunity. *Science* **360**, 449-453 (2018).

45 Samuvel, D. J., Sundararaj, K. P., Nareika, A., Lopes-Virella, M. F. & Huang, Y. Lactate boosts TLR4 signaling and NF-κB pathway-mediated gene transcription in macrophages via monocarboxylate transporters and MD-2 up-regulation. *The Journal of Immunology* **182**, 2476-2484 (2009).

46 Dezfuli, S. N. *et al.* Influence of HEPES buffer on the local pH and formation of surface layer during in vitro degradation tests of magnesium in DMEM. *Progress in Natural Science: Materials International* **24**, 531-538 (2014).

47 Lin, A. & Agrawal, P. Glutamine decomposition in DMEM: effect of pH and serum concentration. *Biotechnology letters* **10**, 695-698 (1988).

48 Zhou, H.-c. *et al.* Lactic acid in macrophage polarization: The significant role in inflammation and cancer. *International Reviews of Immunology*, 1-15 (2021).

49 Yang, K. *et al.* Lactate Suppresses Macrophage Pro-Inflammatory Response to LPS Stimulation by Inhibition of YAP and NF-κB Activation via GPR81-Mediated Signaling. *Frontiers in Immunology* **11**, 2610 (2020).

50 Agüero, A. *et al.* Study of the influence of the reprocessing cycles on the final properties of polylactide pieces obtained by injection molding. *Polymers* **11**, 1908 (2019).

51 Karst, D. & Yang, Y. Molecular modeling study of the resistance of PLA to hydrolysis based on the blending of PLLA and PDLA. *Polymer* **47**, 4845-4850 (2006).

52 Raghu, H. *et al.* CCL2/CCR2, but not CCL5/CCR5, mediates monocyte recruitment, inflammation and cartilage destruction in osteoarthritis. *Annals of the rheumatic diseases* **76**, 914-922 (2017).

53 Kyriakides, T. R. *et al.* The CC chemokine ligand, CCL2/MCP1, participates in macrophage fusion and foreign body giant cell formation. *The American journal of pathology* **165**, 2157-2166 (2004).

54 Loi, F. *et al.* Inflammation, fracture and bone repair. *Bone* **86**, 119-130 (2016).

55 Sadtler, K. *et al.* Developing a pro-regenerative biomaterial scaffold microenvironment requires T helper 2 cells. *Science* **352**, 366-370 (2016).

56 Hussey, G. S., Dziki, J. L. & Badylak, S. F. Extracellular matrix-based materials for regenerative medicine. *Nature Reviews Materials* **3**, 159-173 (2018).

57 Christman, K. L. Biomaterials for tissue repair. *Science* **363**, 340-341 (2019).

CHAPTER 4: Glycolytic reprogramming underlies immune cell activation by polyethylene wear particles

This chapter is a preprint of the following manuscript, currently submitted to Acta Biomaterialia:

Glycolytic reprogramming underlies immune cell activation by polyethylene wear particles

Chima V. Maduka, Oluwatosin M. Habeeb, Maxwell M. Kuhnert, Maxwell Hakun, Stuart B. Goodman, Christopher H. Contag

Abstract

Primary total joint arthroplasties (TJAs) are widely and successfully applied reconstructive procedures to treat end-stage arthritis. Nearly 50% of TJAs are now performed in young patients, posing a new challenge: performing TJAs which last a lifetime. The urgency is justified because subsequent TJAs are costlier and fraught with higher complication rates, not to mention the toll taken on patients and their families. Polyethylene particles, generated by wear at joint articulations, drive aseptic loosening by inciting insidious inflammation associated with surrounding bone loss. Down modulating polyethylene particle-induced inflammation enhances integration of implants to bone (osseointegration), preventing loosening. A promising immunomodulation strategy could leverage immune cell metabolism, however, the role of immunometabolism in polyethylene particle-induced inflammation is unknown. Our findings reveal that immune cells exposed to sterile or contaminated polyethylene particles show fundamentally altered metabolism, resulting in glycolytic reprogramming. Inhibiting glycolysis controlled inflammation, inducing a pro-regenerative phenotype that could enhance osseointegration.

Keywords: Polyethylene wear particles, glycolytic reprogramming, total joint arthroplasty, immune cells

Introduction

End-stage arthritis can be successfully treated by primary total joint arthroplasties (TJAs)[1]. With nearly 50% of TJAs performed in patients younger than 65 years[2], the vision of TJAs is now to reconstruct joints which will last a lifetime, despite patients' daily activities[3]. This is especially crucial because revision TJAs are costlier and fraught with higher complication rates, technical difficulties, and poorer surgical outcomes than primary TJAs[4]. Such revision TJAs commonly arise from aseptic loosening, frequently incited by polyethylene wear particles generated by relative motion at joint articulations[5]. Aseptic loosening may occur with or without adsorbed contaminants, such as bacterial lipopolysaccharides (LPS). Wear particles induce prolonged, low-grade inflammation with macrophages and fibroblasts as key immune cellular players[6]. This pathology is often radiographically detected only when surrounding bone loss (periprosthetic osteolysis) occurs[3]. By then, compromised implant stability results in loosening and implant failure, necessitating revision surgeries.

To minimize generation of wear particles, ultrahigh molecular weight polyethylene liners at the bearing surfaces of reconstructed joints are currently being replaced by highly crosslinked polyethylene. Crosslinked polyethylene has significantly reduced the amount of generated wear particles and accompanied chronic inflammation with periprosthetic osteolysis[7]. However, crosslinking does not completely block the generation of wear

particles from bearing surfaces of implants and subsequent inflammation[8]. Up to 9% of patients with crosslinked polyethylene liners present with chronic inflammation-induced periprosthetic osteolysis 15 years later[9]. Moreover, crosslinking has little effect on particles from third body wear, backside wear and impingement[10]; and there are currently no agents that specifically treat polyethylene particle-induced inflammatory osteolysis[11]. Consequently, there is an unmet clinical need to develop methods that will mitigate aseptic loosening from polyethylene particle-induced chronic inflammation to improve implant longevity.

Metabolic reprogramming refers to changes in glycolytic flux and oxidative phosphorylation (OXPHOS), traditional bioenergetic pathways, that are inextricably linked to macrophage activation toward proinflammatory[12,13] or pro-regenerative phenotypes[14,15]. Advances in understanding macrophage-mesenchymal stem cell crosstalk[16] has revealed that down modulating inflammation induced by polyethylene particles can prevent implant loosening by enhancing osseointegration through increased pro-regenerative macrophage activity. For example, using mesenchymal stem cells (MSCs)[17] and engineered IL-4 expressing MSCs[18]; targeting inflammatory pathways using decoy molecules for NF-kB[19], TNF-α[20] and MCP-1[21]; and using antioxidants like vitamin E[11] have shown promise for enhanced osseointegration by reducing inflammation. However, the metabolic underpinnings underlying macrophage activation by polyethylene particles are largely undefined. A detailed understanding of metabolic programs could be leveraged for immunomodulation toward extending the longevity of implants. Here, we show that both macrophages and fibroblasts exposed to sterile or LPS-contaminated polyethylene particles undergo metabolic reprogramming and differential changes in bioenergetics. Glycolytic

reprogramming underlies increased levels of proinflammatory cytokines, including MCP-1, IL-6, IL-1β and TNF-α. Specific inhibition of different glycolytic steps not only modulated these proinflammatory cytokines but stimulated pro-regenerative cytokines, including IL-4 and IL-10, without affecting cell viability. Concomitant elevation of both glycolytic flux and oxidative phosphorylation by polyethylene particles and inhibitory effects on inflammatory cytokines in addition to IL-1β[13] suggest a unique metabolic program that could be targeted for pro-regenerative clinical outcomes following TJAs.

Results

Bioenergetics is differentially altered in immune cells exposed to polyethylene particles

We had previously optimized an in-vitro, live-cell, bioenergetic workflow where ATP is rate-limiting to measure spatiotemporal bioenergetic alterations in cells exposed to biomaterials[22]. This involved transfecting mouse embryonic fibroblasts (MEFs) with a Sleeping Beauty transposon plasmid (pLuBIG) having a bidirectional promoter driving an improved firefly luciferase gene (fLuc) and a fusion gene encoding a Blasticidin-resistance marker (BsdR) linked to eGFP (BGL)[23]. Both highly crosslinked[8] and ultrahigh molecular weight[21] polyethylene particles similarly incite inflammation and are clinically used. Ultrahigh molecular weight polyethylene particles whose doses and sizes have been previously characterized were examined herein after polyethylene particles were determined to be endtoxin-free[17-19,21]. Since adsorbed bacterial lipopolysaccharide (LPS; a.k.a. endotoxin) could play a role in aseptic loosening[24], we compared key results to cells exposed to polyethylene particles and LPS.

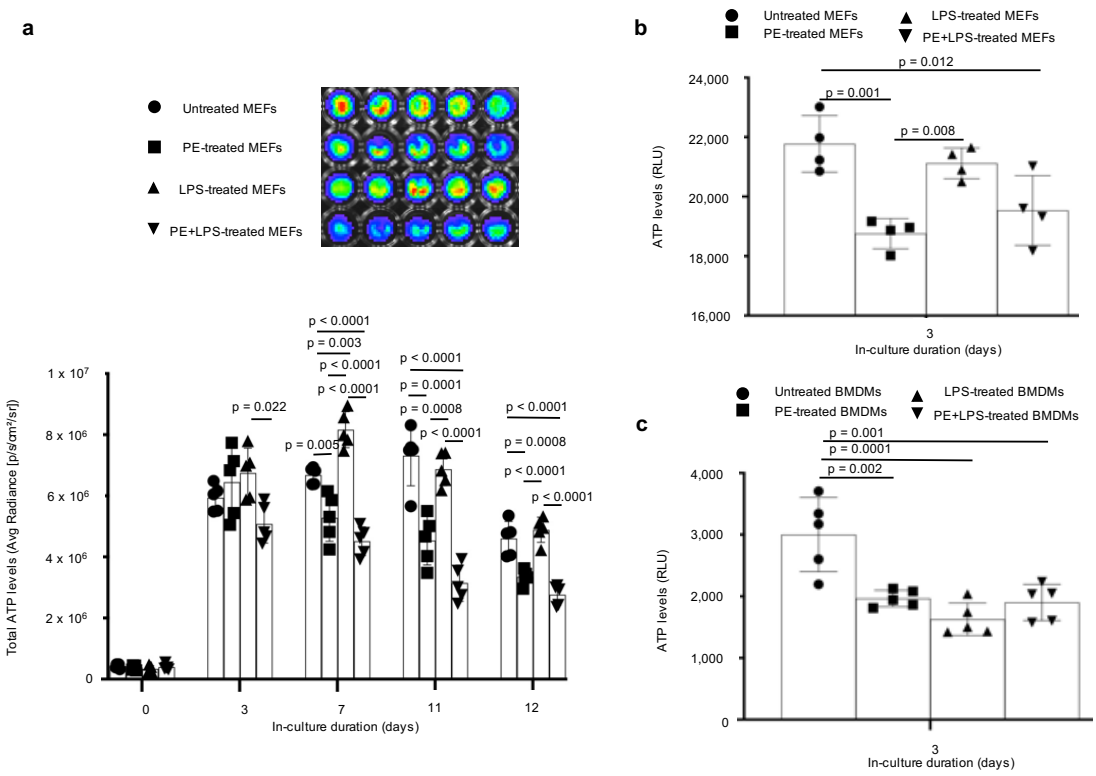

Figure 12. Ultrahigh molecular weight polyethylene (PE) particles, alone or in combination with endotoxin (LPS), alter bioenergetic (ATP) levels. **a**, Over time, PE particles lower bioenergetics in blasticidin-eGFP-luciferase (BGL)-transfected mouse embryonic fibroblasts (MEFs) compared to untreated cells; combining PE particles and LPS lowers ATP levels compared to PE particles or LPS alone (representative bioluminescent wells shown). **b**, In lysed wild-type MEFs, bioenergetics is lowered after exposure to PE particles. **c**, In primary bone marrow-derived macrophages (BMDMs), PE particles and LPS, alone or in combination, decrease bioenergetics. Mean (SD), n = 5 (Fig. 1a, 1c), n = 4 (Fig. 1b), one-way ANOVA followed by Tukey's post-hoc test.

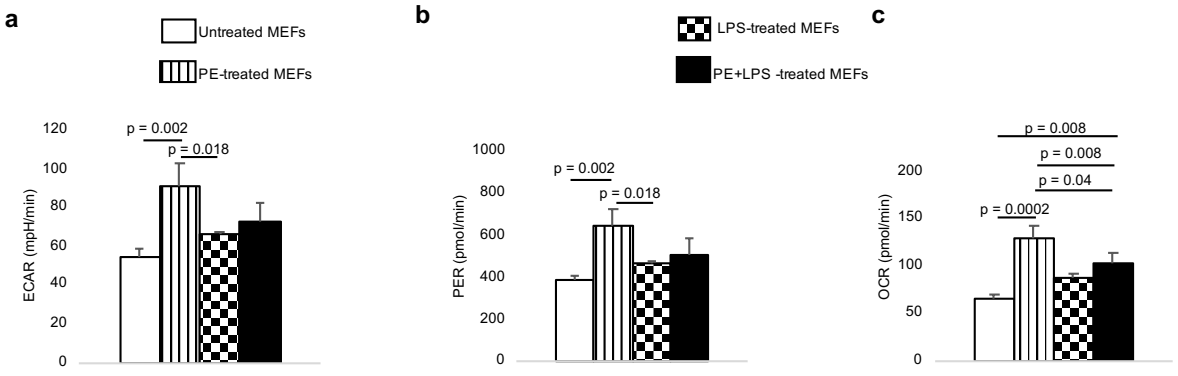

Figure 13. Mouse embryonic fibroblasts (MEFs) exposed to ultrahigh molecular weight polyethylene (PE) particles alone show increased functional metabolic indices. a-c, In comparison to untreated cells, PE particle-treated MEFs have higher extracellular acidification rate (ECAR; **a**), proton efflux rate (PER; **b**) and oxygen consumption rate (OCR; **c**). Mean (SD), n = 3, one-way ANOVA followed by Tukey's post-hoc test.

Whereas only polyethylene particles consistently lowered bioenergetic (ATP) levels in live BGL cells, overall, LPS alone did not affect ATP levels when compared to untreated fibroblasts over time (Fig. 12a). In comparison to polyethylene particles or LPS alone, combining polyethylene particles and LPS further decreased ATP levels after prolonged exposure (Fig. 12a). D-luciferin used in live-cell assays could be limited by its ability to permeate cell membranes[25]; accordingly, bioenergetic measurement in lysed fibroblasts was more sensitive, corroborating decreases in ATP levels after exposure to only polyethylene particles (by 1.2-fold) or a combination of polyethylene particles and LPS (by 1.1-fold) relative to untreated cells at day 3 (Fig. 12b). Primary bone marrow-derived macrophages revealed a 1.5-, 1.8-, and 1.6-fold decrease in ATP levels relative to untreated cells following exposure to only polyethylene particles, only LPS, and polyethylene particles with LPS, respectively (Fig. 12c).

Exposure to polyethylene particles alters functional metabolism in immune cells

To explore what bioenergetic pathways were responsible for alterations in ATP levels, we used the Seahorse assay to probe extracellular acidification rate (ECAR), lactate-linked proton efflux rate (PER) and oxygen consumption rate (OCR). ECAR, PER and OCR are indices of glycolytic flux, monocarboxylate transporter (MCT) function[26,27] and mitochondrial oxidative phosphorylation, respectively, and are used to assess metabolic reprogramming[12,13]. Following exposure to LPS alone, fibroblasts did not reveal changes in ECAR, PER or OCR compared to untreated cells (Fig. 13a-c). In contrast, exposure to polyethylene particles resulted in a 1.7-, 1.7-, and 2-fold increase in ECAR, PER and OCR, respectively, relative to untreated fibroblasts (Fig. 13a-c). Similarly, a combination of

polyethylene particles and LPS increased OCR by 1.6-fold in comparison to untreated fibroblasts (Fig. 13c).

Exposure to only polyethylene particles increased ECAR, PER and OCR by 13.1-, 13.1- and 3.1-fold, respectively, in primary macrophages compared to untreated cells (Fig. 14a, c, e). Macrophages exposed to polyethylene particles and LPS increased ECAR, PER and OCR by 23-, 23.1- and 2.8-fold, respectively, compared to untreated cells (Fig. 14b, d, f). To reduce abnormal increments in ECAR, PER and OCR, we targeted different stages of glycolysis using 3-(3-pyridinyl)-1-(4-pyridinyl)-2-propen-1-one (3PO), 2-deoxyglucose (2DG) and aminooxyacetic acid (a.a.). 3PO inhibits 6- phosphofructo-2-kinase which is the rate limiting glycolytic enzyme[28]; 2DG inhibits hexokinase, the first enzyme in glycolysis[13]; and a.a. prevents the mitochondrion from utilizing glycolytic pyruvate[29]. In a dose-dependent manner, 3PO, 2DG and a.a. decreased ECAR, PER and OCR among macrophages exposed to only polyethylene particles or a combination of polyethylene particles and LPS (Fig. 14a-f), suggesting efficient cellular uptake and pharmacologic effects of these small molecule inhibitors.

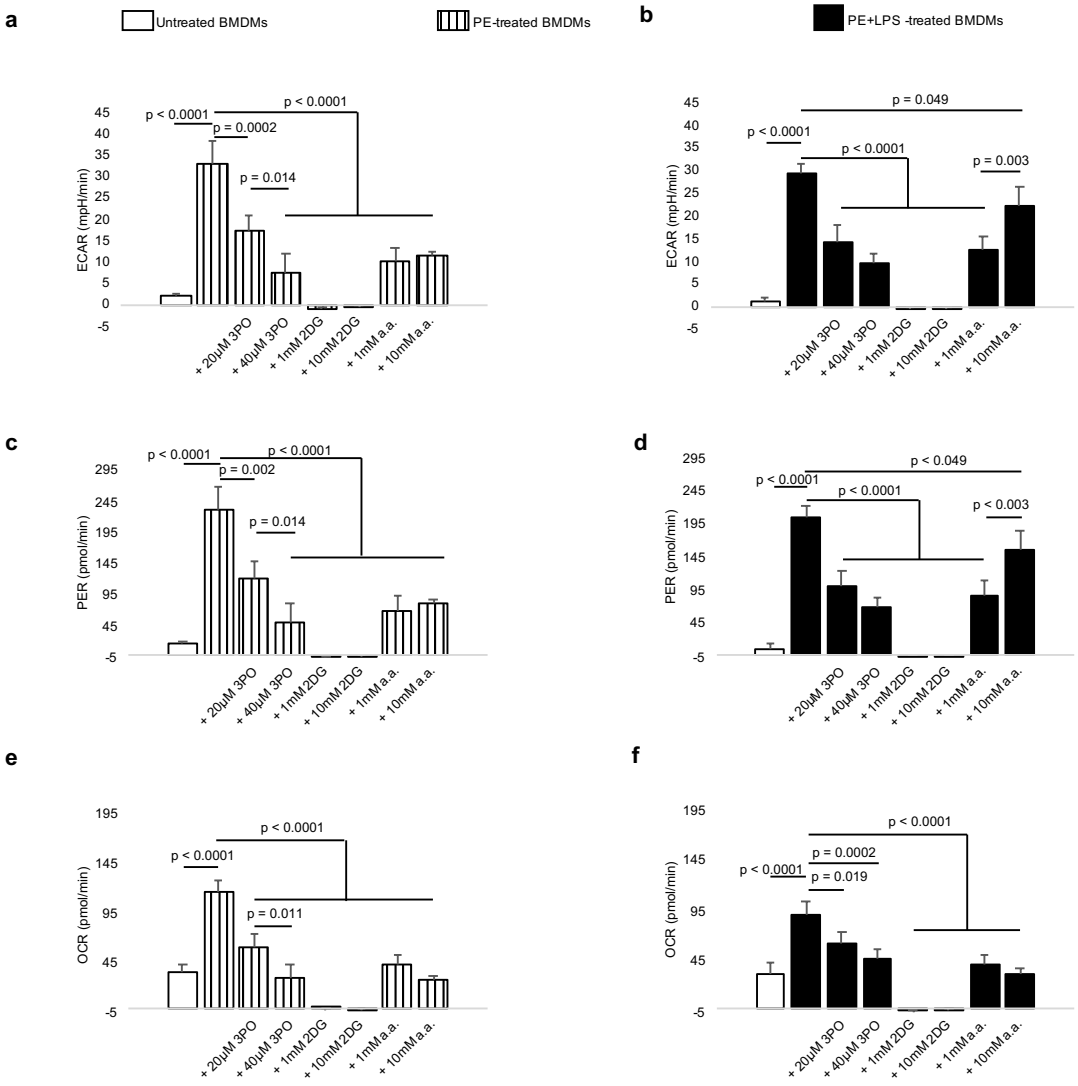

Figure 14. Primary bone marrow-derived macrophages (BMDMs) exposed to ultrahigh molecular weight polyethylene (PE) particles or both PE particles and endotoxin (LPS) reveal greater extracellular acidification rate (ECAR), proton efflux rate (PER) and oxygen consumption rate (OCR) than untreated cells; this increment is reduced upon addition of various glycolytic inhibitors. a-f, ECAR (**a-b**), PER (**c-d**) and OCR (**e-f**) are increased in BMDMs treated with PE particles, alone or in combination with LPS; elevated levels are decreased upon addition of 3-(3-Pyridinyl)-1-(4-pyridinyl)-2-propen-1-one (3PO), 2-deoxyglucose (2DG) or aminooxyacetic acid (a.a.). Mean (SD), n = 3, one-way ANOVA followed by Tukey's post-hoc test.

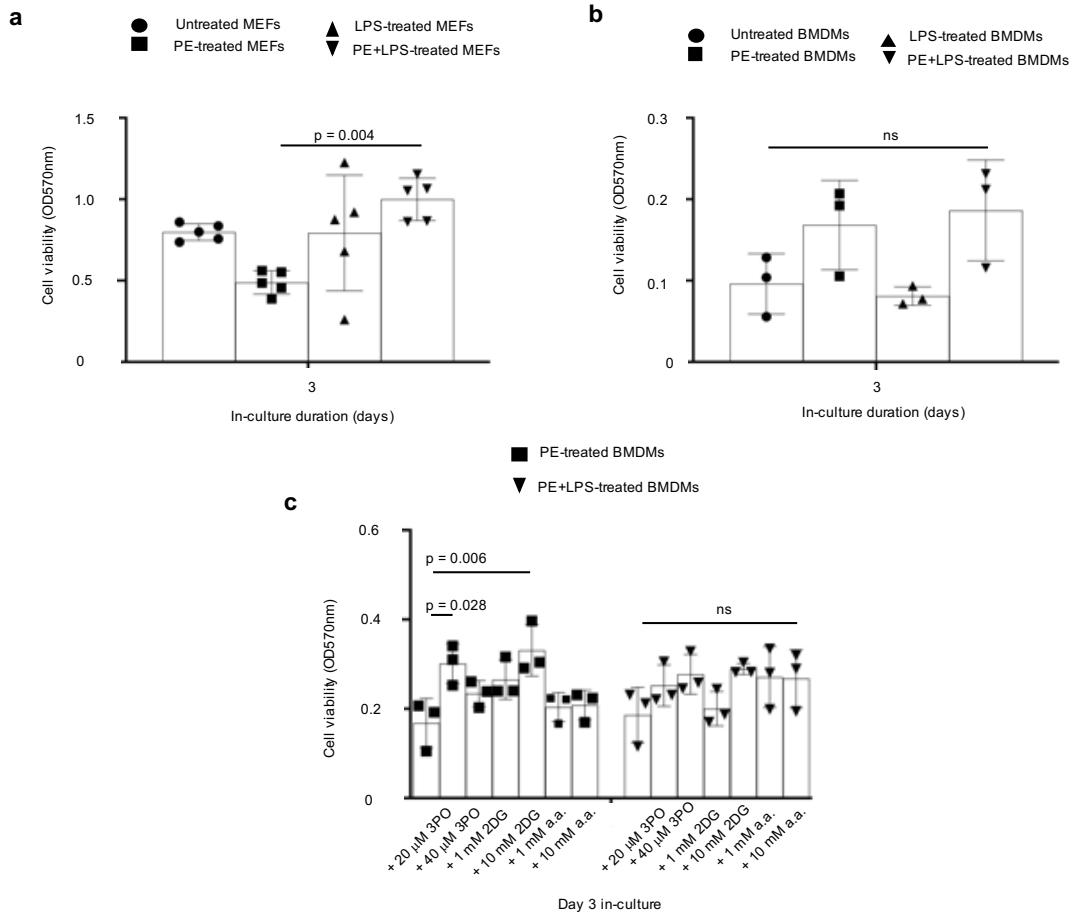

Figure 15. Compared to untreated cells, treatment with ultrahigh molecular weight polyethylene (PE) particles, endotoxin (LPS) or a combination of PE particles and LPS does not change cell numbers; addition of glycolytic inhibitors does not decrease cell numbers. a-b, In mouse embryonic fibroblasts (MEFs; **a**) or primary bone marrow-derived macrophages (BMDMs; **b**), exposure to PE particles, LPS or PE particles and LPS does not change cell numbers relative to untreated controls. **c**, Addition of various doses of 3-(3-Pyridinyl)-1-(4-pyridinyl)-2-propen-1-one (3PO), 2-deoxyglucose (2DG) or aminooxyacetic acid (a.a.) to PE particle-treated or PE particle- and LPS-treated BMDMs does not decrease cell numbers. Mean (SD), n = 5 (Fig. 4a), n = 3 (Fig. 4b, c), one-way ANOVA followed by Tukey's post-hoc test.

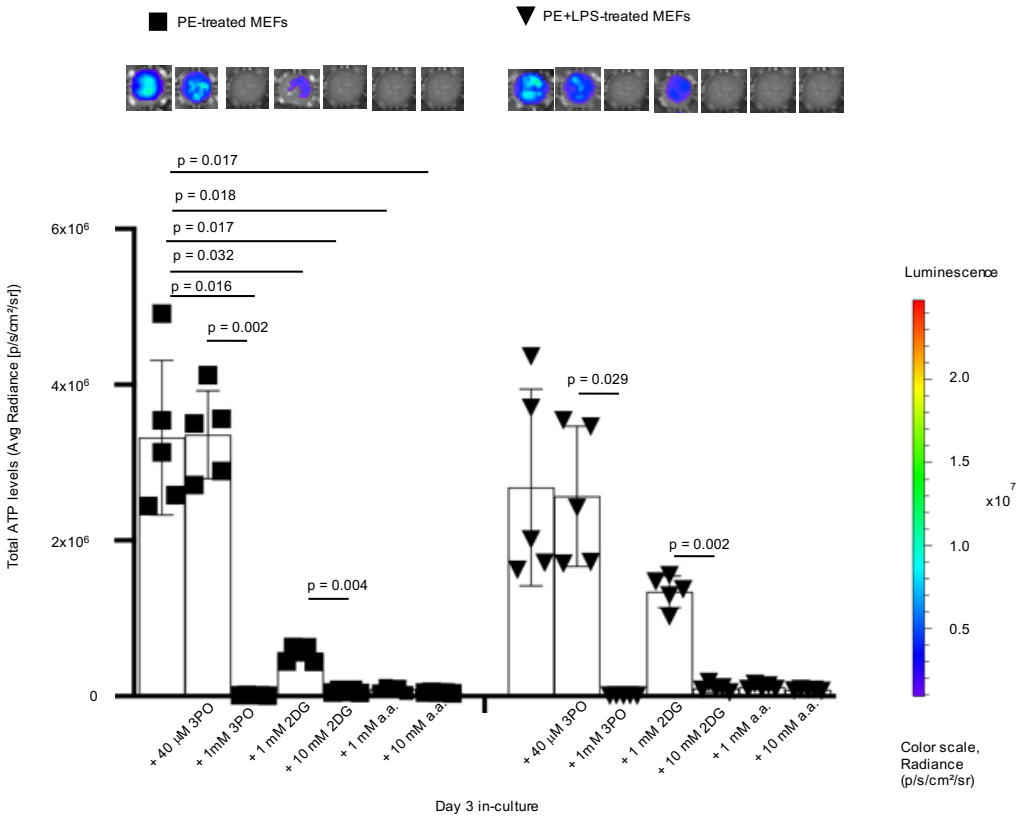

Figure 16. Glycolytic inhibitors decrease bioenergetic levels in treated mouse embryonic fibroblasts (MEFs). Following treatment of blasticidin-GFP-Luciferase (BGL)-transfected MEFs with ultrahigh molecular weight polyethylene (PE) particles alone or in combination with endotoxin (LPS), addition of 3-(3-pyridinyl)-1-(4-pyridinyl)-2-propen-1-one (3PO), 2-deoxyglucose (2DG) and aminooxyacetic acid (a.a.; representative wells are shown) tend to decrease bioenergetics in a dose-dependent manner. Not significant (ns), mean (SD), Brown-Forsythe and Welch ANOVA followed by Dunnett's T3 multiple comparisons test, n = 5.

Compared to untreated cells, there was no difference in cell numbers following exposure to polyethylene particles, LPS or polyethylene particles with LPS among fibroblasts (Fig. 15a) or macrophages (Fig. 15b). Additionally, exposure of macrophages to pharmacologic inhibitors, including 3PO, 2DG and a.a. did not lower cell viability (Fig. 15c). Importantly, in fibroblasts exposed to polyethylene particles alone or polyethylene particles and LPS, addition of 3PO, 2DG or a.a. further lowered bioenergetics in a dose-dependent manner (Fig. 16).

Immunometabolism underlies macrophage polarization by polyethylene particles

To evaluate how metabolism affects immune cellular function, we assayed levels of cytokine and chemokine expression using a magnetic bead-based technique[30]. We observed that proinflammatory proteins, including MCP-1 (Fig. 17a), IL-6 (Fig. 17b), IL-1β (Fig. 17c) and TNF-α (Fig. 17d) were increased by 4.1-, 97.3-, 41.8- and 7-fold, respectively, after exposure to polyethylene particles in comparison to untreated macrophages. Addition of 3PO or 2DG consistently decreased proinflammatory cytokine or chemokine levels (Fig. 17a-d) relative to macrophages exposed to only polyethylene particles; however, addition of a.a. selectively decreased MCP-1 expression (Fig. 17a).

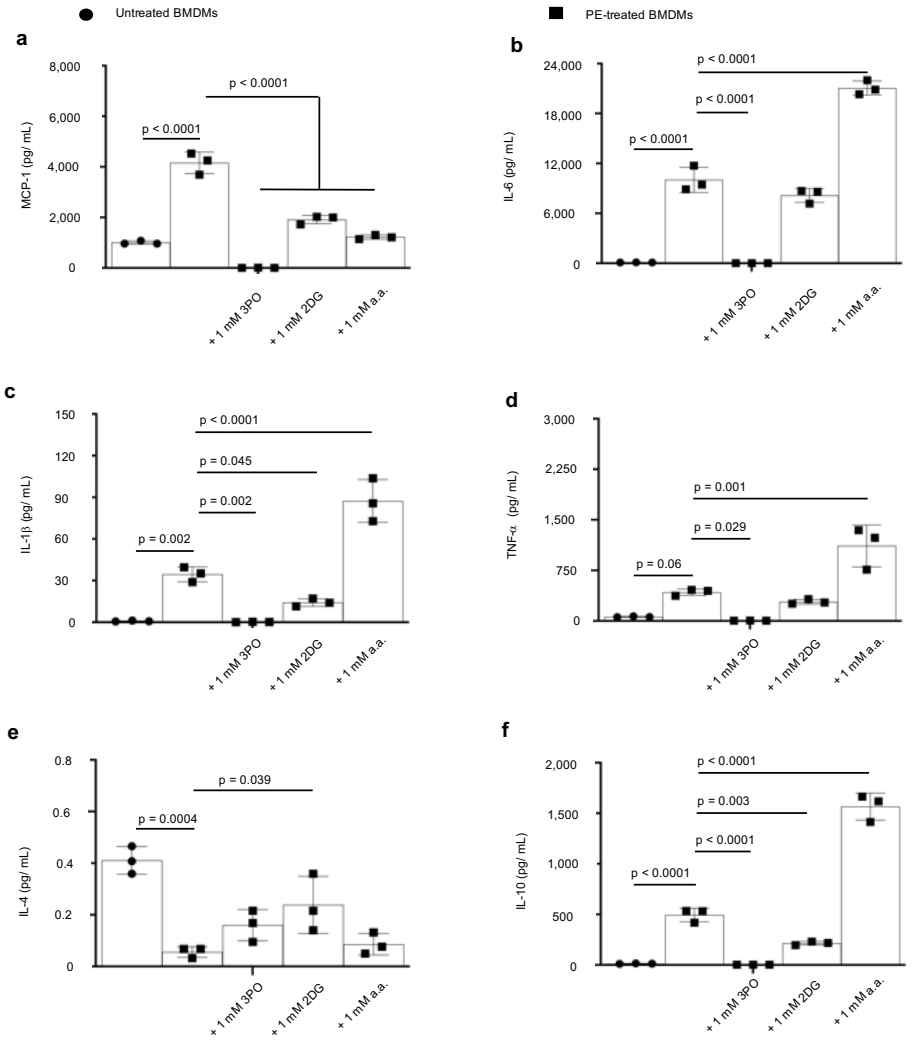

Figure 17. Elevated proinflammatory cytokine (protein) levels are decreased following addition of glycolytic inhibitors to primary bone marrow-derived macrophages (BMDMs). a-d, In BMDMs, exposure to ultrahigh molecular weight polyethylene (PE) particles increase proinflammatory cytokines, including MCP-1 (**a**), IL-6 (**b**), IL-1β (**c**) and TNF- (**d**) in comparison to untreated BMDMs. Addition of 3-(3-Pyridinyl)-1-(4-pyridinyl)-2-propen-1-one (3PO) or 2-deoxyglucose (2DG) decreases proinflammatory cytokines; aminooxyacetic acid (a.a.) selectively decreases MCP-1 levels. **e**, Exposure of BMDMs to PE particles decreases IL-4 levels in comparison to untreated cells; IL-4 levels tend to increase following addition of glycolytic inhibitors. **f**, Compared to BMDMs exposed to only PE particles, exposure to PE particles and a.a. increase IL-10 levels. Mean (SD), n = 3, one-way ANOVA followed by Tukey's post-hoc test; assay was performed after 3 days in-culture.

Exposure of macrophages to polyethylene particles decreased IL-4 levels by 7.4-fold compared to untreated cells; addition of 3PO, 2DG or a.a. increased IL-4 levels by 2.9-, 4.3-, and 1.5- fold, respectively, relative to polyethylene particles alone; however, only the increase by 2DG was statistically significant (Fig. 17e). Levels of IL-13 and IFN-λ were unchanged (data not shown). Consistent with macrophage polarization being a continuum[31,32], polyethylene particles increased IL-10 expression in comparison to untreated macrophages (Fig. 17f). Whereas addition of 3PO or 2DG did not increase IL-10 levels, a.a. increased IL-10 expression by 3.2-fold relative to macrophages exposed to only polyethylene particles (Fig. 17f).

Discussion

When macrophages are exposed to bacterial lipopolysaccharide (LPS), their bioenergetic (ATP) levels are decreased as part of cell activation and inflammation[33]. This results from reprogrammed metabolism that shifts bioenergetic dependence from mitochondrial oxidative phosphorylation (OXPHOS) to glycolysis, with crucial consequences on proinflammatory[12,13] and anti-inflammatory[14,15] events. While immunometabolism in response to LPS has been well characterized for such clinical applications as bacterial sepsis, the role of immunometabolism in sterile inflammation induced by clinically relevant implant materials is unknown.

Macrophages are the dominant immune cell type implicated in the chronic inflammatory response to ultrahigh molecular weight polyethylene (PE) particles[2], likely acting through Toll-like receptors (TLRs)[34,35]. Following exposure to PE particles of particular sizes and over a threshold, transcriptional signaling occurs through NF-kB[36],

MyD88[37] and chemerin/ChemR23[38]. Consequently, there is increased production of proinflammatory cytokines that accompany resulting pathologies, including periprosthetic osteolysis. Likewise, fibroblasts play a synergistic role with macrophages. Fibroblasts exposed to PE particles [39,40] express MCP-1, RANKL, IL-1β, IL-6, MMP1 and MMP2 which activate osteoclasts, accentuate inflammation and degrade surrounding bone extracellular matrix.

Adsorbed LPS could be a contaminant on sterilized implants and has been documented in a subset of patients diagnosed with aseptic loosening of implants from chronic inflammation[24]. Therefore, PE and LPS-contaminated PE (cPE) particles were examined and compared to LPS. Our findings reveal that bioenergetic imbalances differentially occur in macrophages and fibroblasts exposed to PE particles, LPS or cPE particles. For example, although LPS did not affect ATP levels in fibroblasts, PE particles lowered cellular bioenergetics. Furthermore, fibroblasts exposed to PE particles but not LPS were metabolically reprogrammed, revealing increases in glycolysis, OXPHOS and monocarboxylate transporter (MCT) function. On the other hand, decreased ATP levels were observed in primary bone marrow-derived macrophages exposed to PE particles, LPS or cPE particles consistent with reliance on glycolysis. Immune cells depend on glycolysis during inflammatory activation as glycolysis produces ATP quicker than OXPHOS, albeit OXPHOS results in overall higher ATP levels. Additionally, this switch to glycolysis is crucial for IL-1β production by stabilizing HIF-1α in macrophages[13] and fibroblast activation in fibrosis[41]. Surprisingly, in addition to elevated glycolysis, OXPHOS was increased in macrophages exposed to PE or cPE particles, independent of changing cell numbers. Concomitant elevation in both glycolysis and OXPHOS suggests a unique metabolic reprogram induced by PE

particles relative to LPS; LPS increases glycolysis while reducing OXPHOS[12]. Accompanied decrease in ATP levels suggests that increased OXPHOS is directed at functions other than cellular energy supply. In a septic model, LPS was shown to repurpose mitochondrial function toward superoxide formation in macrophages[12]. At earlier time points than used in this study, LPS decreased OXPHOS[12], likely reflecting as yet uncharacterized temporal changes in metabolic reprogramming. Notably, glycolytic flux and MCT function but not OXPHOS were higher in macrophages exposed to cPE than PE particles, relative to respective controls. This may likely be from synergistic signaling with cPE particles, as PE particles and LPS are known to activate TLR2 and TLR4 receptors, respectively[34,35].

Elevated glycolytic flux in macrophages exposed to PE or cPE particles could be lowered by specific pharmacologic inhibition of different glycolytic steps using 3-(3-pyridinyl)-1-(4-pyridinyl)-2-propen-1-one (3PO)[28], 2-deoxyglucose (2DG)[13] and aminooxyacetic acid (a.a.)[29]. Lactate from glycolysis is converted to pyruvate which feeds mitochondrial OXPHOS, and proton-linked lactate is bidirectionally shuttled through MCT[26,27]. Consequently, pharmacologic inhibition of glycolysis lowered aberrantly elevated OXPHOS and MCT function. Pharmacologic inhibition did not result in reduced cell viability, excluding potential toxicity. Using fibroblasts expressing luciferase, we observed that glycolytic inhibition further reduced ATP levels following exposure to PE particles, corroborating cellular bioenergetic dependence on glycolysis.

Macrophages exposed to PE particles became polarized to a proinflammatory phenotype as measured by elevated protein expression of MCP-1, IL-6, IL-1β and TNF-α. Additionally, IL-10 was increased, consistent with macrophage polarization being a spectrum[31]. Both IL-1β and TNF-α induce RANKL expression which drives osteoclast

maturation and differentiation, together with M-CSF[6]. Osteolysis, associated with PE particle-induced chronic inflammation, is the result of net bone loss from osteoclast-mediated bone resorption exceeding osteoblast-mediated bone formation. Similarly, IL-6[42] and MCP-1[43] are associated with increased osteolysis and cartilage destruction. Interestingly, 2DG and 3PO decreased aberrantly elevated proinflammatory cytokines. In particular, 2DG allowed for some level of proinflammatory cytokine expression. This is clinically important because a suitable level of inflammation is required for tissue repair and osseointegration[44]; compromised osseointegration is a leading cause of implant failure[4]. Remarkably, whereas 2DG decreased MCP-1, IL-6, IL-1β and TNF-α protein levels which were elevated by PE particles, 2DG is known to selectively decrease IL-1β protein levels from LPS[13], suggesting unique differences. In contrast to 2DG and 3PO, a.a. selectively decreased MCP-1 but not IL-6, IL-1β and TNF-α; and increased IL-10 levels. Central to macrophage-stem cell crosstalk, IL-10 signaling is critical for tissue regeneration[45]. Glycolytic inhibition using 2DG increased IL-4 levels which were reduced by PE particles. Increment of IL-4 levels suggest a pro-regenerative macrophage phenotype. Acute and chronic inflammation as well as bone loss induced by PE particles is reversed by inducing a pro-regenerative macrophage phenotype using IL-4[18].

In conclusion, all clinically relevant biomaterials undergo wear at articulations, resulting in different levels of chronic inflammation and undermining the longevity of biomaterials used in arthroplasties. By characterizing immune cell metabolism as being pivotal in the inflammatory pathology induced by polyethylene particles, we reveal a unique vulnerability which could be harnessed for the dual purposes of controlling inflammation and stimulating pro-regenerative immune cell phenotypes. Targeting immunometabolism

can be extended to other implant materials[46,47], improving osseointegration and long-term clinical outcomes for patients undergoing various arthroplasties.

Methods

Materials

Ultrahigh molecular weight polyethylene particles were sourced, characterized and determined to be endotoxin-free as previously described[18]. Concentrations of 100ng/ mL of lipopolysaccharide (LPS) from *Escherichia coli* O111:B4 (MilliporeSigma) and 1.25 mg/ mL of ultrahigh molecular weight polyethylene particles were used. Furthermore, 3-(3-pyridinyl)-1-(4-pyridinyl)-2-propen-1-one (MilliporeSigma), 2-deoxyglucose (MilliporeSigma) and aminooxyacetic acid (Sigma-Aldrich) were used for glycolytic inhibition.

Bioenergetic measurement

Bioluminescence was measured using the IVIS Spectrum in vivo imaging system (PerkinElmer) after adding 150 μg/mL of D-luciferin (PerkinElmer). Living Image (Version 4.5.2, PerkinElmer) was used for acquiring bioluminescence on the IVIS Spectrum. Standard ATP/ADP kits (Sigma-Aldrich) containing D-luciferin, luciferase and cell lysis buffer were used to according to manufacturer's instructions. Luminescence at integration time of 1,000 ms was obtained using the SpectraMax M3 Spectrophotometer (Molecular Devices) using SoftMax Pro (Version 7.0.2, Molecular Devices).

Cells

Mouse embryonic fibroblast (MEFs) cell line (NIH 3T3 cell line; ATCC) and primary bone-marrow derived macrophages (BMDMs) derived from C57BL/6J mice (Jackson Laboratories) of 3-4 months[12,48] were used. NIH 3T3 cells were stably transfected with a Sleeping Beauty transposon plasmid (pLuBIG) having a bidirectional promoter driving an improved firefly luciferase gene (fLuc) and a fusion gene encoding a Blasticidin-resistance marker (BsdR) linked to eGFP (BGL)[23]. This enabled us to monitor bioenergetic changes in live cells[22]. For temporal (IVIS) experiments lasting 12 days, 5,000 BGL cells were initially seeded in each well of a 96-well tissue culture plate in 200 μL of complete medium (see below). For ATP, crystal violet and Seahorse assays, 20,000 wild-type MEFs were seeded. For ATP, crystal violet and cytokine/ chemokine assays, 50,000 BMDMs were seeded; 60,000 BMDMs were seeded for Seahorse experiments. For IVIS experiments with glycolytic inhibitors, 20,000 BGL cells were initially seeded. All time points are indicated on respective graphs. Complete medium comprised of DMEM medium, 10% heat-inactivated Fetal Bovine Serum and 100 U/mL penicillin-streptomycin (all from ThermoFisher Scientific).

Cell viability

Cell viability was assessed using the crystal violet assay[49]. Absorbance (optical density) was acquired at 570 nm using the the SpectraMax M3 Spectrophotometer (Molecular Devices) and SoftMax Pro software (Version 7.0.2, Molecular Devices).

Functional metabolism

Basal measurements of oxygen consumption rate (OCR), extracellular acidification rate (ECAR) and lactate-linked proton efflux rate (PER) were obtained in real-time using the Seahorse XFe-96 Extracellular Flux Analyzer (Agilent Technologies)[12,13,15]. Prior to running the assay, cell culture medium was replaced by the Seahorse XF DMEM medium (pH 7.4) supplemented with 25 mM D-glucose and 4 mM Glutamine. The Seahorse ATP rate assay was run according to manufacturer's instruction and all reagents for the Seahorse assays were sourced from Agilent Technologies. Wave software (Version 2.6.1) was used to export Seahorse data directly as means ± standard deviation (SD).

Chemokine and cytokine measurements

Cytokine and chemokine levels were measured using a MILLIPLEX MAP mouse magnetic bead multiplex kit (MilliporeSigma)[30] to assess for IL-6, MCP-1, TNF-α, IL-1β, IL-4, IL-10, IFN-λ and 1L-13 protein expression in supernatants. Data was acquired using Luminex 200 (Luminex Corporation) by the xPONENT software (Version 3.1, Luminex Corporation). Using the glycolytic inhibitor, 3PO, expectedly decreased cytokine values to < 3.2 pg/ mL in some experiments. For statistical analyses, those values were expressed as 3.1 pg/ mL. Values exceeding the dynamic range of the assay, in accordance with manufacturer's instruction, were excluded. Additionally, IL-6 ELISA kits (RayBiotech) for supernatants were used according to manufacturer's instructions.

Statistics and reproducibility

Statistical software (GraphPad Prism) was used to analyse data presented as mean with standard deviation (SD). Significance level was set at $p < 0.05$, and details of statistical tests and sample sizes, which are biological replicates, are provided in figure legends. Exported data (mean, SD) from Wave in Seahorse experiments had the underlying assumption of normality and similar variance, and thus were tested using corresponding parametric tests as indicated in figure legends.

Acknowledgements

Euthanized C57BL/6J mice were a gift from RR Neubig (facilitated by J Leipprandt) and the Campus Animal Resources at Michigan State University (MSU). Funding for this work was provided in part by the James and Kathleen Cornelius Endowment at MSU.

Author contributions

Conceptualization, C.V.M. and C.H.C.; Methodology, C.V.M., S.B.G., and C.H.C.; Investigation, C.V.M., M.O.B., M.M.K. and M.H.; Writing – Original Draft, C.V.M.; Writing – Review & Editing, C.V.M., M.O.B., M.M.K., M.H., S.B.G. and C.H.C.; Funding Acquisition, C.H.C.; Resources, S.B.G. and C.H.C.; Supervision, S.B.G. and C.H.C.

Competing interests

The authors declare no competing interests.

REFERENCES

REFERENCES

1 Ingham, E. & Fisher, J. Biological reactions to wear debris in total joint replacement. *Proceedings of the Institution of Mechanical Engineers, Part H: Journal of Engineering in Medicine* **214**, 21-37 (2000).

2 Cobelli, N., Scharf, B., Crisi, G. M., Hardin, J. & Santambrogio, L. Mediators of the inflammatory response to joint replacement devices. *Nature Reviews Rheumatology* **7**, 600-608 (2011).

3 Sivananthan, S., Goodman, S. & Burke, M. in *Joint Replacement Technology* 373-402 (Elsevier, 2021).

4 Goodman, S. B., Gallo, J., Gibon, E. & Takagi, M. Diagnosis and management of implant debris-associated inflammation. *Expert review of medical devices* **17**, 41-56 (2020).

5 Bistolfi, A. *et al.* Ultra-high molecular weight polyethylene (UHMWPE) for hip and knee arthroplasty: The present and the future. *Journal of Orthopaedics* **25**, 98-106 (2021).

6 Kandahari, A. M. *et al.* A review of UHMWPE wear-induced osteolysis: the role for early detection of the immune response. *Bone research* **4**, 1-13 (2016).

7 Tsukamoto, M., Mori, T., Ohnishi, H., Uchida, S. & Sakai, A. Highly cross-linked polyethylene reduces osteolysis incidence and wear-related reoperation rate in cementless total hip arthroplasty compared with conventional polyethylene at a mean 12-year follow-up. *The Journal of Arthroplasty* **32**, 3771-3776 (2017).

8 Ormsby, R. T. *et al.* Osteocytes respond to particles of clinically-relevant conventional and cross-linked polyethylene and metal alloys by up-regulation of resorptive and inflammatory pathways. *Acta biomaterialia* **87**, 296-306 (2019).

9 Hopper Jr, R. H., Ho, H., Sritulanondha, S., Williams, A. C. & Engh Jr, C. A. Otto Aufranc Award: crosslinking reduces THA wear, osteolysis, and revision rates at 15-year followup compared with noncrosslinked polyethylene. *Clinical orthopaedics and related research* **476**, 279 (2018).

10 Greenfield, E. M. *et al.* Does endotoxin contribute to aseptic loosening of orthopedic implants? *Journal of Biomedical Materials Research Part B: Applied Biomaterials: An Official Journal of The Society for Biomaterials, The Japanese Society for Biomaterials, and The Australian Society for Biomaterials and the Korean Society for Biomaterials* **72**, 179-185 (2005).

11 Liu, F., Dong, J., Zhou, D. & Zhang, Q. Identification of key candidate genes related to inflammatory osteolysis associated with vitamin E-Blended UHMWPE debris of

orthopedic implants by integrated bioinformatics analysis and experimental confirmation. *Journal of Inflammation Research* **14**, 3537 (2021).

12 Mills, E. L. *et al.* Succinate Dehydrogenase Supports Metabolic Repurposing of Mitochondria to Drive Inflammatory Macrophages. *Cell* **167**, 457-470.e413, doi:10.1016/j.cell.2016.08.064 (2016).

13 Tannahill, G. *et al.* Succinate is a danger signal that induces IL-1β via HIF-1α. *Nature* **496**, 238-242, doi:10.1038/nature11986 (2013).

14 Mills, E. L. *et al.* Itaconate is an anti-inflammatory metabolite that activates Nrf2 via alkylation of KEAP1. *Nature* **556**, 113 (2018).

15 Ip, W. E., Hoshi, N., Shouval, D. S., Snapper, S. & Medzhitov, R. Anti-inflammatory effect of IL-10 mediated by metabolic reprogramming of macrophages. *Science* **356**, 513-519 (2017).

16 Pajarinen, J. *et al.* Mesenchymal stem cell-macrophage crosstalk and bone healing. *Biomaterials* **196**, 80-89 (2019).

17 Lin, T. *et al.* Preconditioning of murine mesenchymal stem cells synergistically enhanced immunomodulation and osteogenesis. *Stem cell research & therapy* **8**, 1-9 (2017).

18 Pajarinen, J. *et al.* Interleukin-4 repairs wear particle induced osteolysis by modulating macrophage polarization and bone turnover. *Journal of Biomedical Materials Research Part A* **109**, 1512-1520 (2021).

19 Lin, T.-H. *et al.* NF-κB decoy oligodeoxynucleotide enhanced osteogenesis in mesenchymal stem cells exposed to polyethylene particle. *Tissue engineering Part A* **21**, 875-883 (2015).

20 Zhao, Y.-p. *et al.* Progranulin suppresses titanium particle induced inflammatory osteolysis by targeting TNFα signaling. *Scientific reports* **6**, 1-13 (2016).

21 Gibon, E. *et al.* Selective inhibition of the MCP-1-CCR2 ligand-receptor axis decreases systemic trafficking of macrophages in the presence of UHMWPE particles. *Journal of Orthopaedic Research* **30**, 547-553 (2012).

22 Maduka, C. V., Alhaj, M., Ural, E., Habeeb, M. O., Kuhnert, M. M.,Chung, S., Hakun, M., Makela, A. V., Hankenson, K. D., Goodman, S. B., Narayan, R., & Contag, C. H. Polylactide degradation activates immune cells by metabolic reprogramming. *Nature Biomedical Engineering* **2022** (**under revision**).

23 Kanada, M. *et al.* Differential fates of biomolecules delivered to target cells via extracellular vesicles. *Proceedings of the National Academy of Sciences* **112**, E1433-E1442 (2015).

24 Bonsignore, L. A., Anderson, J. R., Lee, Z., Goldberg, V. M. & Greenfield, E. M. Adherent lipopolysaccharide inhibits the osseointegration of orthopedic implants by impairing osteoblast differentiation. *Bone* **52**, 93-101 (2013).

25 Lee, K. *et al.* Cell uptake and tissue distribution of radioiodine labelled D-luciferin: implications for luciferase based gene imaging. *Nuclear medicine communications* **24**, 1003-1009 (2003).

26 Tan, Z. *et al.* in *The Journal of biological chemistry* Vol. 290 46-55 (2015).

27 Payen, V. L., Mina, E., Van Hee, V. F., Porporato, P. E. & Sonveaux, P. Monocarboxylate transporters in cancer. *Mol Metab* **33**, 48-66, doi:10.1016/j.molmet.2019.07.006 (2020).

28 Clem, B. *et al.* Small-molecule inhibition of 6-phosphofructo-2-kinase activity suppresses glycolytic flux and tumor growth. *Molecular cancer therapeutics* **7**, 110-120 (2008).

29 Kauppinen, R. A., Sihra, T. S. & Nicholls, D. G. Aminooxyacetic acid inhibits the malate-aspartate shuttle in isolated nerve terminals and prevents the mitochondria from utilizing glycolytic substrates. *Biochim Biophys Acta* **930**, 173-178, doi:10.1016/0167-4889(87)90029-2 (1987).

30 Sprague, L. *et al.* Dendritic cells: in vitro culture in two-and three-dimensional collagen systems and expression of collagen receptors in tumors and atherosclerotic microenvironments. *Experimental cell research* **323**, 7-27 (2014).

31 Sadtler, K. *et al.* Design, clinical translation and immunological response of biomaterials in regenerative medicine. *Nature Reviews Materials* **1**, 1-17 (2016).

32 Mishra, P. K. *et al.* Sterile particle-induced inflammation is mediated by macrophages releasing IL-33 through a Bruton's tyrosine kinase-dependent pathway. *Nature materials* **18**, 289-297 (2019).

33 O'Neill, L. A. & Pearce, E. J. in *J Exp Med* Vol. 213 15-23 (2016).

34 Maitra, R., Clement, C. C., Crisi, G. M., Cobelli, N. & Santambrogio, L. Immunogenecity of modified alkane polymers is mediated through TLR1/2 activation. *PloS one* **3**, e2438 (2008).

35 Tamaki, Y. *et al.* Increased expression of toll-like receptors in aseptic loose periprosthetic tissues and septic synovial membranes around total hip implants. *The Journal of rheumatology* **36**, 598-608 (2009).

36 Hodges, N. A., Sussman, E. M. & Stegemann, J. P. Aseptic and septic prosthetic joint loosening: Impact of biomaterial wear on immune cell function, inflammation, and infection. *Biomaterials* **278**, 121127 (2021).

37 Goodman, S. B., Pajarinen, J., Yao, Z. & Lin, T. Inflammation and bone repair: from particle disease to tissue regeneration. *Frontiers in Bioengineering and Biotechnology*, 230 (2019).

38 Zhao, F., Cang, D., Zhang, J. & Zheng, L. Chemerin/ChemR23 signaling mediates the effects of ultra-high molecular weight polyethylene wear particles on the balance between osteoblast and osteoclast differentiation. *Annals of Translational Medicine* **9** (2021).

39 Koreny, T. *et al.* The role of fibroblasts and fibroblast-derived factors in periprosthetic osteolysis. *Arthritis & Rheumatism: Official Journal of the American College of Rheumatology* **54**, 3221-3232 (2006).

40 Man, K., Jiang, L.-H., Foster, R. & Yang, X. B. Immunological responses to total hip arthroplasty. *Journal of functional biomaterials* **8**, 33 (2017).

41 Xie, N. *et al.* Glycolytic reprogramming in myofibroblast differentiation and lung fibrosis. *American journal of respiratory and critical care medicine* **192**, 1462-1474 (2015).

42 Udagawa, N. *et al.* Interleukin (IL)-6 induction of osteoclast differentiation depends on IL-6 receptors expressed on osteoblastic cells but not on osteoclast progenitors. *The Journal of experimental medicine* **182**, 1461-1468 (1995).

43 Raghu, H. *et al.* CCL2/CCR2, but not CCL5/CCR5, mediates monocyte recruitment, inflammation and cartilage destruction in osteoarthritis. *Annals of the rheumatic diseases* **76**, 914-922 (2017).

44 Loi, F. *et al.* Inflammation, fracture and bone repair. *Bone* **86**, 119-130 (2016).

45 Liu, J. *et al.* Macrophage polarization in periodontal ligament stem cells enhanced periodontal regeneration. *Stem cell research & therapy* **10**, 1-11 (2019).

46 Ma, C., Kuzma, M. L., Bai, X. & Yang, J. Biomaterial-based metabolic regulation in regenerative engineering. *Advanced Science* **6**, 1900819 (2019).

47 Saborano, R. *et al.* Metabolic reprogramming of macrophages exposed to silk, poly (lactic-co-glycolic acid), and silica nanoparticles. *Advanced Healthcare Materials* **6**, 1601240 (2017).

48 Gonçalves, R. & Mosser, D. M. The isolation and characterization of murine macrophages. *Current protocols in immunology* **111**, 14.11. 11-14.11. 16 (2015).

49 Feoktistova, M., Geserick, P. & Leverkus, M. Crystal violet assay for determining viability of cultured cells. *Cold Spring Harbor Protocols* **2016**, pdb. prot087379 (2016).

CHAPTER 5: Elevated oxidative phosphorylation is critical for immune cell activation by polyethylene wear particles

This chapter is a preprint of the following manuscript, currently under review in the Journal of Immunology and Regenerative Medicine:

Elevated oxidative phosphorylation is critical for immune cell activation by polyethylene wear particles

Chima V. Maduka, Maxwell M. Kuhnert, Oluwatosin M. Habeeb, Anthony Tundo, Ashley V. Makela, Stuart B. Goodman, Christopher H. Contag

Abstract

Chronic inflammation is a major concern after total joint replacements (TJRs), as it is associated with bone loss, limited bone-implant integration (osseointegration), implant loosening and failure. Inflammation around implants could be directed away from adverse outcomes and toward enhanced osseointegration and improved surgical outcome. Activated macrophages exposed to polyethylene particles play a dominant inflammatory role, and exhibit elevated mitochondrial oxidative phosphorylation (OXPHOS) whose role is unclear. By probing the contribution of the electron transport chain (ETC), we show that increased oxygen consumption does not contribute to bioenergetic (ATP) levels in fibroblasts and primary bone marrow-derived macrophages activated by polyethylene particles. Rather, it generates reactive oxygen species (ROS) at complex I by increasing mitochondrial membrane potential in macrophages. Inhibition of OXPHOS in a dose-dependent manner without affecting glycolysis was accomplished by targeting complex I of the ETC using either rotenone or metformin. Metformin decreased mitochondrial ROS and, subsequently,

expression of proinflammatory cytokines, including IL-1β, IL-6 and MCP-1 but not TNF-α in macrophages. These results highlight the contribution of mitochondrial bioenergetics to activation of immune cells by polyethylene wear particles, offering new opportunities to modulate macrophage states toward desired clinical outcomes.

Keywords: Polyethylene wear particles, macrophage, mitochondrial oxidative phosphorylation, total joint replacement

Introduction

Degenerative osteoarthritis is commonly treated by primary total joint replacements (TJRs). Bearing surfaces of articulations are often lined by polyethylene to prevent metal-on-metal articulation which is associated with metal ion toxicities and aseptic lymphocyte-dominated vasculitis-associated lesions[1]. However, wear particles of polyethylene generated by relative motion of artificially reconstructed joints after TJRs activate macrophages, resulting in chronic inflammation and bone loss[2,3]. This limits bone-implant integration (osseointegration) necessary for implant longevity[4,5]. Implant longevity is crucial because revision surgeries are costlier, more difficult and associated with higher complication rates than primary TJAs. Crosslinking polyethylene increases its resistance to wear, significantly reducing, but not eliminating, wear particle generation[6]. Wear particles of ultrahigh molecular weight polyethylene (UHMWPE) or highly crosslinked polyethylene (XLPE) are clinically relevant and result in inflammation[6,7]. Advances in understanding the role of macrophage polarization in macrophage-mesenchymal stem cell crosstalk show that inflammation induced by wear particles represents an opportunity to re-direct inflammation

toward desired surgical outcomes, such as enhanced osseointegration and implant longevity[8-13].

The mitochondrion is the center of energy (adenosine triphosphate; ATP) production in the cell, meeting bioenergetic demands by oxygen consumption (oxidative phosphorylation; OXPHOS) under resting conditions. As part of OXPHOS, electron transfer through the mitochondrial electron transport chain (ETC) generates ATP[14]. The ETC consists of a series of protein complexes, including complex I, II, III, IV and V with diverse roles. Beyond meeting energy demands, the ETC plays key regulatory and effector roles in inflammation[15-18]. In neutrophils and T-cells, increased oxygen consumption results in superoxide formation. Although oxygen consumption is reduced in macrophages exposed to bacterial lipopolysaccharide (LPS) as part of the switch from OXPHOS to glycolysis for ATP production[19,20], residual oxygen consumption is directed to superoxide formation[19], eventually producing reactive oxygen species (ROS)[21] as part of inflammation.

The immunometabolic changes in macrophages exposed to UHMWPE wear particles includes elevated OXPHOS[22], but its precise role is unclear. Herein, we set out to probe the role of increased oxygen consumption in macrophages activated by polyethylene particles. Elucidating the role of mitochondrial bioenergetics in immune cells activated by polyethylene particles could offer new insights toward controlling inflammation around implants. Clinically, this could translate to enhanced osseointegration, improved surgical outcome and implant longevity.

Materials and methods

Cells

Primary bone-marrow derived macrophages (BMDMs) derived from C57BL/6J mice (Jackson Laboratories) of 3-4 months[19,23] as well as wild-type mouse embryonic fibroblast (MEFs) cell line (NIH 3T3 cell line; ATCC) which tested negative for Mycoplasma were used. Cells were seeded in complete medium comprising DMEM medium, 10% heat-inactivated Fetal Bovine Serum and 100 U/mL penicillin-streptomycin; all reagents were sourced from ThermoFisher Scientific. For the different assays, 50,000 BMDMs or 20,000 MEFs were seeded for 3 days in a 96-well tissue culture plate in 200 μL of complete medium.

Materials

The generation, characteristics and concentration (1.25 mg/ mL) of UHMWPE particles used in this study have been previously described[7]. Additionally, 100ng/ mL of lipopolysaccharide (LPS) from *Escherichia coli* O111:B4 (MilliporeSigma) was used. Reagents including rotenone, metformin, oligomycin and antimycin A were sourced from MilliporeSigma and used at concentrations shown in each figure for probing mitochondrial functions. These reagents were reconstituted in complete medium and added at the time of seeding cells for experiments.

Bioenergetic (ATP) measurement

Bioenergetics was measured using ATP/ADP kits (Sigma-Aldrich) according to manufacturer's instructions. Luminescence was measured using the SpectraMax M3

Spectrophotometer (Molecular Devices) by SoftMax Pro (Version 7.0.2, Molecular Devices) at integration time of 1,000 ms.

Seahorse assay

Basal measurements of oxygen consumption rate (OCR), extracellular acidification rate (ECAR) and lactate-linked proton efflux rate (PER) were acquired using the Seahorse XFe-96 Extracellular Flux Analyzer (Agilent Technologies)[19,24,25]. The Seahorse XF DMEM medium (pH 7.4) was used after supplementation with 25 mM D-glucose and 4 mM Glutamine; seeded cells were washed off and incubated in a non-CO_2 incubator an hour prior to the assay, according to manufacturer's instructions for the Seahorse ATP rate assay. Afterwards, wave software (Version 2.6.1) was used to export Seahorse data directly as means ± standard deviation (SD).

Crystal Violet assay

The crystal violet assay was used to assess for cell viability[26]. Absorbance (optical density) measurements at 570 nm were acquired using the SpectraMax M3 Spectrophotometer (Molecular Devices) and SoftMax Pro software (Version 7.0.2, Molecular Devices).

Milliplex assay

Cytokine and chemokine expression in cell culture supernatants were evaluated using a MILLIPLEX MAP mouse magnetic bead multiplex kit (MilliporeSigma)[27]. Assays were performed for IL-6, MCP-1, TNF-α, IL-1β, IL-4, IL-10, IFN-λ and 1L-13. Data was acquired

using a Luminex 200 instrument (Luminex Corporation) and xPONENT software (Version 3.1, Luminex Corporation).

Flow cytometry

Macrophages were detached from 96-well plates after incubation using 1X PBS with 4mM EDTA (Teknova) at 37 °C for 10 minutes, followed by gentle pipetting. Cells were assessed for mitochondrial mass (MitoTracker Green FM, MTG; ThermoFisher Scientific), mitochondrial membrane potential (tetramethylrhodamine methyl ester, TMRM; ThermoFisher Scientific) and mitochondrial superoxide (MitoSOX Red, MSOX; ThermoFisher Scientific). Unstained cells from each condition, single-stained TMRM, MTG and MSOX cells were used for controls. A mix of 1X PBS (ThermoFisher Scientific) containing Live/Dead Blue (1:1000) and MTG (50 nM)/TMRM (20 nM) or MTG (50 nM)/MSOX (2.5 uM) were added to samples containing 650,000 cells in 100 μL, followed by incubation at 37 °C and 5% CO_2 in the dark for 30 min. Cells were collected by centrifugation followed by two washes using flow buffer. Flow buffer comprised 0.5% bovine serum albumin (MilliporeSigma) made in 1X PBS. Cells were fixed using 4% paraformaldehyde for 10 minutes at room temperature in the dark. Cells were collected by centrifugation followed by resuspension in 100 μL flow buffer for analysis using the Cytek Aurora flow cytometer. Cells were identified and singlets gated using FSC/SSC. MTG+ cells were gated from live cells and MSOX/TMRM were identified from the MTG+ population. Data were analyzed using FCS Express software (De Novo Software; version 7.12.0005).

Statistics and reproducibility

Data were presented as mean with standard deviation (SD) and analysed using statistical software (GraphPad Prism, version 9.3.1). Although exact p-values were presented, significance level was set at $p < 0.05$. Specific details of statistical tests and sample sizes (biological replicates) are provided in figure legends. Exported data (mean, SD) from Wave in Seahorse experiments had the underlying assumption of normality and similar variance, and thus were tested using corresponding parametric tests as indicated in figure legends.

Results

We have previously uncovered a role for glycolytic reprogramming in the inflammatory response to UHMWPE wear particles. Specific inhibition of different steps in glycolysis prevented the expression of proinflammatory cytokines while stimulating anti-inflammatory cytokines[22]. However, in addition to increased glycolysis, elevated mitochondrial oxygen consumption was observed whose role was unclear. To elucidate the role of mitochondrial OXPHOS, the function of putative sites of oxygen consumption[28], including complex I and III of the ETC were probed, and compared to complex V where ATP is synthesized. Inhibition of complex I was accomplished using rotenone[28]; for clinical translatability, metformin which has similar pharmacologic action was also used[29,30]. Additionally, complex III and V were inhibited by antimycin A and oligomycin, respectively.

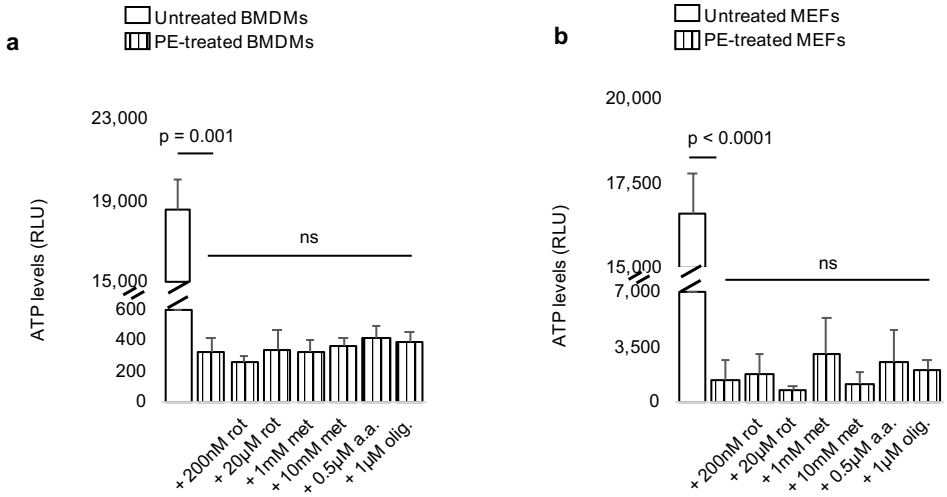

Figure 18. Decreased bioenergetic (ATP) levels in immune cells exposed to ultrahigh molecular weight polyethylene (PE) particles are not affected by pharmacologic inhibition of mitochondrial respiration. a-b, Primary bone marrow-derived macrophages (BMDMs; **a**) or mouse embryonic fibroblasts (MEFs; **b**) have decreased ATP levels after exposure to ultrahigh molecular weight polyethylene (PE) particles; decreased ATP levels are unaffected following inhibition of the electron transport chain by rotenone (rot), metformin (met), antimycin A (a.a.) or oligomycin (olig.). Not significant (ns), mean (SD), n = 4 (Fig. 1a), n = 5 (Fig. 1b), Brown-Forsythe and Welch ANOVA followed by Dunnett's T3 multiple comparisons test or one-way ANOVA followed by Tukey's post-hoc test.

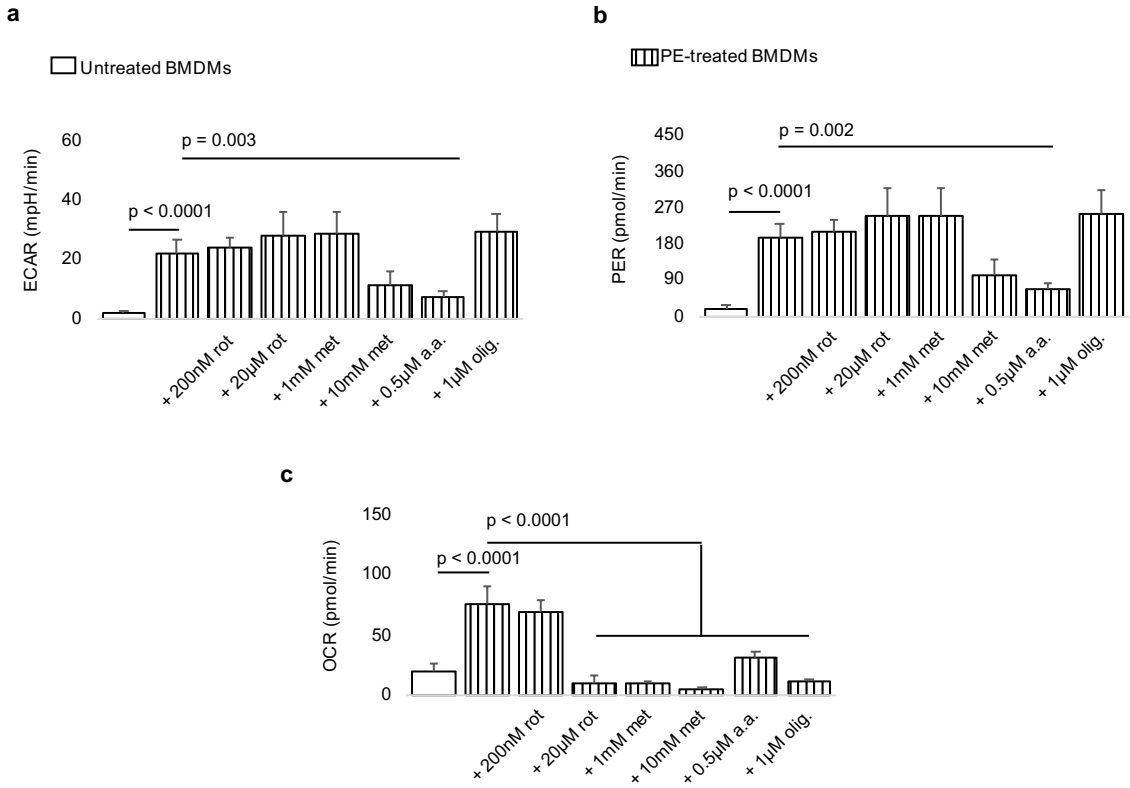

Figure 19. Exposure to ultrahigh molecular weight polyethylene (PE) particles increases extracellular acidification rate (ECAR), proton efflux rate (PER) and oxygen consumption rate (OCR) in macrophages; inhibitors of mitochondrial respiration reduce OCR. **a-c**, Compared to untreated primary bone marrow-derived macrophages (BMDMs), exposure to PE particles increase ECAR, PER and OCR. Inhibition of mitochondrial respiration using rotenone (rot), metformin (met), antimycin A (a.a.) or oligomycin (olig.) decreases elevated OCR but not ECAR or PER; with antimycin A, there is accompanied decrease in ECAR and PER. Mean (SD), n = 5, one-way ANOVA followed by Tukey's post-hoc test.

Macrophages and fibroblasts are dominant cellular actors in polyethylene particle-induced chronic inflammation and associated pathologies[3]. Compared to respective controls, exposure of primary bone marrow-derived macrophages or mouse embryonic fibroblasts to polyethylene particles decreased bioenergetics in lysed cells (Fig. 18a-b)[22]. Importantly, specific inhibition of complex I by rotenone or metformin did not further decrease ATP levels (Fig. 18a-b) in immune cells exposed to polyethylene particles. Similarly, complex III and V did not appear to contribute to ATP production in exposed immune cells (Fig. 18a-b).

Exposure of macrophages to polyethylene particles resulted in simultaneous elevation of extracellular acidification rate (ECAR), lactate-linked proton efflux rate (PER) and oxygen consumption rate (OCR) (Fig. 19a-c)[22]. Whereas ECAR is indicative of glycolytic flux, OCR is an index of mitochondrial OXPHOS, and lactate-linked PER is a surrogate of monocarboxylate transporter function[31,32], all of which are key to inflammatory activation. Compared to groups exposed to only polyethylene particles, we observed that specific inhibition of complex I and V of the ETC did not affect ECAR (Fig. 19a) or PER (Fig. 19b); however, they reduced OCR (Fig. 19c). With complex I, the reduction in OCR (Fig. 19c) was dose-dependent. On the other hand, inhibition of complex III using antimycin A reduced ECAR, PER and OCR (Fig. 19a-c) compared to groups exposed only to polyethylene particles. Importantly, pharmacological inhibition of the ETC was not the result of reduced cell numbers, excluding toxicity (Fig. 20a-b).

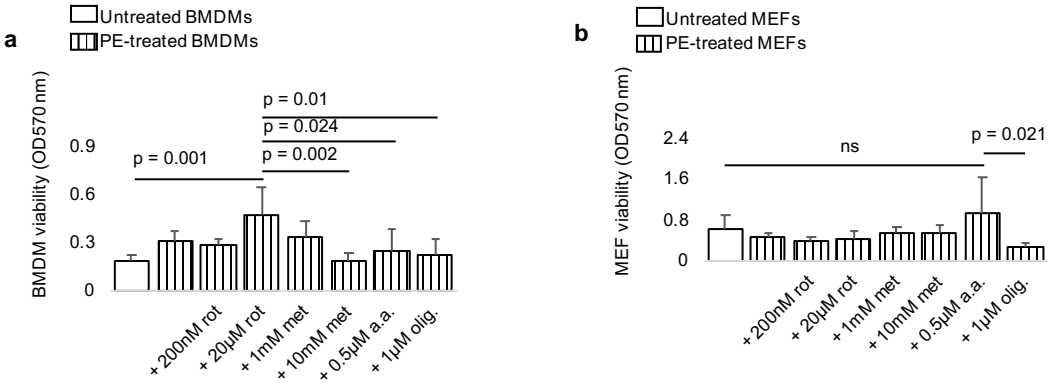

Figure 20. Inhibition of mitochondrial respiration does not reduce cell viability. a-b, In comparison to untreated cells, primary bone marrow-derived macrophages (BMDMs; **a**) or mouse embryonic fibroblasts (MEFs; **b**) have similar cell numbers after exposure to ultrahigh molecular weight polyethylene (PE) particles; cell viability is not reduced following inhibition of the electron transport chain by rotenone (rot), metformin (met), antimycin A (a.a.) or oligomycin (olig.). Not significant (ns), mean (SD), n = 5 (Fig. 1a), n = 4-5 (Fig. 1b), one-way ANOVA followed by Tukey's post-hoc test.

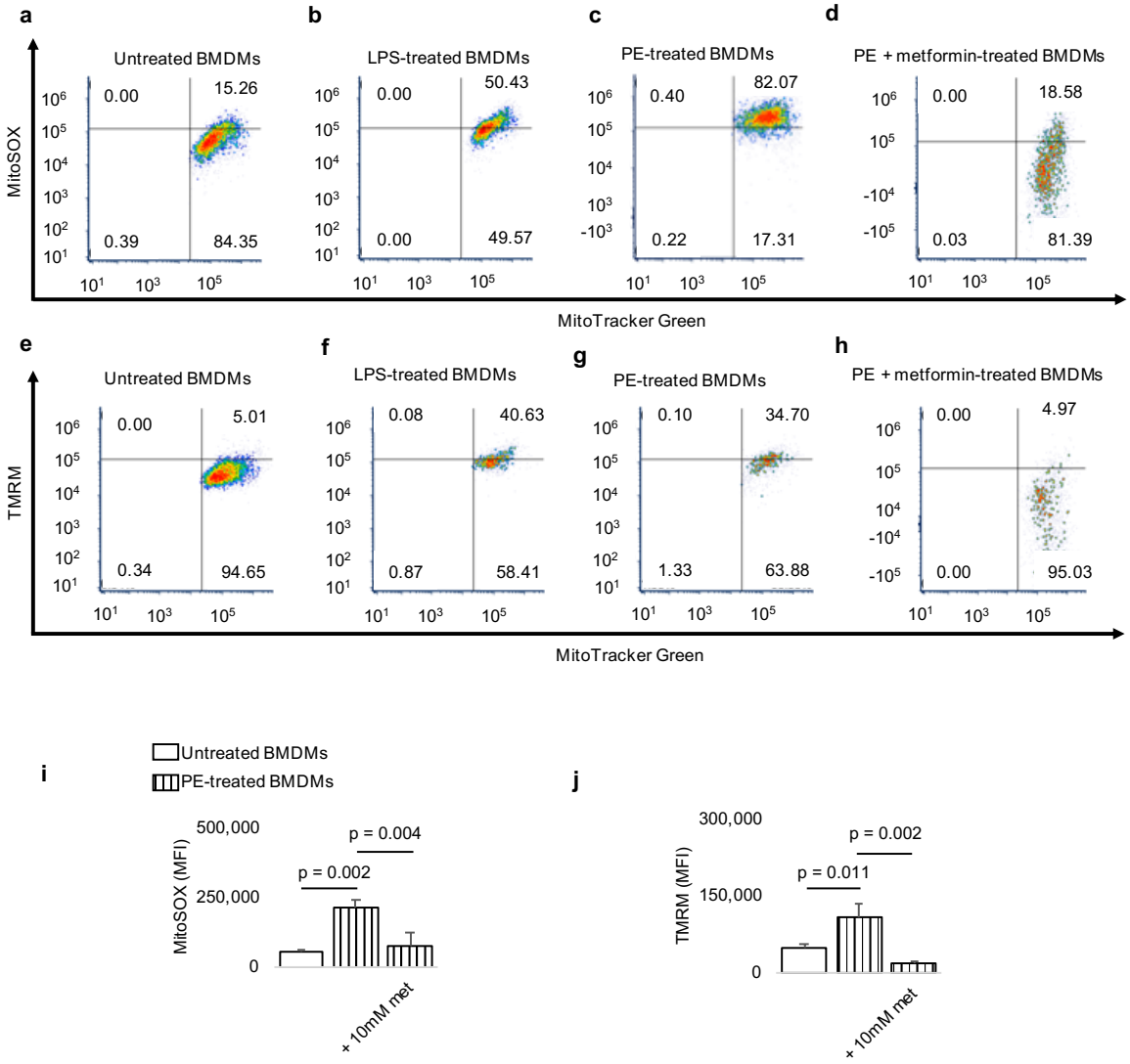

Figure 21. Exposure of macrophages to ultrahigh molecular weight polyethylene (PE) particles elevates mitochondrial membrane potential and reactive oxygen species (ROS) production which are decreased by metformin. a-d, In representative fluorescence-activated cell sorting (FACS) plots, compared to untreated primary bone marrow-derived macrophages (BMDMs; **a**), exposure to lipopolysaccharide (LPS; **b**) or PE particles (**c**) increases mitochondrial ROS as measured by MitoSOX Red (MitoSOX); elevated mitochondrial ROS levels are decreased by metformin (met). **e-h,** Similarly, mitochondrial membrane potential (measured by tetramethylrhodamine methyl ester, TMRM) of untreated BMDMs (**e**) is increased by LPS (**f**) or PE particles (**g**); increased

To test whether increased OCR at complex I (Fig. 19c) fueled ROS production in the mitochondrion, macrophages were stained with mitoSOX Red, with a bacterial lipopolysaccharide (LPS)-treated group included for comparison. Exposure to LPS or PE particles increased mitochondrial ROS relative to untreated macrophages (Fig. 21a-c). Addition of metformin decreased mitochondrial ROS compared to macrophages exposed to only PE particles (Fig. 21d). Mitochondrial membrane potential is critical for reverse electron transport (RET) at complex I, and subsequent generation of mitochondrial ROS[19]. Tetramethylrhodamine methyl ester (TMRM) staining demonstrated that LPS or PE particles increased mitochondrial membrane potential relative to untreated macrophages (Fig. 21e-g), with metformin decreasing elevated mitochondrial membrane potential (Fig. 21h). Quantified median fluorescence intensities (MFI) corroborated these findings (Fig. 21i-j).

Seeing that inhibition of complex I reduced aberrantly elevated OCR (Fig. 19c) without further decreasing bioenergetics (Fig. 18a), ECAR (Fig. 19a) or PER (Fig. 19b) in comparison to groups exposed to only polyethylene particles, we sought to determine the selective contribution of OCR from complex I to macrophage activation by polyethylene particles. Exposure to polyethylene particles increased proinflammatory cytokines, including IL-1β, IL-6, MCP-1 and TNF-α in comparison to untreated cells (Fig. 22a-d)[22]. Levels of IL-13 and IFN-γ were unchanged (data not shown).

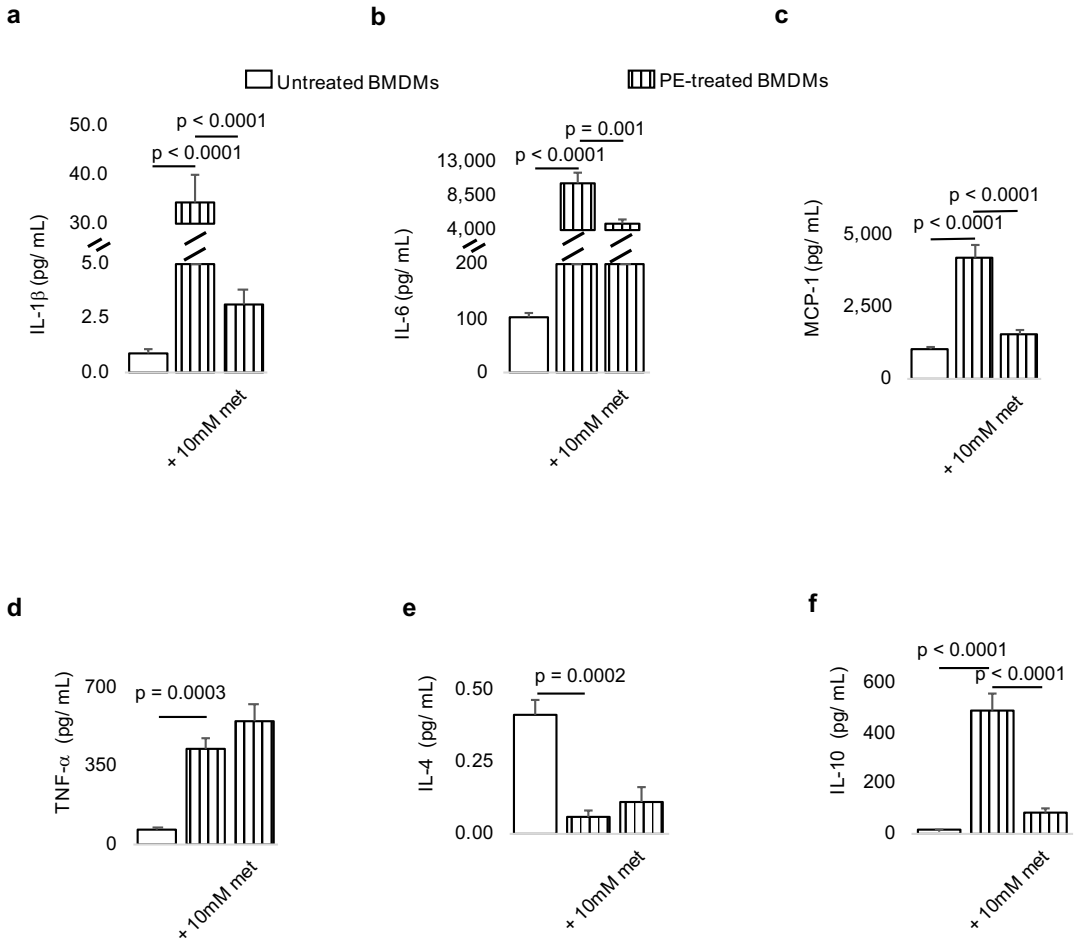

Figure 22. Exposure of macrophages to ultrahigh molecular weight polyethylene (PE) particles elevates proinflammatory cytokines which are decreased by metformin. **a-c,** In primary bone marrow-derived macrophages (BMDMs), proinflammatory cytokine (protein) levels, including IL-1β (**a**), IL-6 (**b**) and MCP-1 (**c**) are increased by exposure to PE particles, however, inhibition of the mitochondrial electron transport chain by metformin (met) decreases proinflammatory cytokine levels. **d**, Although the proinflammatory cytokine TNF-α is increased by exposure to PE particles, metformin does not decrease its levels. **e-f,** Whereas PE particles decrease IL-4 protein expression (**e**), they increase IL-10 levels (**f**); addition of metformin does not increase either anti-inflammatory cytokine relative to groups treated with PE particles alone. Mean (SD), n=3, one-way ANOVA followed by Tukey's post-hoc test.

Metformin decreased elevated IL-1β (Fig. 22a), IL-6 (Fig. 22b) and MCP-1 (Fig. 22c) but not TNF-α protein levels (Fig. 22d) when compared to groups exposed to only polyethylene particles. Furthermore, metformin neither increased IL-4 (Fig. 22e) nor IL-10 (Fig. 22f) protein expression in comparison to groups treated with only polyethylene particles.

Discussion

When immune cells are exposed to UHMWPE particles, bioenergetic (ATP) levels decrease, but mitochondrial OXPHOS is elevated. What role OXPHOS plays in immune cellular activation by polyethylene particles is not fully understood. Within the mitochondrial inner membrane and as part of OXPHOS, embedded complexes of the ETC generate ATP by electron transfer[14]. We show that OXPHOS does not contribute to ATP production in macrophages and fibroblasts exposed to polyethylene particles. Whereas inhibition of the ETC at complex I, III or V does not affect ATP production, inhibition of various glycolytic steps in immune cells exposed to polyethylene particles reduces ATP levels in a dose-dependent manner[22]. This suggests that glycolysis is primarily responsible for ATP production in immune cells exposed to polyethylene particles. HMGB1/ RAGE signaling is an inflammatory pathway associated with activation after exposure to polyethylene particles[33]. As part of its inflammatory role in promoting growth of pancreatic cancers, HMGB1/ RAGE signaling directly increases ATP levels by increasing mitochondrial OXPHOS[34]. In particular, elevated oxygen consumption at complex I was observed to enhance ATP production. Inhibition of complex I activity using rotenone decreased ATP production by HMGB1 in normal fibroblasts and pancreatic tumor cells, and cancer cell

proliferation and migration were decreased[34]. In contrast to observations in the HMGB1/ RAGE signaling pathway, oxygen consumption is reduced in macrophages exposed to LPS[19,20]. Mitochondrial function was shown to be repurposed toward increased superoxide formation at complex I[19], generating ROS[21]. Unlike LPS, PE particles increase oxygen consumption. Similar to macrophages exposed to polyethylene particles, concomitantly elevated glycolysis and OXPHOS for immune cellular functions is observed in neutrophils, wherein oxygen consumption is directed at activation and release of neutrophil extracellular traps (termed NETosis)[35] and superoxide formation[36]. Similarly, CD4+ T cells obtained from humans with systemic lupus erythematosus[37], an autoinflammatory disorder, also concomitantly elevate glycolysis and OXPHOS.

In macrophages exposed to polyethylene particles, specific pharmacologic inhibition of glycolysis was accompanied by a reduction in OXPHOS[22]. Similarly, inhibition of OXPHOS at complex III reduced both OXPHOS and glycolysis, consistent with their interdependence[38]; additionally, monocarboxylate transporter (MCT) function was reduced. Proton-linked shuttle of lactate occurs via MCTs, and these transporters are emerging targets for immunomodulation[31,32]. However, their specific role in pathologies associated with polyethylene particles requires further investigation. In contrast to complex III inhibition, inhibition of OXPHOS at complex I was not accompanied by reduction in glycolysis, allowing us to probe the selective contribution of oxygen consumption at complex I to macrophage activation by polyethylene particles. Both rotenone and metformin decreased oxygen consumption at complex I in a dose-dependent manner, consistent with their known pharmacodynamics[29].

Our findings suggest that elevated oxygen consumption at complex I of the ETC in macrophages exposed to PE particles is directed toward mitochondrial ROS production in a manner that is dependent on mitochondrial membrane potential. During inflammation, oxygen consumption at complex I leads to superoxide formation[19]. When oxygen consumption is inhibited at complex I by rotenone, a role for reverse electron transport in superoxide formation is likely[28] and has been shown for LPS-induced responses[19].

Inhibition of oxygen consumption at complex I using metformin decreased only some proinflammatory cytokines, including MCP-1, IL-1β and IL-6 in primary macrophages exposed to polyethylene particles. Metformin had no effect on TNF-α protein levels which are elevated in macrophages exposed to polyethylene particles. In septic models of inflammation due to LPS, inhibition of glycolysis[24] or OXPHOS[29] selectively decreased IL-1β without effects on TNF-α or IL-6 expression. In addition to the ability of metformin to inhibit oxygen consumption at complex I, it could also stimulate adenosine monophosphate (AMP)-activated kinase (AMPK). Stimulation of AMPK, a pro-survival pathway often activated during starvation, has been shown to be anti-inflammatory in macrophages exposed to polyethylene particles[39] or LPS[40]. Importantly, metformin was shown to reverse bone loss that accompanies chronic inflammation to polyethylene particles[39].

NF-kB is the master transcriptional regulator of macrophage activation by polyethylene particles[41]. The dominant NF-kB transactivating subunit called NF-kB3 (p65, encoded by the *RelA* gene) regulates mitochondrial OXPHOS in colon carcinoma cells, and silencing *RelA* results in decreased oxygen consumption[42]. Aside from being closely associated with the mitochondrion[43], NF-kB regulates OXPHOS by increasing cytochrome c oxidase 2[44], a complex IV subunit, in a p53-dependent manner[45]. Consistent with this notion,

p53 activation increases generation of ROS[46]. Similar to colon carcinoma, elevated oxygen consumption is an emerging feature of several types of cancers where the role of OXPHOS is multipronged. For example, elevated mitochondrial biogenesis driven by PGC-1α is associated with the invasive and metastatic capabilities of breast cancer[47]. In this role, administration of only rotenone accounts for differential oxygen consumption[47]. Pancreatic cancer stem cells exhibit a unique metabolic phenotype regulated by PGC-1α and c-MYC, and they require increased oxygen consumption for survival associated with increased ATP production[48]. Administration of oligomycin accounted for differential oxygen consumption while reducing elevated ATP levels in these cells[48]. For metastasis in pancreatic ductal adenocarcinoma, increased oxygen consumption driven by COX6B2 elevated ATP production which was abolished by oligomycin[49]. Here, ATP signaling was used by purinergic pathways required for epithelial-mesenchymal transition in metastasis[49]. In prostate, colon and breast cancers, elevated OXPHOS sustains drug resistance[50-52].

As part of their anti-inflammatory effect, macrophages could exhibit increased mitochondrial oxygen consumption. For instance, IL-4 has been shown to increase oxygen consumption[53]. However, this increment is accounted for by administration of oligomycin which inhibits ATP synthase[53], suggesting a need for increased levels of ATP in the anti-inflammation response. Consistent with this, inhibition of OXPHOS by nitric oxide prevents, polarization of inflammatory macrophages to an anti-inflammatory phenotype by limiting mitochondrial ATP production[20]. IL-4 induces mitochondrial biogenesis in a PGC-1β-dependent mechanism to meet the enhanced bioenergetic needs of anti-inflammatory macrophages[54]. It has been proposed that IL-4 and IL-13 enhance OXPHOS by inhibiting mTOR[55]. In this regard, IL-4 fails to induce an anti-inflammatory phenotype when mTOR is

constitutively activated in a genetic model[56]. Oxymoronically, mTOR signaling is critical for OXPHOS through PGC-1α[57], challenging this theory and necessitating further research to reconcile the diverse roles of OXPHOS in immune cell states.

In conclusion, we show that increased oxygen consumption does not contribute to bioenergetic (ATP) levels in activated macrophages exposed to UHMWPE particles. Rather, it is directed toward mitochondrial ROS production in a manner that is dependent on mitochondrial membrane potential, suggesting a role for reverse electron transport. Inhibition of OXPHOS in a dose-dependent manner without affecting glycolysis was accomplished by targeting complex I of the ETC using either rotenone or metformin. Consequently, this decreased expression of proinflammatory cytokines, including IL-1β, IL-6 and MCP-1 but not TNF-α in primary bone marrow-derived macrophages. These results highlight the contribution of mitochondrial respiration to activation of immune cells by polyethylene wear particles, offering new opportunities that target mitochondrial respiration to control macrophage states toward desired clinical outcomes.

Author contributions

Conceptualization, C.V.M. and C.H.C.; Methodology, C.V.M., S.B.G., A.V.M. and C.H.C.; Investigation, C.V.M., M.M.K., O.M.B, A.T. and A.V.M.; Writing – Original Draft, C.V.M.; Writing – Review & Editing, C.V.M., M.M.K., O.M.B, A.T., A.V.M., S.B.G., and C.H.C.; Funding Acquisition, C.H.C.; Resources, S.B.G. and C.H.C.; Supervision, S.B.G. and C.H.C.

Data availability

Data generated during this study are included in this published article.

Declaration of competing interest

The authors declare no conflict of interest.

Acknowledgements

Euthanized C57BL/6J mice were a gift from RR Neubig (facilitated by J Leipprandt and E Lisabeth) and the Campus Animal Resources at Michigan State University (MSU). Funding for this work was provided in part by the James and Kathleen Cornelius Endowment at MSU.

REFERENCES

REFERENCES

1 Pelt, C. E. *et al.* Histologic, serologic, and tribologic findings in failed metal-on-metal total hip arthroplasty: AAOS exhibit selection. *JBJS* **95**, e163 (2013).

2 Goodman, S. B., Gallo, J., Gibon, E. & Takagi, M. Diagnosis and management of implant debris-associated inflammation. *Expert review of medical devices* **17**, 41-56 (2020).

3 Sivananthan, S., Goodman, S. & Burke, M. in *Joint Replacement Technology* 373-402 (Elsevier, 2021).

4 Agarwal, R. & García, A. J. Biomaterial strategies for engineering implants for enhanced osseointegration and bone repair. *Adv Drug Deliv Rev* **94**, 53-62, doi:10.1016/j.addr.2015.03.013 (2015).

5 Ho-Shui-Ling, A. *et al.* Bone regeneration strategies: Engineered scaffolds, bioactive molecules and stem cells current stage and future perspectives. *Biomaterials* **180**, 143-162 (2018).

6 Tsukamoto, M., Mori, T., Ohnishi, H., Uchida, S. & Sakai, A. Highly cross-linked polyethylene reduces osteolysis incidence and wear-related reoperation rate in cementless total hip arthroplasty compared with conventional polyethylene at a mean 12-year follow-up. *The Journal of Arthroplasty* **32**, 3771-3776 (2017).

7 Pajarinen, J. *et al.* Interleukin-4 repairs wear particle induced osteolysis by modulating macrophage polarization and bone turnover. *Journal of Biomedical Materials Research Part A* **109**, 1512-1520 (2021).

8 Goodman, S. B., Pajarinen, J., Yao, Z. & Lin, T. Inflammation and bone repair: from particle disease to tissue regeneration. *Frontiers in Bioengineering and Biotechnology*, 230 (2019).

9 Christman, K. L. Biomaterials for tissue repair. *Science* **363**, 340-341 (2019).

10 Eming, S. A., Wynn, T. A. & Martin, P. Inflammation and metabolism in tissue repair and regeneration. *Science* **356**, 1026-1030 (2017).

11 Chung, L., Maestas Jr, D. R., Housseau, F. & Elisseeff, J. H. Key players in the immune response to biomaterial scaffolds for regenerative medicine. *Advanced drug delivery reviews* **114**, 184-192 (2017).

12 Franz, S., Rammelt, S., Scharnweber, D. & Simon, J. C. Immune responses to implants–a review of the implications for the design of immunomodulatory biomaterials. *Biomaterials* **32**, 6692-6709 (2011).

13 Li, C. *et al.* Design of biodegradable, implantable devices towards clinical translation. *Nature Reviews Materials* **5**, 61-81 (2020).

14 Nolfi-Donegan, D., Braganza, A. & Shiva, S. Mitochondrial electron transport chain: Oxidative phosphorylation, oxidant production, and methods of measurement. *Redox biology* **37**, 101674 (2020).

15 Garaude, J. *et al.* Mitochondrial respiratory-chain adaptations in macrophages contribute to antibacterial host defense. *Nature immunology* **17**, 1037-1045 (2016).

16 Olive, A. J., Kiritsy, M. & Sassetti, C. (Am Assoc Immnol, 2021).

17 Sena, L. A. *et al.* Mitochondria are required for antigen-specific T cell activation through reactive oxygen species signaling. *Immunity* **38**, 225-236 (2013).

18 Di Gioia, M. *et al.* Endogenous oxidized phospholipids reprogram cellular metabolism and boost hyperinflammation. *Nature immunology* **21**, 42-53 (2020).

19 Mills, E. L. *et al.* Succinate Dehydrogenase Supports Metabolic Repurposing of Mitochondria to Drive Inflammatory Macrophages. *Cell* **167**, 457-470.e413, doi:10.1016/j.cell.2016.08.064 (2016).

20 Van den Bossche, J. *et al.* Mitochondrial dysfunction prevents repolarization of inflammatory macrophages. *Cell reports* **17**, 684-696 (2016).

21 West, A. P. *et al.* TLR signalling augments macrophage bactericidal activity through mitochondrial ROS. *Nature* **472**, 476-480 (2011).

22 Maduka, C. V., Habeeb, O. M., Kuhnert, M. M., Hakun, M., Goodman, S. B. & Contag, C. H. Glycolytic reprogramming underlies immune cell activation by polyethylene wear particles. *Biomaterials Advances* **2022** (submitted).

23 Gonçalves, R. & Mosser, D. M. The isolation and characterization of murine macrophages. *Current protocols in immunology* **111**, 14.11. 11-14.11. 16 (2015).

24 Tannahill, G. *et al.* Succinate is a danger signal that induces IL-1β via HIF-1α. *Nature* **496**, 238-242, doi:10.1038/nature11986 (2013).

25 Ip, W. E., Hoshi, N., Shouval, D. S., Snapper, S. & Medzhitov, R. Anti-inflammatory effect of IL-10 mediated by metabolic reprogramming of macrophages. *Science* **356**, 513-519 (2017).

26 Feoktistova, M., Geserick, P. & Leverkus, M. Crystal violet assay for determining viability of cultured cells. *Cold Spring Harbor Protocols* **2016**, pdb. prot087379 (2016).

27 Sprague, L. *et al.* Dendritic cells: in vitro culture in two-and three-dimensional collagen systems and expression of collagen receptors in tumors and atherosclerotic microenvironments. *Experimental cell research* **323**, 7-27 (2014).

28 Murphy, M. P. How mitochondria produce reactive oxygen species. *Biochemical journal* **417**, 1-13 (2009).

29 Kelly, B., Tannahill, G. M., Murphy, M. P. & O'Neill, L. A. Metformin inhibits the production of reactive oxygen species from NADH: ubiquinone oxidoreductase to limit induction of interleukin-1β (IL-1β) and boosts interleukin-10 (IL-10) in lipopolysaccharide (LPS)-activated macrophages. *Journal of biological chemistry* **290**, 20348-20359 (2015).

30 Pålsson-McDermott, E. M. & O'Neill, L. A. Targeting immunometabolism as an anti-inflammatory strategy. *Cell research* **30**, 300-314 (2020).

31 Samuvel, D. J., Sundararaj, K. P., Nareika, A., Lopes-Virella, M. F. & Huang, Y. Lactate boosts TLR4 signaling and NF-κB pathway-mediated gene transcription in macrophages via monocarboxylate transporters and MD-2 up-regulation. *The Journal of Immunology* **182**, 2476-2484 (2009).

32 Tan, Z. *et al.* in *The Journal of biological chemistry* Vol. 290 46-55 (2015).

33 Koivu, H. *et al.* Autoinflammation around AES total ankle replacement implants. *Foot & Ankle International* **36**, 1455-1462 (2015).

34 Kang, R. *et al.* The HMGB1/RAGE inflammatory pathway promotes pancreatic tumor growth by regulating mitochondrial bioenergetics. *Oncogene* **33**, 567-577 (2014).

35 Sack, M. N. Mitochondrial fidelity and metabolic agility control immune cell fate and function. *The Journal of clinical investigation* **128**, 3651-3661 (2018).

36 Guthrie, L. A., McPHAIL, L. C., Henson, P. M. & Johnston Jr, R. Priming of neutrophils for enhanced release of oxygen metabolites by bacterial lipopolysaccharide. Evidence for increased activity of the superoxide-producing enzyme. *The Journal of experimental medicine* **160**, 1656-1671 (1984).

37 Yin, Y. *et al.* Normalization of CD4+ T cell metabolism reverses lupus. *Science translational medicine* **7**, 274ra218-274ra218 (2015).

38 Van Raam, B. J. *et al.* Mitochondrial membrane potential in human neutrophils is maintained by complex III activity in the absence of supercomplex organisation. *PloS one* **3**, e2013 (2008).

39 Yan, Z. *et al.* Metformin suppresses UHMWPE particle-induced osteolysis in the mouse calvaria by promoting polarization of macrophages to an anti-inflammatory phenotype. *Molecular Medicine* **24**, 1-12 (2018).

40 Sag, D., Carling, D., Stout, R. D. & Suttles, J. Adenosine 5′-monophosphate-activated protein kinase promotes macrophage polarization to an anti-inflammatory functional phenotype. *The Journal of Immunology* **181**, 8633-8641 (2008).

41 Lin, T.-H. *et al.* NF-κB decoy oligodeoxynucleotide enhanced osteogenesis in mesenchymal stem cells exposed to polyethylene particle. *Tissue engineering Part A* **21**, 875-883 (2015).

42 Mauro, C. *et al.* NF-κB controls energy homeostasis and metabolic adaptation by upregulating mitochondrial respiration. *Nature cell biology* **13**, 1272-1279 (2011).

43 Albensi, B. C. What is nuclear factor kappa B (NF-κB) doing in and to the mitochondrion? *Frontiers in cell and developmental biology*, 154 (2019).

44 Matoba, S. *et al.* p53 regulates mitochondrial respiration. *Science* **312**, 1650-1653 (2006).

45 Johnson, R. F., Witzel, I.-I. & Perkins, N. D. p53-dependent regulation of mitochondrial energy production by the RelA subunit of NF-κB. *Cancer research* **71**, 5588-5597 (2011).

46 Karawajew, L., Rhein, P., Czerwony, G. & Ludwig, W.-D. Stress-induced activation of the p53 tumor suppressor in leukemia cells and normal lymphocytes requires mitochondrial activity and reactive oxygen species. *Blood* **105**, 4767-4775 (2005).

47 LeBleu, V. S. *et al.* PGC-1α mediates mitochondrial biogenesis and oxidative phosphorylation in cancer cells to promote metastasis. *Nature cell biology* **16**, 992-1003 (2014).

48 Sancho, P. *et al.* MYC/PGC-1α balance determines the metabolic phenotype and plasticity of pancreatic cancer stem cells. *Cell metabolism* **22**, 590-605 (2015).

49 Nie, K. *et al.* COX6B2 drives metabolic reprogramming toward oxidative phosphorylation to promote metastasis in pancreatic ductal cancer cells. *Oncogenesis* **9**, 1-13 (2020).

50 Ippolito, L. *et al.* Metabolic shift toward oxidative phosphorylation in docetaxel resistant prostate cancer cells. *Oncotarget* **7**, 61890 (2016).

51 Bacci, M. *et al.* miR-155 drives metabolic reprogramming of ER+ breast cancer cells following long-term estrogen deprivation and predicts clinical response to aromatase inhibitors. *Cancer research* **76**, 1615-1626 (2016).

52 Denise, C. *et al.* 5-fluorouracil resistant colon cancer cells are addicted to OXPHOS to survive and enhance stem-like traits. *Oncotarget* **6**, 41706 (2015).

53 Tan, Z. *et al.* Pyruvate dehydrogenase kinase 1 participates in macrophage polarization via regulating glucose metabolism. *The Journal of immunology* **194**, 6082-6089 (2015).

54 Vats, D. *et al.* Oxidative metabolism and PGC-1β attenuate macrophage-mediated inflammation. *Cell metabolism* **4**, 13-24 (2006).

55 Kelly, B. & O'neill, L. A. Metabolic reprogramming in macrophages and dendritic cells in innate immunity. *Cell research* **25**, 771-784 (2015).

56 Byles, V. *et al.* The TSC-mTOR pathway regulates macrophage polarization. *Nature communications* **4**, 1-11 (2013).

57 Cunningham, J. T. *et al.* mTOR controls mitochondrial oxidative function through a YY1–PGC-1α transcriptional complex. *Nature* **450**, 736-740 (2007).

CHAPTER 6: Conclusion

Summary

We reveal that functional metabolism and bioenergetics are emerging paradigms in defining the body's foreign body response to implanted biomaterials, including polylactide (PLA) and polyethylene (PE) as they degrade. At least for PLA, this is a paradigm shift away from the proposed pH changes by lactate to seeing lactate, and oligomers of this monomer, as signaling molecules that reprogram immune cell metabolism to drive a proinflammatory pattern of immune modulators. Alterations include concomitant increases in glycolytic flux as well as oxidative phosphorylation, and are consequential to the mechanism by which PLA and PE degradation products activate macrophages and fibroblasts. As such, we show that metabolism can be leveraged to control immune cellular responses toward phenotypes that result in favorable regenerative and anti-inflammatory outcomes. Additionally, we demonstrate that differential metabolic reprogramming explains the role of stereochemistry in unique immune cellular responses to multiple PLA types, shedding light on long-standing controversies on differential inflammatory responses to PLA of varied stereochemistries. Accordingly, small molecules that specifically target glycolysis or oxidative phosphorylation to modulate these pathways guide inflammatory reactions to materials implanted in the body. These studies have laid a solid foundation on which to build programs in tissue regeneration with PLA as the matrix with embedded metabolic reprogramming molecules that drive regenerative processes. Our findings build on PLA's strength as the most widely used polymer in medicine, yet, offers opportunities for significantly expanding current biomedical applications of PLA. For example, almost solely highly crystalline formulations of PLA are approved for orthopedic PLA applications. Using amorphous PLA which is often avoided because it degrades faster than crystalline formulations (with the potential for

greater inflammation), we show that physicochemical properties of PLA should no longer be a rate limiting step in PLA's application in biomedicine because metabolic inhibitors effectively abrogates adverse responses to both crystalline and amorphous PLA. Similarly, PE particles that result in implant failures and loosening after eliciting insidious inflammatory activities have a metabolic basis. By targeting altered metabolic pathways, we show that proinflammatory responses can not only be suppressed, but directed toward pro-regenerative phenotypes. This offers new opportunities to enhance bone-implant integration (osseointegration), ensuring the longevity of implants applied in total joint replacements and advancing tissue engineering.

Future Directions

To realize our long-term goal of building synthetic tissues by leveraging immunometabolism, ongoing and future studies will:

1. Incorporate metabolic inhibitors in PLA by melt-blending and examine the potential for controlled and sustained release: Loading and distribution of metabolic inhibitors will be validated by Scanning electron microscopy with energy dispersive X-ray spectrometry (SEM–EDX).
2. Validate our finding that metabolic reprogramming underlies immune cellular activation by PLA degradation using fluorodeoxyglucose (FDG)-positron emission tomography (PET) imaging: PLA with and without incorporating metabolic inhibitors will be subcutaneously implanted in wild-type mice, alongside appropriate controls.
3. Examine immune cell trafficking in the implant microenvironment using intravital microscopy: PLA with and without incorporating metabolic inhibitors will be subcutaneously implanted in the ears of $Ccr2^{RFP}Cx3cr1^{GFP}$ dual-reporter mice.

4. Examine the effect of metabolic inhibitors on bone regeneration: A critical-sized femoral defect will be made in rats wherein 3D printed PLA scaffolds will be implanted. PLA Scaffolds with and without incorporating metabolic inhibitors will be implanted in the defect and bone regeneration will be evaluated.
5. Examine the effects of metabolic inhibitors on neovascularization after PLA Scaffolds with and without incorporating metabolic inhibitors are implanted.